

IJAE

Italian Journal of Anatomy and Embryology

Official Organ of the Italian Society
of Anatomy and Histology

Vol. 126
N. 2

2022

ISSN 1122-6714


FIRENZE
UNIVERSITY
PRESS

Founded by Giulio Chiarugi in 1901

Editor-in-Chief

Domenico Ribatti, University of Bari, Italy

Managing Editor

Ferdinando Paternostro, University of Firenze, Italy

Editorial Board

Gianfranco Alpini, Indiana University, USA
Giuseppe Anastasi, University of Messina, Italy
Juan Arechaga, University of Leioa, Spagna
Erich Brenner, University of Innsbruck, Austria
Marina Bentivoglio, University of Verona, Italy
Anca M. Cimpean, University of Timisoara, Romania
Lucio I. Cocco, University of Bologna, Italy
Bruna Corradetti, Houston Methodist Hospital, USA
Raffaele De Caro, University of Padova, Italy
Valentin Djonov, University of Berne, Switzerland
Amelio Dolfi, University of Pisa, Italy
Roberto di Primio, University of Ancona, Italy
Gustavo Egea, University of Barcellona, Spagna
Antonio Filippini, University “La Sapienza”, Roma, Italy
Eugenio Gaudio, University of Roma “La Sapienza”, Italy
Paolo Mazzarello, University of Pavia, Italy
Thimios Mitsiadis, University of Zurich, Switzerland
John H. Martin, City University New York, USA
Paolo Mignatti, New York University, USA
Stefania Montagnani, University of Napoli, Italy
Michele Papa, University of Napoli, Italia
Jeroen Pasterkamp, University of Utrecht, The Netherlands
Francesco Pezzella, University of Oxford, UK
Marco Presta, University of Brescia, Italy
Jose Sañudo, University of Madrid, Spain
Gigliola Sica, University “Cattolica”, Roma, Italy
Michail Sitkovsky, Harvard University, Boston, USA
Carlo Tacchetti, University “Vita-Salute San Raffaele”, Milano, Italy
Sandra Zecchi, University of Firenze, Italy

Past-Editors

I. Fazzari; E. Allara; G.C. Balboni; E. Brizzi; G. Gheri; P. Romagnoli

Journal e-mail: ijae@unifi.it – Web site: <http://www.fupress.com/ijae>

Italian Journal of Anatomy and Embryology

IJAE

Vol. 126, n. 2 - 2022

Firenze University Press

Italian Journal of Anatomy and Embryology

Published by

Firenze University Press – University of Florence, Italy

Via Cittadella, 7 - 50144 Florence - Italy

<http://www.fupress.com/substantia>

Direttore responsabile: **Ferdinando Paternostro, University of Firenze, Italy**

Direttore scientifico: **Domenico Ribatti, University of Bari, Italy**

Copyright © 2022 **Authors**. The authors retain all rights to the original work without any restriction.

Open Access. This issue is distributed under the terms of the [Creative Commons Attribution 4.0 International License \(CC-BY-4.0\)](https://creativecommons.org/licenses/by/4.0/) which permits unrestricted use, distribution, and reproduction in any medium, provided you give appropriate credit to the original author(s) and the source, provide a link to the Creative Commons license, and indicate if changes were made. The Creative Commons Public Domain Dedication (CC0 1.0) waiver applies to the data made available in this issue, unless otherwise stated.



Citation: Gianfranco Natale, Emanuele Armocida (2022) The vascular structure of the urethra: a historical overview. *Italian Journal of Anatomy and Embryology* 126(2): 3-8. doi: 10.36253/ijae-11104

Copyright: © 2022 Gianfranco Natale, Emanuele Armocida. This is an open access, peer-reviewed article published by Firenze University Press (<http://www.fupress.com/ijae>) and distributed under the terms of the Creative Commons Attribution License, which permits unrestricted use, distribution, and reproduction in any medium, provided the original author and source are credited.

Data Availability Statement: All relevant data are within the paper and its Supporting Information files.

Competing Interests: The Author(s) declare(s) no conflict of interest.

The vascular structure of the urethra: a historical overview

GIANFRANCO NATALE^{1,2,*}, EMANUELE ARMOCIDA³

¹ Department of Translational Research and New Technologies in Medicine and Surgery, University of Pisa, Pisa, Italy

² Museum of Human Anatomy “Filippo Civinini”, University of Pisa, Pisa, Italy

³ Department of Medicine and Surgery, University of Parma, Parma, Italy

*Corresponding author. E-mail: gianfranco.natale@unipi.it

Abstract. Penile structure and function aroused interest since ancient times, when the erectile activity was mainly attributed to an accumulation of air by Greek and Roman physicians. In the Renaissance period Leonardo da Vinci was one of the first to recognize the right functional importance of the presence of blood in penile tissues. Since then, although with different techniques and interpretations, the morphological studies reported the description of blood vessels differently arranged in complicated networks. The discovery of blood circulation by William Harvey in his famous *Exercitatio anatomica de motu cordis* (1628) and the demonstration of capillaries by Marcello Malpighi stimulated a deeper research. In particular, the presence of a non vascular spongy tissue (cavernous bodies) with cellular texture (cellular theory) was postulated and interpreted as consisting of a loose and elastic spongy tissue arranged in several cells into which, during erection, blood is poured from the arteries, and from which it is afterwards removed by veins. In the beginning of the 19th century, when both vascular and cellular texture theories concerning the penile anatomy were still coexisting, a particular attention was paid to the urethral structure. Thanks to improved injection techniques, Paolo Mascagni and Alessandro Moreschi provided accurate works on this subject, demonstrating the vascular nature of the cavernous bodies. Finally, in 1899 Victor Vecki von Gyurkovechky confirmed the vascular theory, histologically demonstrated by the presence of endothelium.

Keywords: cavernous body of the penis, corpus spongiosum, urethra, cellular theory.

The dynamics of penile erection evoked an anatomical and physiological interest since ancient times. In Greek and Roman medicine, represented by the great figures of Hippocrates and Galen, respectively, an accumulation of air (*pneuma*) was believed responsible for such a phenomenon (Driel, 2015). Significantly, the mythological Priapus just embodied this particular condition, with oversized genitals and permanent erection, giving rise to the medical term priapism.

Although influenced by the previous tradition, in the Renaissance period Leonardo da Vinci (1452-1519) was one of the first anatomists to recognize the presence of blood instead of air in the penile tissues during erection and

a similar conclusion was achieved also by the anatomist Costanzo Varolio (1543-1575) (Driel, 2015).

The first anatomical description of erectile tissues can be found in the book V, chapter XIV (*De virilis membri, penisque structura*; On the male organ and the structure of the penis) of the famous *De Humani corporis fabrica* published in 1543 by the father of modern anatomy, Andreas Vesalius (1514-1564) (Fig. 1), who also illustrated male genitals. In his masterpiece Vesalius denied the nature of cavernous bodies of the penis in terms of blood vessels, nerves, tendons, bones or ligaments, but he recognized the presence of venous (dark) blood, describing several *fasciculi* of arteries and veins closely interwoven, within an investing sheath (Vesalius, 2007, p. 163):

The Creator constructed the penis from two bodies that resemble nothing else in the human frame (with the possible exception of the nipple). These two bodies can become erect, grow longer, and swell considerably when they are filled with spirit; and when the spirit disperses they contract, collapse, become flaccid, and shorten. They are not veins or arteries or nerves, for they take origin from bones. They are not tendons, for they are not enervations of muscles, they cannot (as they can in dogs and weasels) be regarded as bones or cartilages, for when they are slack and relaxed they can easily be bent and folded like a ligament. But you cannot call them ligaments either, for they definitely have sensation, show clear holes or cavities within them, are rather fleshy and soft in the middle and, quite unlike ligaments, are filled with dark blood.

The Italian physician and anatomist Giovanni Filippo Ingrassia (1510-1580), student of Vesalius, in his work *De tumoribus praeter naturam*, published in 1552, clearly stated that *corpora cavernosa* are an aggregate of blood vessels (Levi, 1835).

The development of injection techniques and the creation of anatomical models contributed significantly to anatomical discoveries and were very effective in convincing that an accumulation of blood, rather than its mere presence, was important during erection. When Regnier de Graaf (1641-1673) injected the hypogastric artery with water, he observed an engorgement of penile blood vessels, as well. Similar results were obtained by Frederik Ruysch (1638-1731), who also performed injection techniques, realizing wax-like casts of penis (Driel, 2015).

After the discovery of the blood circulation described by William Harvey (1578-1657) in the famous *Exercitatio anatomica de motu cordis et sanguinis in animalibus* (Harvey, 1628), and the microscopic identification of capillaries by Marcello Malpighi (1628-1694) in the *De pulmonibus observationes anatomicae* (Malpighi, 1661), it became clear the continuity between arter-



Figure 1. Plaster bust of Andreas Vesalius. Museum of Human Anatomy “Filippo Civinini”, University of Pisa.

ies and veins. In particular, in its *Dissertatio epistolica varii argumenti de cornuum vegetatione, utero, viviparorum ovis, plantis &c*, Malpighi (1687, p. 211) considered the structure of the penis as composed of diverticula or appendices of veins. In 1703 the surgeon and anatomist William Cowper (1666-1709) admitted the large communication between arteries and veins in the spleen and penis, as reported in *An answer to Dr Wright’s Letter, concerning the Cure of an Aposthumation of the Lungs*, published in *Philosophical Transactions* (Cowper, 1703).

However, in the late 18th century this vascular disposition was not recognized in all organs. In some particular tissues, such as spleen and genitals, the anatomical continuity between arterial and venous system still had to be clearly demonstrated.

One of the first anatomists who showed a vascular structure on the surface of the cavernous body of the urethra was Lorenz Heister (1683-1758). In the footsteps of his master Ruysch, he examined this part more closely, so that in the fifth table of his *Compendium anatomicum*, published in Nuremberg in 1741, he included two figures, illustrating both dorsal and ventral sides of the penis, clearly and accurately demonstrating blood vessels of the surface of the glans behind the mercury injection pushing for the dorsal vein. With this method, not only the perfusion of the surface of the glans, but also of the whole corpus cavernosum of the urethra was easily obtained. Surprisingly, Heister did not note the real anatomical nature of the urethra and the whole glans (Levi, 1835).

This uncertainty favored alternative hypotheses. For instance, in the case of erectile tissues of genitals, the presence of a non vascular spongy tissue with cellular texture (cellular theory) was postulated. In detail, in spite of advanced injection techniques, the nature of the cavernous tissue of the glans and around the male urethra still had to be structurally elucidated. In *Elementa physiologiae corporis humani*, published in 1765, Albrecht von Haller (1708-1777) described *corpora cavernosa penis* as *ex tenacissima cellulosa stipata natura facti*. Furthermore, he found the spongy tissue of urethra distinct form that of the two cavernous body of penis, but he observed a communication between arteries and veins (Haller, 1765). Similarly, Guichard Joseph Duverney (1648-1730), Herman Boerhaave (1668-1738), and Marie François Xavier Bichat (1771-1802) also interpreted the cavernous bodies of the penis and urethra as consisting of a loose and elastic spongy tissue arranged in several cells into which, during erection, blood is poured from the arteries, and from which it is afterwards removed by veins (Todd, 1839).

On the contrary, the famous surgeon John Hunter (1728-1793), who also dealt with the concept of angiogenesis (Lenzi et al., 2016; Natale et al., 2017), in *Observations on certain parts of the animal oeconomy* observed that cavernous bodies were not spongy or cellular, but consisting of a plexus of veins (Hunter, 1792, p. 43):

In the perfect male the penis is large; the corpora cavernosa being capable of dilatation. The corpus spongiosum is very vascular; that part of the canal which is called the bulb is considerably enlarged, forming a cavity; and the muscoli acceleratores urinae, as they are termed, are strong and healthy.*

The notes are very illuminating:

** The cells of the corpora cavernosa are muscular, although no such appearance is to be observed in men: for the penis in erection is not at all times equally distended. The penis in a cold day is not so large in erection as in a warm one; which, probably, arises from a kind of spasm that could not act upon it if it were not muscular.*

† It may not be improper to observe, that the corpus spongiosum urethrae, and glans penis, are not spongy or cellular, but made up of a plexus of veins. This structure is discernable in the human subject; but much more distinctly seen in many animals, as the horse, &c.

Accordingly, other authors, including Georges Cuvier (1769-1832), Friedrich Tiedemann (1781-1861), Bartolomeo Panizza (1785-1867), and Ernst Heinrich Weber (1795-1878), also recognized the vascular nature of the cavernous tissue in man and other animals (Todd, 1839). In particular, Pierre Augustin Bécларd (1785-1825) provided the following definition of the erectile tissue in his *Éléments d'anatomie générale, ou Description de tous les genres d'organes qui composent le corps humain*, published posthumously in 1828 (Bécларd, 1828, p. 172):

Le tissu érectile, caveux ou spongieux, consiste en des terminaisons de vaisseaux sanguins, en des racines de veines surtout, qui, au heu d'avoir la ténuité capillaire, ont plus d'ampleur, sont très-extensibles, et réunies à beaucoup de filets nerveux.

The earliest and most commonly used anatomical technique was to obtain the turbulence of the cavernous bodies of the penis and urethra by pushing the waxy material for a random hole in the cavernous body of the urethra in the bulb region, or in the root of the cavernous bodies of the penis. In fact, examining the anatomical preparations included in the *Index Rerum Musei Anatomici Ticinensis*, published in 1804 by Antonio Scarpa (1752-1832), the preparations number 129, 134, 311 and, in particular, the number 130 realized by Giacomo Rezia (1745-1825), obtained with the procedure just described, clearly demonstrated the superficial vascular network of the cavernous body of the urethra (Levi, 1835).

In the beginning of the 19th century, when both vascular and cellular texture theories concerning the penile anatomy were still coexisting, a particular attention was paid to the urethral structure. Two figures contributed to the understanding of the vascular nature of the urethra. In the *Elogio del celebre anatomico Paolo Mascagni*, Farnese (1816) attributed to his mentor Mascagni (1755-1815) the demonstration in 1809 of the continuity between arteries and veins and the description of venous plexuses, this term replacing the previous and misled-

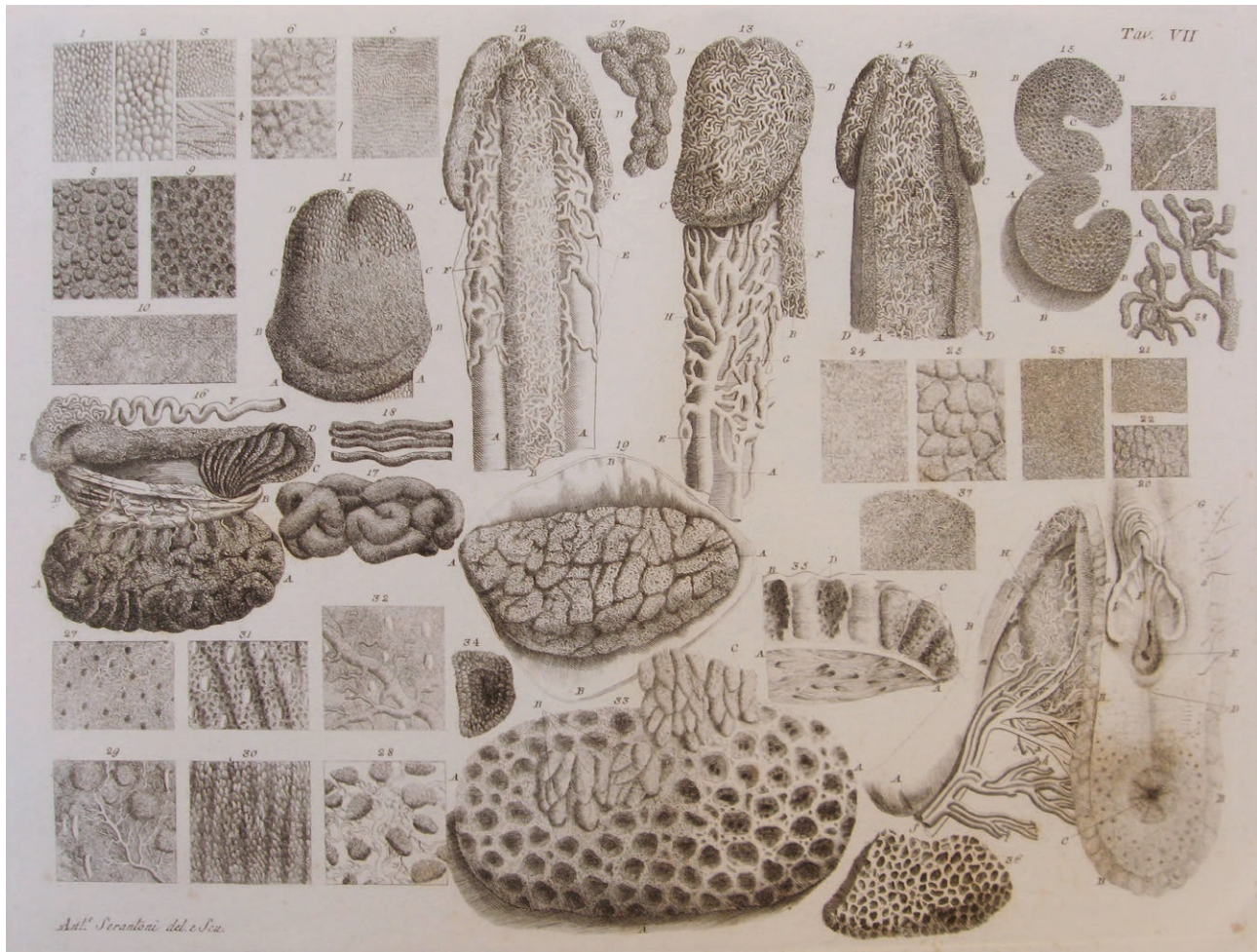


Figure 2. Plate VII, taken from *Tavole figurate di alcune parti organiche del corpo umano, degli animali e dei vegetabili, esposte nel Prodomo della grande anatomia di Paolo Mascagni* by Francesco Antommarchi (1819b). Library of Medicine and Pharmacy, University of Pisa.

ing name of spongy body attributed to the inner part of penis. In 1817 Alessandro Moreschi (1771-1826) also published two important works on the same subject (Moreschi, 1817a; 1817b) and a dispute also arose. A detailed description of the dynamics of this scientific controversy has been recently published (Armocida and Natale, 2019). The *Prodromo della grande anatomia*, a posthumous work by Mascagni edited in 1819, included a plate dedicated to the structure of the urethra (Fig. 2) and a comprehensive view of this scientific story (Antommarchi, 1819a; 1819b). Then, Mascagni developed a technique to inject urethral blood vessels, but Moreschi was the first to publish an accurate work on this subject.

In *Medico-Chirurgical Transactions* the demonstrator of anatomy John Shaw (1792-1827) published *On the structure of the membranous part of the urethra*, where he stated that Italian anatomists did not extend their

observations to the membranous part of the urethra (Shaw, 1819). For this reason, he considered himself the first to demonstrate the vascular structure of this tract of the urethra, as also affirmed in *A manual for the Student of Anatomy* (Shaw, 1825, p. 76):

There is, likewise, a set of vessels immediately below the membrane, which, when empty, are very similar in appearance to muscular fibres. I have discovered that these vessels form an internal spongy body, which passes down to the membranous part of the urethra, and forms even a small bulb there.

In *Additions to the general anatomy of Xavier Bichat*, when dealing with erectile texture, Béclard (1823, p. 118) stated that its vascular nature was recognized by several anatomists, including the Italian ones:

In our time Mess. Cuvier, Ribes and others in France, Mascagni, Paul Farnese and Moreschi in Italy, and Tiedmann in Germany have perfectly demonstrated this fact, both in man and various other animals.

Some years later, the anatomist and physiologist Johannes Peter Müller (1801-1858) anticipated in his *Handbuch der Physiologie des Menschen für Vorlesungen* (Müller, 1833) a very detailed study with eight magnificent illustrations on the vascular arrangement of erectile tissues, published in 1835 in the second number of *Archiv für Anatomie, Physiologie und wissenschaftliche Medicin*, directed by himself: *Entdeckung der bei der Erektion des männlichen Gliedes wirksamen Arterien bei dem Menschen und den Thieren* (Müller, 1835a). The study included the description of the deep artery of penis and, besides nutrient ramified arteries, a second set of tendril-like branches, named *arteriae helicinae*, demonstrated with an injection technique. An English translation of Müller's work summary appeared in different journals (Müller, 1835b,c,d; 1836). A Müller's lecture dealing with the innervation of erectile tissues was also published (Müller, 1837): *Über die organischen Nerven der erectilen männlichen Geschlechtsorgane*. The famous French physiologist Flourens (1835) also dedicated a short work to the history of vascular structure of the penis, where he praised Müller's findings.

In the second edition of his *Elements*, Craigie (1851) included also Müller's observations and proposed a hemodynamic role for the vascular structure of erectile tissues:

It seems not doubtful that the accumulation of blood in these helicine arteries is the physiological cause of the phenomena of erection. [...] In the tissue now described it is manifest that the physiologist ought to place the phenomena of the process distinguished by the name of vital turgescence (turgor vitalis) by Hebenstreit, Reil, Ackermann, and Schlosser. Though these authors suppose vital turgescence in different degrees in almost all the textures of the animal body, their most distinct examples are taken from those parts which consist of erectile vessels.

Finally, Victor Vecki von Gyurkovechky (1857-1938) in his *Pathologie und Therapie der Männlichen Impotenz* reported the vascular nature of the cavernous spaces, as histologically demonstrated by the presence of endothelium (Vecki, 1899, English edition, p. 51): *These small hollow interspaces of the three corpora are coated with endothelium resembling that of the veins, and are consequently venous spaces.*

REFERENCES

- Antommarchi F. (1819a) Prodrómo della grande anatomia. Seconda opera postuma di Paolo Mascagni, posta in ordine e pubblicata a spese di una società innominata da Francesco Antommarchi, dissettore anatomico nell'Imp. e R. Arcispedale di S.M.N. e socio di varie Accademie. Dalla tipografia di Giovanni Marenigh, Firenze.
- Antommarchi F. (1819b) Tavole figurate di alcune parti organiche del corpo umano, degli animali e dei vegetabili, esposte nel Prodrómo della grande anatomia di Paolo Mascagni. Presso Giovanni Marenigh, Firenze.
- Armocida E., Natale G. (2019) Paolo Mascagni and Alessandro Moreschi: who discovered the vascular structure of urethra? Anatomy of an intellectual property dispute. *Medicina Historica* 3(3): 170-180.
- Béclard P.A. (1823) Additions to the general anatomy of Xavier Bichat. Translated from French by George Hayward. Richardson and Lord, Boston.
- Béclard P.A. (1828) *Éléments d'anatomie générale, ou Description de tous les genres d'organes qui composent le corps humain*. Chez C.J. de Mat et H. Remy, Bruxelles.
- Cowper W. (1703) An answer to Dr Wright's Letter, concerning the Cure of an Aposthumation of the Lungs. *Philos. Trans. R. Soc. Lond.* 23(285): 1386-1393.
- Craigie D. (1851) *Elements of General and Pathological Anatomy*, presenting a view of the present state of knowledge in these branches of science. Lindsay and Blakiston, Philadelphia.
- Driel M.F. van (2015) Physiology of Penile Erection – A Brief History of the Scientific Understanding up till the Eighties of the 20th Century. *Sex. Med.* 3: 349-357.
- Farnese T. (1816) *Elogio del celebre anatomico Paolo Mascagni toscano*. Coi Tipi di Gio. Giuseppe Destefanis, Milano.
- Flourens M.J.P. (1835) Lectures on human embryology. Lecture V. The penis in man. *The Lancet* 7(618): 433-437.
- Haller A. von (1765) *Elementa physiologiae corporis humani*. Vol. seven, book XXVII. Apud Cornelium Haak, Lugduni Batavorum.
- Harvey W. (1628) *Exercitatio anatomica de motu cordis et sanguinis in animalibus*. Sumptibus Guilielmi Fitzeri, Francofurti.
- Hunter J. (1792) *Observations on certain parts of the animal oeconomy*. 2nd Ed. Printed and sold at no. 13, Castle-Street, Leicester-Square; and by Mr. G. Nichol, Pall-Mall; and Mr. J. Johnson, St. Paul's Church-Yard, London.

- Lenzi P., Bocci G., Natale G. (2016) John Hunter and the origin of the term “angiogenesis”. *Angiogenesis* 19: 255-256.
- Levi M.G. (translator) (1835) *Dizionario classico di medicina interna ed esterna*. Tomo 20. Giuseppe Antonelli Editore, Venezia. Pp. 460-470.
- Malpighi M. (1661) *De pulmonibus observationes anatomicae*. Bononiae.
- Malpighi M. (1687) *Opera omnia*. Apud Petrum Vander Lugduni Batavorum.
- Moreschi A. (1817a) Cenni preliminari intorno alla scoperta della struttura vascolare del corpo dell'uretra e della ghianda creduta sin qui spugnosa o cellulosa ed osservazioni sull'Elogio del cel. Anatomico Paolo Mascagni, divulgato dal sig. Tommaso Farnese, Dottore in Medicina e Chirurgia, ecc. Presso A.F. Stella, Milano.
- Moreschi A. (1817b) *Commentarium de urethrae corporis glandisque structura: VI. idus Decembris ann. M.DCCC.X. detecta ab I.R. Scientiarum, Literarum Artiumque Instituto approbatum. Accedunt de vasorum splenicorum in animalibus constitutione nec non de utero gravido epitomae. Ex Typographia Joannis Pirottae, Mediolani*.
- Müller J. (1833) *Handbuch der Physiologie des Menschen für Vorlesungen*. J. Hölscher, Koblenz.
- Müller J. (1835a) Entdeckung der bei der Erektion des männlichen Gliedes wirksamen Arterien bei dem Menschen und den Thieren. *Archiv für Anatomie, Physiologie und Wissenschaftliche Medicin* 202-213.
- Müller J. (1835b) Newly discovered arrangement of the Arteries in the Erectile Tissue of the Penis. *The London Medical and Surgical Journal* 7(180): 753-754.
- Müller J. (1835c) Newly discovered arrangement of the Arteries in the Erectile Tissue of the Penis. *The Edinburgh Medical and Surgical Journal* 44: 243-244.
- Müller J. (1835d) Newly discovered arrangement of the Arteries in the Erectile Tissue of the Penis. *The American Journal of the Medical Sciences* 17: 179-181.
- Müller J. (1836) The discovery of the arteries producing erection of the penis in man and other animals. *The London Medical Gazette* 17: 566-71.
- Müller J. (1837) Über die organischen Nerven der erectilen männlichen Geschlechtsorgane des Menschen und der Säugethiere. Gelesen in der Königlichen Akademie der Wissenschaften zu Berlin im Jahre 1835. In: *Abhandlungen der Königlichen Akademie der Wissenschaften zu Berlin*. Druckerei der Königlichen Akademie der Wissenschaften, Berlin. Pp. 93-140.
- Natale G., Bocci G., Lenzi P. (2017) Looking for the Word “Angiogenesis” in the History of Health Sciences: From Ancient Times to the First Decades of the Twentieth Century. *World J. Surg.* 41: 1625-1634.
- Shaw J. (1819) On the structure of the membranous part of the urethra. *Medico-Chirurgical Transactions* 10(part II, XXIII): 339-357.
- Shaw J. (1825) *A Manual for the Student of Anatomy; Containing Rules for Displaying the Structure of the Body, so as to Exhibit the Elementary Views of Anatomy, and Their Application to Pathology and Surgery*. J. Disturnell, Troy.
- Todd R.B. (editor) (1839) *The cyclopaedia of anatomy and physiology*. Vol. 2. Longman, Brown, Green, Longmans, & Roberts, London. Pp. 144-147.
- Vecki V.G. *The pathology and treatment of sexual impotence*. From the author's second German edition, revised and rewritten. WB Saunders, Philadelphia, 1899.
- Vesalius A. (2007) *De Humani corporis fabrica. On the Fabric of the Human Body. A translation of De Humani Corporis Fabrica Libri Septem. Book V. The Organs of Nutrition and Generation*. Edited by William Frank Richardson and John Burd Carman. Norman Publishing Novato, California.



Citation: Rita M. Serra, Paolo Melis, Andrea Montella, Pasquale Bandiera (2022) Bioarcheological and paleopathological study of a multiple deposition burial from S. Antine- Genoni (SU) – Sardegna - Italy. *Italian Journal of Anatomy and Embryology* 126(2): 9-16. doi: 10.36253/ijae-13842

Copyright: © 2022 Rita M. Serra, Paolo Melis, Andrea Montella, Pasquale Bandiera. This is an open access, peer-reviewed article published by Firenze University Press (<http://www.fupress.com/ijae>) and distributed under the terms of the Creative Commons Attribution License, which permits unrestricted use, distribution, and reproduction in any medium, provided the original author and source are credited.

Data Availability Statement: All relevant data are within the paper and its Supporting Information files.

Competing Interests: The Author(s) declare(s) no conflict of interest.

ORCID

AM: 0000-0002-5514-4453
PB: 0000-0002-0589-4539

Bioarcheological and paleopathological study of a multiple deposition burial from S. Antine-Genoni (SU) – Sardegna - Italy

RITA M. SERRA^{1,2}, PAOLO MELIS³, ANDREA MONTELLA^{1,2}, PASQUALE BANDIERA^{1,2,*}

¹ Department of Biomedical Sciences, University of Sassari, Italy

² Center for Anthropological, Paleopathological and Historical Studies of the Sardinian and Mediterranean populations, Department of Biomedical Sciences, University of Sassari, Italy

³ Department of History, Human Sciences and Education, University of Sassari, Italy

*Corresponding author. E-mail: bandiera@uniss.it

Abstract. A multiple deposition burial in a lithic coffin was found on a hill located in the Campidano valley, in Central South Sardinia (Italy). The site was used from 1800 BC to 500 AD, the burial seems to be dated to the Roman age (238 BC-470AD). A total of 98 human bones and 3 human teeth were present. Anthropological and paleopathological analyses were made. The biological profile was defined with standard anthropological methodologies. The anthropological analysis. A large part of the bones can be referred to as an adult male. Most of the bones display the presence of pathologies, in most cases osteophytosis, the correlation of the same pathologies in contiguous bones indicate that they may belong to the same individual. Very interesting is a possible blade injury in the lateral epicondyle of the right male humerus and a plausible pertrochanteric fracture. The presence, in the same coffin, of a small number of individuals, with the presence of one subadult, can't completely exclude that they were members of the same family group. More analyses will be necessary to better understand the context.

Keywords: Sardinia, anthropology, paleopathology, blade injury.

INTRODUCTION

Sardinia is an island located in the middle of the Mediterranean Sea. Its history started with local people's civilization: two different phases named "Pre-Nuragic" (450.000-1.800 BC) and "Nuragic" (1.800-238 BC) ages (Lilliu G. 2004). Nuragic age gets its name from a truncated cone megalithic structure called "Nuraghe", present all over the island.

From 800 BC, there were many dominions in Sardinia, perhaps due to its position in the middle of the most important trade routes of the past. These dominions were present mostly near the coast, while the middle of the island was interested in the survival of the previous domination.

Phoenicians and Punics (Bartoloni P. et al 1997), and Roman (Angiolillo S. et al 2017), mentioning some of them, settled their village along the Sardinian coast, at the beginning; just later their presence is evidenced also in inland. Historical changes in Sardinia have influenced the native population and civilization and marked the history of the island. A recent study (Marcus J.H. et al 2020) has investigated the genetic history of the island, underling the introduction of new genetic inheritance and the survival of the local population at the same time. Many studies have concerned humans remain in all ages all over the island, evidencing life-style, feed, occupational markers, origin, and migration.

The anthropological study provides a better understanding of the evolution and changes of Sardinian civilization. The southern region characterized by the Campidano valley was interested in a more significant presence of eastern dominance than the northern part. That part of the island has, at the present time, a lack of studies and information.

MATERIALS AND METHODS

The site of Genoni is located on a hill, in the Campidano valley, in the middle of Sardinia. The area was used from the Nuragic Age (1800-238 BC) to the Punic (470-238BC) and the Roman Age (238 BC-470 AD), evidenced by the presence of many Nuragic and Roman structures.

One of these structures was a lithic coffin that contained human remains from different people. To understand the real use of the site we decided to study the biological profile of these people, using the main standard anthropological methodologies (Ubelaker D.H. 1989; Perrot R. 2012), supported by newer methodologies when it has been necessary (Catteneo C. et al 2004).

Sex was determined using morphologic methodologies (Açsadi C.Y, Nemeskéri J. 1970; Phenice T.W. 1969).

To determine the age of death we use standard methodologies (Iscan M.Y. 1984, Lovejoy C.O et al 1985; Meindel R.S., Lovejoy C.O. 1985, Brooks S., Suckey J.M. 1990), also considering the new evaluation of methodology (Verzeletti et al 2010; Russel K.F. et al 1993).

Estimation of stature was based on the Trotter and Glaser methodology (Trotter M., Gleser G.C. 1952) which considered the maximum length of the bone.

To better understand pathological conditions, markers of occupational stress (Henderson C.Y. et al 2013, Mariotti V. et al 2007) and state of health (Fornaciari G., Giuffra V. 2009; Ortner D.J et al 1985) have been studied. All the analyses were done in the paleoanthropology

laboratory of the Department of Biomedical Sciences at the University of Sassari.

Pathological conditions are assessed according to traditional classification and divided into bones and anatomical regions. Markers of occupational stress were also considered in the same bones.

RESULTS AND DISCUSSION

We have analyzed an amount of 98 human bones (complete and fragmented) and 3 teeth (Table 1). Most of them are vertebrae and ribs (an amount of 57), and among the other bones, the most present is the right femur (3) and the left pelvis (3).

Starting from the total number of bones, only one person could be present; but they are not only the adult's bones, considering that the minimum number of individuals became two. But to understand the number of individuals it is necessary to consider the biological profile, which was calculated for each bone.

Biological profile

Table 2 presented the division of bones among sex after anthropological analysis.

- Three individuals are computed from the pelvis: one adult male, one adult female and one sub-adult.
- Three individuals of the right femur: 2 adult males and 1 subadult.
- Two individuals occur from most other bones, generally two adults or one adult and one subadult.

To summarize, the anthropological analysis of each bone shows a minimum number of 4 individuals: 2 adult males, 1 adult female and 1 subadult.

For determining the age of death, we used the same methodology. The estimation displayed homogeneity in the distribution; the most diagnostic, as usual, is the pelvis.

Table 3 shows the age range of death for each bone, taking into account their gender determination.

Most of the bones showed an age range "older than", sharper data from ribs. They are referred to two sex indeterminate individuals in the age range of 24/35 Y (YA) and 40/50Y (OA), and a female individual of more than 30Y (MA). Another diagnostic data comes from the pelvic bone of three individuals: a male of 50/59Y (OA), an indeterminate adult of 35/45Y (MA) and a subadult of 4/7Y (INF).

Crossing results of age and sex determination, and considering the minimum number of individuals estimated, apparently present a totality of 4 individuals:

Table 1. Bones present with the number of them. Note: Tooth (FDI number of tooth present); vertebra (C=cervical; T=thoracic; L=lumbar); bones (R=Right; L=Left).

Bone	Com(plete)/fr(agmentary)	Nr	Note
skull	fr	1	
tooth	com	3	36;37;46
vertebra	com	31	10C;16T;5L
rib	fr	26	10R; 16L;
clavicula	fr	5	3L;2R
sternum	fr	1	
scapula	fr	2	2L
humerus	com/fr	3	1R; 2L
radius	com	1	1L
ulna	fr	3	2L;1R
hand	fr	4	2 1st metacarpal R; 1 proximal phalanges R; 1 2nd metacarpal L
pelvis	fr	3	2 ilium L; 1 acetabulum L
sacrum	fr	2	
femur	com/fr	6	3 com R; 1 com L; 2 fr L
tibia	fr	5	4 L; 1 R
fibula	fr	1	1R
foot	fr	4	1 talus R; 1 talus L; 1 calcaneus L; 1 2nd metatarsal L

Table 2. Division of bones among sex. (M=male; F=female; I=indeterminate; SubAd=Sub-adult; TOT=total).

Anatomical regions	M	F	I	SubAd	TOT
skull			1		1
teeth			1	1	2
vertebrae			2		2
ribs			2		2
clavicle	1	1			2
scapula	1	1			2
humerus	1	1			2
radius	1				1
ulna	1		1		2
hand			2		2
pelvis	1	1		1	3
sacrum	1		1		2
femur	2			1	3
tibia	1		1		2
fibula			1		1
talus	1	1			2
calcaneus			1		1
II metatarsal			1		1
TOT	2	1	2	1	

Table 3. Age range of death for each bone. (M=male; F=female; I=indeterminate; SubAd=Sub-adult).

Anatomical regions	M	F	I	SubAd
skull				
teeth				7/8y
vertebrae			>18	
ribs			24/32y; 40/50y	
clavicle	>30y	>30yy		
scapula	>22y	>22y		
humerus	>21y	>21y		
radius	>18y			
ulna	>18y		>18y	
hand			>16y	
pelvis	50/59y		35/45y	3/5y
sacrum	>25y		>25y	
femur	>21y			5/7 y
tibia	>21y		>21y	
fibula			>21y	
talus				
calcaneus			>21y	
II metatarsal			>18y	

- Two adult males, the former in the range of young adults (YA) aged between 25 and 35 years, the latter in the range of middle adults (MA) aged between 35 and 45 years.
- One adult female, in the age range of old adult (OA) aged older than 46 years.
- One subadult aged between 5 and 8 years.

The poor conservation of most bones consented to the stim of stature only in five of them (Table 4).

In three cases the individual was a male, and the stature estimated was 164m, 165cm and 158 cm. Is evident a difference between the average of the the first two compared to the last, but it is also important to remember that there are two adult males individuals.

One stature estimation is referred to as a sub-adult, with a height of 107 cm.

The last estimation, 165cm, comes from a talus of sex-undetermined individuals.

Pathologies

A high percentage of bones show pathological conditions: in a total of 98, 36 (37%) of them were pathologic, all of them related to adult individuals (Figure 1)

More than 80% of the observed pathologies were osteophytosis:

Table 4. Stim of stature in cases where complete bones were present, standardized to Trotter e Gleser method.(m=adult male; I=adult indeterminated; inf= subadult; R=right side; L=left side).

Sex	m	m	m	inf	I
Bone	humerus	radius	femur	femur	talus
Com(plete)/ Fr(agmentary)	com	com	com	fr	com
R/L	R	L	R	R	L
Stature (Trotter & Gleser)	165,314	164,06	158,752	107,344	165,21

- 20 of the 31 vertebrae (5 cervical; 10 thoracic, 3 lumbar, 1 sacral);
- 7 ribs of the 26 (6 from left and 1 from right side);
- 3 clavicles of the 4 (1 from the right; 2 from the left);
- 2 humeri from 3 (1 from the right;1 from the left);
- 2 ulnae from the 3 (from the left);
- 2 femora from 6 (1 from the right 1 from the left).

Considering the bones in which pathologies are present (Table 5), with the presence of two left ulnas and two left clavicles, at least two adults are present but

is also true that many of them are ascribable to a male individual.

Very interesting pathological signs occur in the right and left male humerus

The left (Figure 2b; 2d) and right (Figure 2a; 2c) humerus exhibit an abnormal evolution of the distal epiphysis. The lateral epicondyle appears smoother as usual, with the presence of osteophyte lips at the posterior margin.

This abnormality is localized at the origin of the anconeus muscle, an extensor muscle of the forearm inserted in the proximal dorsal epiphysis of the ulna (Figure 2e).

Unfortunately, we have a few presences of forearm bone probably related; only a left proximal ulna, where marked osteophytosis is present.

Another interesting situation is present in the same right humerus. The medial epicondyle of the distal epiphysis has an irregular shape, with an anterior deep groove. Considering the development of new formation bone on the medial edge of the groove, we suppose a traumatic lesion.



Figure 1. Pathologic bones from the burial.

Table 5. Bones with pathological condition with an indication of the type of pathology and location. (R=right side; L=left side; I=adult indeterminate; M=adult male; F=adult female).

Bone	Com(plete)/ fr(agmentary)	R/L	Sex	Pathology
Cervical Vertebra	com		I	Osteophytes vertebral body
Cervical Vertebra	com		I	Diffuse osteophytes
Cervical Vertebra	com		I	Osteophytosis right vertebral body and Right inferior rib facet
Cervical Vertebra	com		I	Diffuse osteophytes
Cervical Vertebra	com		I	Osteophytosis superior left facet and inferior body
Thoracic Vertebra	com		I	Osteophytosis spinous process and anterior left facet
Thoracic Vertebra	com		I	Osteophytosis inferior rib facet and transverse process
Thoracic Vertebra	com		I	Osteophytosis transverse process
Thoracic Vertebra	com		I	Osteophytosis spinous process and vertebral body
Thoracic Vertebra	com		I	Osteophytosis rib facets
Thoracic Vertebra	com		I	Osteophytosis of vertebral foramen
Thoracic Vertebra	com		I	Osteophytosis spinous process
Thoracic Vertebra	com		I	Osteophytosis spinous process and left rib facet
Thoracic Vertebra	com		I	Osteophytosis inferior body
Thoracic Vertebra	com		I	Osteophytes vertebral foramen and hernia in inferior body
Lumbar Vertebra	com		I	Hernia in the inferior body facet
Lumbar Vertebra	com		I	Hernia in the inferior body
Lumbar Vertebra	com		I	Osteophytosis in inferior body and left rib facet, Hernia in superior body
Rib body	fr	L	I	Osteophytosis. tubercle
Rib body/head	fr	L	I	Osteophytosis superior body
Rib body/sternal	fr	L	I	Osteophytosis sternal end
Rib body/head	fr	L	I	Osteophytosis tubercle
Rib body/head	fr	L	I	Osteophytosis tubercle
Rib body	fr	L	I	Osteophytosis tubercle
Rib body/head	fr	R	I	Osteophytosis tubercle
Sternum	fr		I	Ossification of right costal cartilage manubrium
Clavicula	com	L	I	Osteophytosis sternal facets
Clavicula	fr	R	I	Osteophytosis and macroporosity sternal end
Clavicula	fr	L	I	Osteolysis acromial end
Humerus	com	R	M	Abnormal shape in medial epicondyle with osteophytosis; groove probably by a blade in lateral epicondyle;
Humerus	fr	L	M	Abnormal development in medial epicondyle
Ulna	fr	R	M	Pronounced osteophytosis in styloid process
Ulna	fr	L	I	Osteophytosis olecranon
Pelvis	fr	L	F	Neoplasm bone in anterior superior iliac spine and acetabular rim
Sacrum	fr		I	Lumbarization S1
Femur	com	R	M	Osteophytosis in superior articular surface; new formation bone in greater trochanter and transverse acetabular ligament; shape modification and osteophytosis on the top of linea aspera (pertrochanteric fracture?)
Femur	com	L	M	Shape modification and osteophytosis on the top of linea aspera

To study the depth, width, direction and the possible presence of signs, a mould of the groove was made (Figure 3). The analysis of the shape reveals a thinner groove in the deepest part, with a linear pattern and a surface characterized by the presence of parallel lines with an oblique angle, currently, a blade cannot be completely excluded.

Very interesting also, a pathological situation of the right femur (Figure 4). Located in the proximal diaphysis, in the sub-trochanteric position, evident mainly in the anterior (Figure 4b) and cranial (Figure 4c) face of the great trochanter. The shape and location of the lesion can be identified with the consequence of a pertrochanteric fracture.

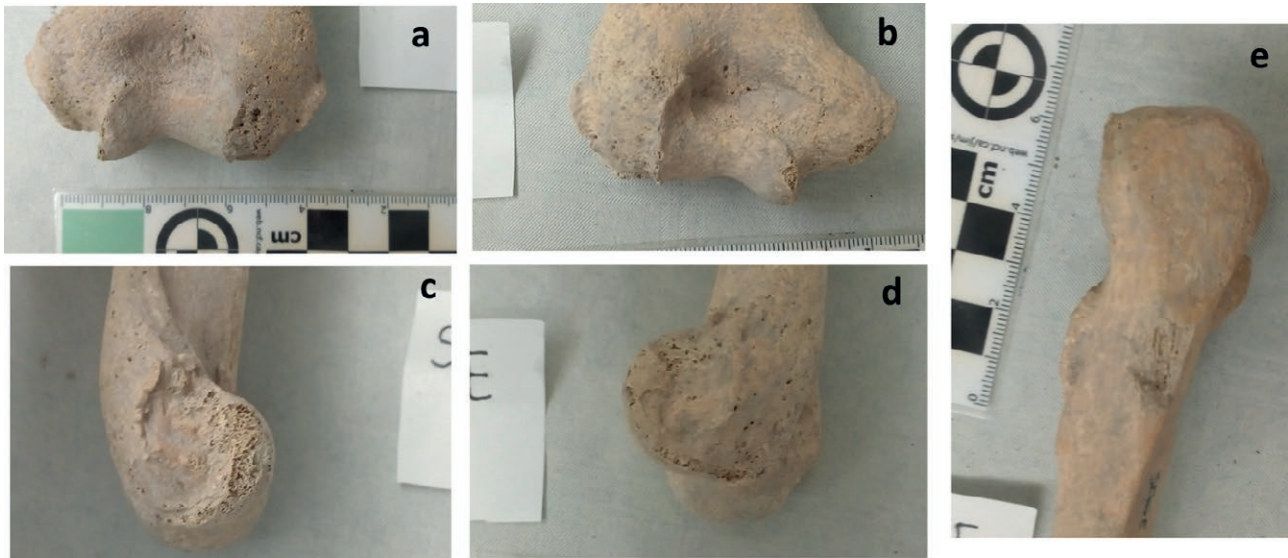


Figure 2. Pathological condition in forearm bones. (a= right humerus- anterior view of distal epiphysis; b= left humerus- anterior view of distal epiphysis; c= right humerus- medial view of distal epiphysis; d= left humerus- medial view of distal epiphysis; e= left ulna-dorsal view of proximal epiphysis).



Figure 3. Mould of the groove in the medial epicondyle of the right humerus.

Some pathologies found in contiguous bones suggest that these modifications may be related to each other. In addition, the general appearance is similar, and they can be attributed to an adult male (as mentioned before) and it is not completely excluded that they could be conferred to the same person.

For this reason, we have decided to consider markers of occupational stress (MOS) in these bones, as well.

Markers of Occupational Stress (MOS)

Analyzing MOS we have noticed the correspondence between lesions and more marked markers (Table 6).

We can see, indeed, in the upper limbs that a robusticity of 3 degrees is present in the right clavicle (Costoclavicular ligament) and distal right humerus (Brachioradialis muscle); high degree also at the insertion of the Deltoides muscle in both humeri. All of these insertions are in the same locations as the lesion mentioned above.

In the lower limbs, we can see a higher degree of MOS in the right femur, corresponding to the Gluteus maximus muscle, where the possible fracture is present. The left side still has a high value, but not as high as the right side.

CONCLUSION

The multiple burials that we analyzed are an interesting case study, because of their composition. Of a total of four individuals, only one may be considered nearly complete.

Very interesting the pathologies present in 37% of the bones. These pathologies are, in most cases, ascribed to male individuals and it is possible that can be attributed to the same person. Considering this possibility, we can analyze the number of pathologies to understand possible relationships between them. A right humerus presents a possible blade injury at the medial epicondyle and this lesion can be related to the strong osteophytosis and macroporosity in the sternal epiphysis of the right clavicle and the pronounced osteophytosis in the styloid process of the right ulna. Moreover, MOS in

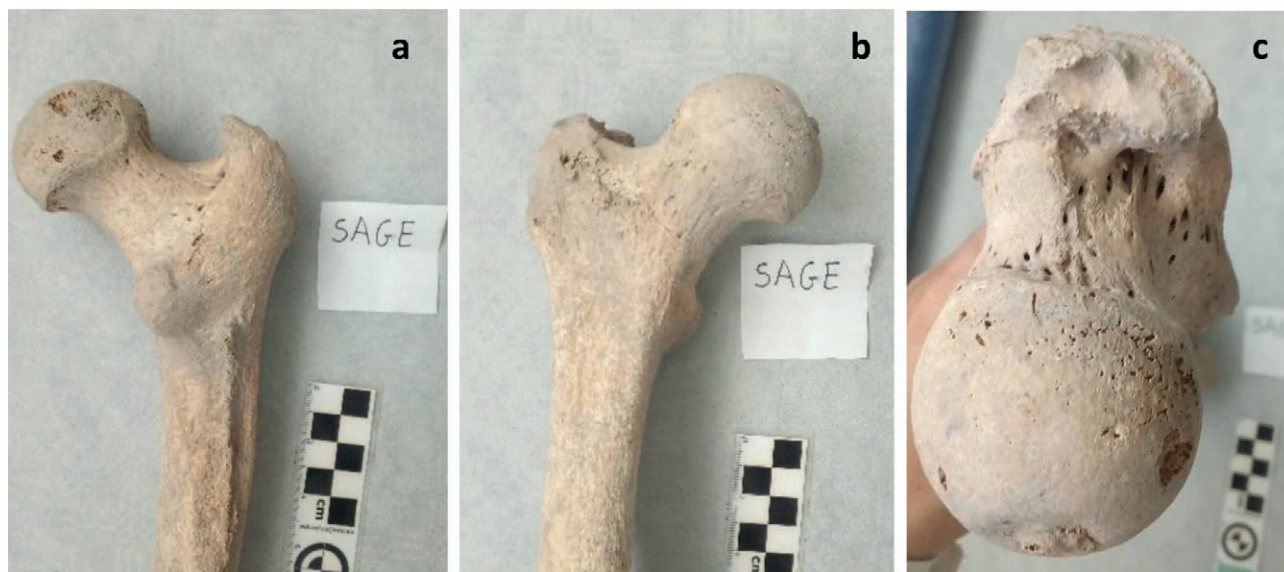


Figure 4. Lesion observed in the proximal epiphysis of the right femur. (a= posterior view; b= anterior view; c=cranial view).

the same bones is very high. Perhaps the movement of the right humerus may have been modified and difficult, with consequences on the whole joint.

Another interesting condition is on the femur. Here is present a lesion that interests the proximal epiphysis, maybe a perthocantheric fracture, resulting in a wrong walk which may have created the osteophytosis and the shape modification at the top of linea aspera of the left femur.

One more aspect of interest is the composition of the individuals in the burial. There are two adult males, one is a middle/old adult, and another one is a young adult. Furthermore is present a young adult female and one subadult (a child). Considering all these aspects, a family burial can't be completely excluded, but an additional genetic study should be done to better understand this aspect.

ACKNOWLEDGEMENT

Supported by the "Fondo di Ateneo per la Ricerca 2019-2020".

REFERENCES

- Açsàdi C.Y., Nemeskéri J. (1970) History of human lifespan and mortality. Akadémiai Kiadó, Budapest.
- Angiolillo S., Martorelli R., Giuman M., Corda A.M., Artizzu D. (2017) La Sardegna romana e altomedievale - storia e materiali. Carlo Delfino Editore, Sassari.
- Bartoloni P., Bondi S.F., Moscati S. (1997) La penetrazione fenicia e punica in Sardegna. Trent'anni dopo. Accademia Naz. dei Lincei, Roma.
- Brooks S., Suckey J.M. (1990) Skeletal age determination based on os pubis: a comparison on Açsàdi-Nemeskéri and Suckey-Brooks methods. *Hum Evol* 5 (3): 227-238.
- Cattaneo C., Grandi M. (2004) Antropologia ed odontologia forense – guida allo studio dei resti umani. Monduzzi editore, Bologna.
- Fornaciari G., Giuffra V. (2009) Lezioni di paleopatologia. ECIG, Genova.
- Henderson C.Y., Mariotti V., Pany-Kucera D., Villotte S., Wilczak C. (2013) Recording Specific Enthesal Changes of Fibrocartilaginous Enteses: Initial Tests Using the Coimbra Method. *International Journal of Osteoarchaeology* 23(2): 152-162.
- Iscan M.Y., Loth S.R., Wright R.K. (1984) Metamorphosis at the sternal rib end: a new method to estimate age of death in white males. *Americ J Phys Anthropol* 65: 147.
- Lilliu G. (2004) La civiltà dei sardi. Dal paleolitico all'età dei nuraghi. Ed il maestrale, Nuoro.
- Lovejoy C.O., Meindel R.S., Pryzbeck T.R., Mensforth R.P. (1985) Chronological metamorphosis of the auricular surface of the ilium: a new method for the determination of adult skeletal age of death. *Amer J Phys Anthropol* 68 (1): 15-28.
- Marcus J.H., Posth C., Ringbauer H., Lai L., Skeates R., Sidore C., Beckett J., Furtwängler A., Olivieri A., Chiang C.W.K., Al-Asadi H., Dey K., Joseph T.A.,

Table 6. Robusticity in Markers of occupational stress observed in pathologic male bones standardized to the Coimbra method protocol. (L=left side; R=right side).

Bone	Side	Male	
		L	R
Scapula	Triceps brachii m.		
	Costoclavicular lig.	1,5	3
	Conoid lig.	1,7	
Clavicle	Trapezoid lig	1,5	
	Pectoralis major m.	1,7	0
	Deltoideus m.	1,7	
	Pectoralis major m.		2
Humerus	latissimus dorsii/teres major mm		1,7
	Deltoideus m.	2	2
	Brachioradialis m.	1,7	3
	Biceps brachii m.		
Radius	Pronator teres m. membr.interossea		
	Triceps brachii m.	1,5	
Ulna	Brachioradialis m.	1,7	
	Supinator m.	1,3	
	Gluteus maximus m.	2	3
Femur	Ileopsoas m.		2
	Vastus medialis m.	1,7	1,5
Patella	Quadriceps tendon		
Tibia	Quadriceps tendon		
	Soleus m.		
Talus	Achilles tendon		
		1,66	2,02

Liu C., Der Sarkissian C., Radzevičiūtė R., Michel M., Gradoli M.G., Marongiu P., Rubino S., Mazzaello V., Rovina D., La Fragola A., Serra R.M., Bandiera P., Bianucci R., Pompianu E., Murgia C., Guirguis M., Pla Orquin R., Tuross N., van Dommelen P., Haak W., Reich D., Schlessinger D., Cucca F., Krause J., Novembre J. (2020) Genetic history from the Middle Neolithic to present on the Mediterranean island of Sardinia. *NATURE COMMUNICATIONS* | (2020) 11:939 | <https://doi.org/10.1038/s41467-020-14523-6> | www.nature.com/naturecommunications.

Mariotti V., Facchini F., Belcastro M.G. (2007) The Study of Enteses: Proposal of a Standardised Scoring Method for Twenty-Three Enteses of the Postcranial Skeleton. *Coll Antropol* 31(1): 291-313.

Meindl R.S., Lovejoy C.O. (1985) Ectocranial suture closure: a revised method for the determination of skel-

etal age at death based on the lateral anterior suture. *Amer J Phys Anthropol* 68(1): 57-66.

Ortner D.J., Putscar W.J. (1985) Identification of pathological condition in human skeletal remains. Academic press-elsevier, San Diego (CA).

Perrot R. (2012) *Precis d'anthropobiologie descriptive et métrique du squelette*. <http://www.laboratoireanthropologieanatomiqueetdepaleopathologie.delyon.fr/PRECIS%20D'ANTHROPOBIOLOGIE%20SOMMAIRE.htm>.

Phenice T.W. (1969) A newly developed visual method of sexing os pubis. *Amer J Phys Anthropol* 30(2): 297-301.

Russell K.F., Simpson S.W., Genovese J., Kinkel M.D., Meindl R.S., Lovejoy C.O. (1993). Independent test of the fourth rib aging technique. *Am J Phys Anthropol* 92(1): 53-62.

Trotter M., Gleser G.C. (1977) Corrigenda the estimation of stature from long bones of americans whites and negroes. *Americ J Phys Anthropol* 47(2): 335-6

Ubelaker D.H. (1989) *Human skeletal remains: Excavation, analysis, interpretation*. Taraxacum. Washington.

Verzeletti A., Cassina M., Micheli L., Conti A., De Ferrari F. (2010). Age estimation from the rib by components method analysis in white males. *Am J Forensic Med Pathol* 31(1): 27-33.



Citation: Jurand Domański, Marta Wanat, Jacek Ciach, Angelika Osuch, Bożena Kurc-Darak, Sławomir Woźniak, Zygmunt Domagała (2022) Off-line or on-line? – near-peer assisted anatomy education in the time of Covid-19 pandemic – a single center randomized controlled study. *Italian Journal of Anatomy and Embryology* 126(2): 17-24. doi: 10.36253/ijae-13877

Copyright: © 2022 Jurand Domański, Marta Wanat, Jacek Ciach, Angelika Osuch, Bożena Kurc-Darak, Sławomir Woźniak, Zygmunt Domagała. This is an open access, peer-reviewed article published by Firenze University Press (<http://www.fupress.com/ijae>) and distributed under the terms of the Creative Commons Attribution License, which permits unrestricted use, distribution, and reproduction in any medium, provided the original author and source are credited.

Data Availability Statement: All relevant data are within the paper and its Supporting Information files.

Competing Interests: The Author(s) declare(s) no conflict of interest.

ORCID

JD: 0000-0003-2416-8062
MW: 0000-0002-6471-3706
JC: 0000-0002-4219-1445
BK-D: 0000-0003-0491-622X
SW: 0000-0002-7450-7993
ZD: 0000-0002-2317-1932

Off-line or on-line? – near-peer assisted anatomy education in the time of Covid-19 pandemic – a single center randomized controlled study

JURAND DOMAŃSKI^{1,*}, MARTA WANAT², JACEK CIACH¹, ANGELIKA OSUCH², BOŻENA KURC-DARAK¹, SŁAWOMIR WOŹNIAK¹, ZYGMUNT DOMAGAŁA¹

¹ Division of Anatomy, Department of Human Morphology and Embryology, Wrocław Medical University, Faculty of Medicine, Wrocław, Poland

² Clinical and Dissecting Anatomy Students Scientific Club, Wrocław Medical University, Wrocław, Poland

*Corresponding author. E-mail: jurand.dom@gmail.com

Abstract. The COVID-19 pandemic significantly changed the way anatomy classes were carried out, depriving students of practical learning using real anatomical specimens. Once COVID restrictions were lifted and students returned to a normal class setting a randomized study was carried out to evaluate effectiveness of practical anatomy didactics. The aim of this study was to evaluate the impact of an anatomy workshop based on demonstrating anatomical structures delivered in a face-to-face format, and to compare it with a standard course based on online learning. The randomization involved 350 students from whom 80 participants were drawn to form both a study and control group. The study consisted of three parts: exam 1, workshop, exam 2. The study group participated in all parts of the project, while the control group participated only in the exam. The workshop was held by near peer teachers (NPT). Statistical analysis showed that participation in the workshop had an effect on the passing score of exam 2 ($p=0.039$). It was also shown that the difference in scores was significantly higher ($p=0.049$) in the study group compared to the control group. The study proved that the workshops which were based on demonstrating anatomical structures by NPT significantly affected the scores obtained by trainees. In conclusion, the project confirmed the importance of student interaction with anatomical specimens and that online teaching is not a substitute for teaching in a dissecting room. Additionally, this study confirmed the high usefulness of NPT as a support for the didactic process conducted by experts.

Keywords: anatomical education, medicine students, human specimen, teaching, Covid, PAL, near-peer teaching.

INTRODUCTION

The didactics of anatomy in Poland differs from other countries in the European Union [3, 4, 20] primarily because the academic teachers play

a dominant role in the learning process, but also the method of teaching is based on anatomical demonstrations. In Germany, teaching of anatomy relies on easily accessible cadavers from the national donation programs. Also important is the didactic activity carried out by medical students in upper years [11], providing young students with direct knowledge from soon-to-be specialists. Some colleges in the United Kingdom shifted the majority of their anatomy course to the post-graduate period, limiting the amount of anatomy classes in the pre-graduate studies. Similarly like in Germany, access to cadavers in the UK is quite easily available, often centralized in a single specialized location [17, 27]. As mentioned earlier teaching anatomy in Poland are structured around the dominance of the academic teacher and their methods of conducting classes as well as preparing specimens. The above mentioned along with the limited availability of cadavers results in practical anatomy classes which are more difficult to conduct [29]. A common solution is demonstrating anatomical structures on previously prepared anatomical specimens [2].

In many European countries as well as in numerous universities in the USA and Canada, a significant portion of the anatomy course consists of practical learning, dissections and preparation of whole cadavers. The theoretical part of classes is limited to an introductory seminar at the beginning of the course [28].

It is worth mentioning that senior medical students play a significant role in these countries, directly influencing the learning process. By taking part in anatomy classes, they generate psychological support for junior colleagues and develop essential teaching skills [12, 26].

In scientific nomenclature, this kind of student teaching is defined as peer-assisted learning [32]. Student-teachers may be peer teachers of students (co-peer teachers) or they may be senior year students - near-peer teachers (NPT) [22].

This is a relatively popular form of education in many countries and it is worth noting that in Germany a near-peer-educator receives a small salary and is employed as a student assistant (personal communication with prof. Lars Brauer, FAU University, Erlangen, Germany).

This type of solution greatly relieves the workload of the staff, who can focus on the individual needs of each student during classes or devote more time towards scientific and organizational activities. Furthermore, near-peer teachers are a necessity due to the shortage of trained and experienced anatomy teachers.

Peer assisted learning has not been implemented in Poland as an educational tool due to legal as well as

financial limitations. Students are not recognized by the legislator as academic teachers, so their employment in such a position is impossible. Such decisions are the result of high expectations for academic lecturers in Poland [31].

The system in German universities proves that even when the dominant role is carried out by the academic teacher, there is still room for peer assisted education. It should be emphasized that the Covid 19 pandemic in Poland made access to anatomical preparations significantly more difficult. In many Polish medical universities, as well as in parts of Europe, dissection classes have been abandoned and replaced with online teaching. Depending on the financial status of the university, in-person classes were substituted by short films showing the stages of anatomical dissections/demonstrations and commercially available 3D solutions such as 3D atlases or 3D films of idealized dissections [13, 24, 37]. Upon return to the dissecting room, halfway through the previous academic year, a project was carried out, evaluating the effectiveness of teaching anatomy using real anatomical specimens. In addition, due to NPT-based didactics demonstrated in the global literature [9, 22], it was decided that the students' first exposure to human cadavers should be carried out in a student-friendly atmosphere in order to minimize any stress and simultaneously increase the sensitivity of the study and improve its quality.

The aim of this study was to evaluate the effectiveness of anatomy workshops based on demonstrating anatomical structures using real human specimens, conducted face-to-face, and compare this to a standard course conducted online using available 3D atlases and online presentations and visualizations.

MATERIAL AND METHODS

All (350 individuals, including 230 females and 120 males) 1st year students of the Faculty of Medicine from the year 2020/2021 were invited to participate in the study. 80 study participants in the age range 19-21 years were selected based on randomization techniques (40 participants were qualified to the control group and 40 participants were qualified to the study group). Randomisation was conducted using the computer program - "R" package, version 4.1.2 (The R Foundation for Statistical Computing, Vienna, Austria). The system numerically selected participants from a group of volunteers who volunteered for the project based on their album number. This guaranteed anonymity and randomness of qualification.



Figure 1. Flow chart of conducting the research project.

During the study, 21 people resigned from both groups (20 people in the control group and 1 person in the study group) for reasons beyond the control of the researchers (lack of consent to continue participation, Covid infection, accidental reasons, fear of the impact of the test result on the final exam, lack of willingness). In order to keep the same conditions of the experiment, no new participants were recruited in their place. Finally, 59 people (25 men, 34 women) participated in the study.

All eligible students were never before exposed to donor specimens/cadaver throughout their anatomical education due to the Covid 19 pandemic restrictions. Each random and qualified participant gave their informed and free willed consent to participate in the study. The limited number of participants in the project was due to restrictions related to the SARS-CoV-2 pandemic. A maximum of 60 subjects could be accommodated in the dissecting rooms at one time.

Recruited participants were coded and then a computer system randomly selected individuals and separated them into a control group as well as a study group (Figure 1). Randomization was conducted by a researcher (ZD) who did not personally know the students or have contact with them at the time of recruitment to the study. The research consisted of three parts: (i) exam 1 (test 1), (ii) workshop, (iii) exam 2 (test 2). The study group participated in all parts of the project and the control group only in the exams (Figure 1). Both groups also participated in a standard course delivered online without access to a dissecting room.

Examination

Each exam consisted of 10 stations with anatomical specimens, 2 arrows (each representing a question) per station (20 arrows in total). The amount of points necessary to pass was set according to the exam regulations published at the beginning of the academic year by the department. On the basis of these regulations standardized sets of questions were prepared from structures similar in area and characterized by a similar level of difficulty. All participants in the study answered the

same questions. The test was carried out simultaneously for all groups. The number of stations and the way that the test was organised was such that no exchange of information between students was possible.

The eligibility of pin sets and selected specimens was decided by consensus. A team of experts (ZD,BKD,SW) was responsible for the substantive assessment of the pins/arrows.

The order of the stations was fixed, and each particular anatomical region was associated with a certain position. Each student had 60s per station (30s per question) and station changes were indicated audibly by an electronic timer. Students wrote their answers on answer sheets prepared by the organizers. There was a maximum of 20 answers available and the passing grade of the exam was at least 14 correct answers (70% of the maximum score). The results were checked twice by the same experts. In case of doubts concerning the correctness of an answer, the decision to credit or not to credit the answer was made jointly by two experts. The experts could not see the personal data of the students and did not know whether the test came from a person from the study group or from the control group. Doubts arose when students used similar names or the names of anatomical details located “near” the indicated structure. The rules of assessment were laid down in the exam regulations. Results were published online no later than one week after the examination due to multiple test checks.

Workshops

The workshop included 4 topics. The topics were chosen by the students in an anonymous questionnaire. A total of 8 workstations were created following the suggestions of the respondents. Two students from higher years were assigned to each station (near peer teachers -NPT). NPT student instructors did not attend the first round of exams. The demonstration time at the station was 30 min. followed by a change of student groups. The presentation was limited to the most important, relevant information with emphasis on clues to quickly identify the marked anatomical structure. Continuous supervision of

student tutors was provided by experts (BKD/SW) with over 10 years of experience in anatomy education.

Final evaluation.

In order to evaluate the impact of the workshop and assess its quality, the results of the study group from the first and second test dates were compared and analyzed in relation to the final results of the control group.

Statistical analysis

A significance level of $p = 0.05$ was assumed for the experimental design. The randomisation and statistical calculations were performed using the statistical package “R”, version 4.1.2 (The R Foundation for Statistical Computing, Vienna, Austria) and the PyCharm 2021.2.3 environment (Community Edition, Vienna, Austria), graphing was performed using the ggplot2 library for the R package (R-Studio, Boston, USA) [14]. The software was used to calculate descriptive statistics, non-parametric tests: the Shapiro-Wilk normality test, the McNemar’s test, to look for inter-group differences, and a paired Wilcoxon signed rank test with continuity correction and Mann-Whitney test with correction for continuity.

The research project received a positive opinion from the UMW local bioethics committee (No. of approval: 451/2021).

RESULTS

The evaluation of both the control group and the study group showed that 49% of the participants passed the first test and 69% of the participants passed the second test (Table 1). Based on McNemar’s test, there is no reason ($p=0.37$) to reject the hypothesis that retaking the exam, not preceded by a workshop, had no effect on the pass rate in the control group. In the control group, the number of points obtained by students in E2 was significantly higher ($p = 0.029$) than the number of points obtained in E1 (Wilcoxon signed rank test with continuity correction) (Figure 2).

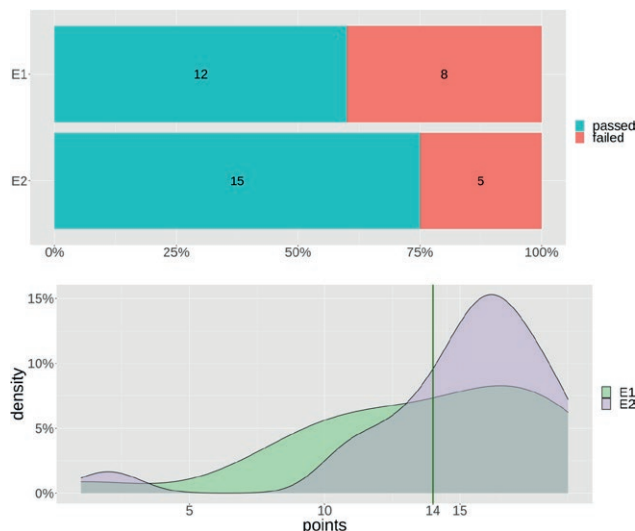


Figure 2. Assessment of the effect of a second attempt on the pass rate and scores in the control group.

Evaluating the impact of workshops on pass rates and scores

It was demonstrated that attending a workshop had an effect on the score pass rate of test 2 (McNemar test; $p=0.039$) (Figure 3). In the study group, the number of points obtained by students in test E2 is statistically and significantly higher ($p<10^{-4}$) than the number of points gained in test E1 (Wilcoxon signed rank test with continuity correction).

Comparison of the impact of workshops on pass rates and scores between the control and research groups

In the study group the workshops had a significant impact on the pass rate in the group, but at the same time in the control group there is no reason to reject the assumption that the workshops had no impact on the pass rate .

Due to the significantly higher ($p=0.042$) scores

Table 1. Comparison of all participants’ results - pass rate (Z) and number of achieved points, E1-first test, E2-second test, Q- quartile

All participant	N	Z (N)	Z (%)	min	Q1	median	mean	Q3	max
E1	59	29	49%	1.0	9.0	13.0	12.1	16.0	19.0
E2	59	41	69%	2.0	13.0	15.0	14.4	16.5	20.0

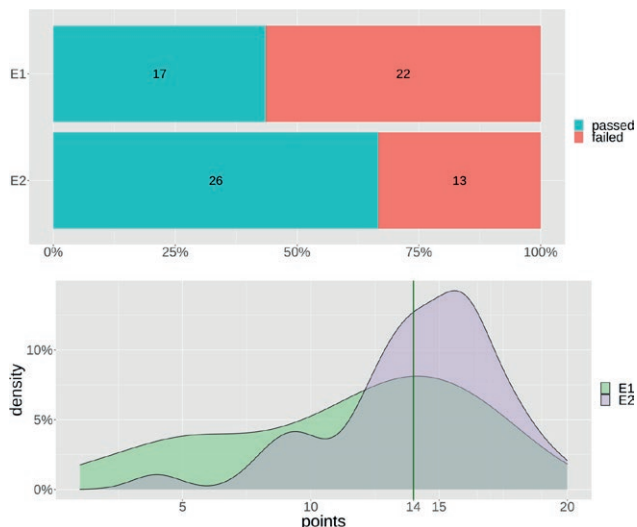


Figure 3. The results of exams in the study group (E1- exam 1 before the workshop, E2- exam 2 after the workshop)

Table 2. Difference in the number of scores in the study group and the control group between examination 1 (E1) and examination 2 (E2); Q- quartile, N-number of participants.

	N	E2 - E1					
		min	Q1	median	mean	Q3	max
Control group	20	- 2.0	0.0	0.0	1.3	2.3	9.0
Study group	39	- 5.0	0.0	2.0	2.9	5.5	11.0

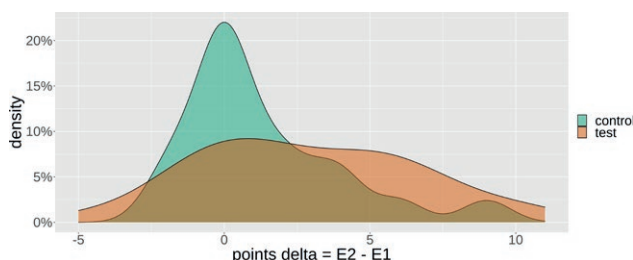


Figure 4. Individual (for each student) differences in the number of credits obtained between E2 and E1 in both groups (E1 - exam 1; E2 - exam 2).

achieved by the students in the control group in test E1 compared to E1 of the study group, and the higher pass rate in E1 and E2 of the control group - in order to compare the effect of the workshops on the number of obtained points - the individual differences in the number of obtained points between E2 and E1 in both groups were calculated (Figure 4). It was shown that the difference in the number of obtained points was signifi-

cantly higher ($p=0.049$) in the study group compared to the control group (Table 2) (Mann-Whitney test, Wilcoxon rank sum test with continuity correction).

DISCUSSION

In the present study, the effectiveness of practical training in anatomy was proven. The participants in the control group achieved better results during the second test, which the researchers interpret as the effect of familiarizing the students with this form of examination, training better concentration and developing strategies for completing it.

Furthermore, it has been shown that this result can be improved by a series of demonstrations carried out by the NPT using anatomical preparations made before the start of the study and cadavers obtained through a local conscious donation programme.

The first medical anatomical dissections were initiated in antiquity by Herophilus of Chalcedon (325-255 BC). In contrast, the use of the human body for the systematized study of anatomy was introduced in the late 14th and early 15th centuries by Italian anatomists [19]. The most famous of these (from Brussels) working in Padua- Andrea Vesalius- through the creation of anatomical atlases based on experiments and observations, brought anatomy into medical sciences [10, 30]. The study of anatomy is a challenge that requires the acquisition of a vast amount of knowledge which can only be studied in the appropriate setting. As early as the 16th century, Charles Estienne argued that anatomy can only be learned accurately in specially equipped places [35]. Students themselves used to proclaim that there is no better teacher of anatomy, teacher of empathy and teacher of the human body, than the corpse itself [15]. The topic of concern for the ethos of anatomy and the humanistic basis of medicine, is threatened by the need to digitalize the classroom in the age of the pandemic, as particularly relevant in the twenty-first century [23].

The COVID-19 pandemic made it impossible for students to interact with cadavers and participate in autopsies. While theory can be discussed through distance learning, there is no substitute for dissecting in any way [33]. Among the various methods of teaching anatomy (e.g. dissecting room classes, lectures, e-learning), the most highly rated are those that allow contact with human cadavers, based on demonstrations in small groups of students [6]. The reduced availability of cadavers in some universities has naturally forced the partial replacement of learning at the dissecting table

with teaching using modern technologies. Centers where donor cadavers are still available put an emphasis on the active participation of students in autopsy. Ghosh et al. stated that this is the only possibility that combines theoretical knowledge with medical practice [16].

Current works prove the crucial importance of contact, even limited, with real human bodies in anatomical didactics. Direct exposure to the specimen is a more effective way of learning anatomy than using alternative - digital or traditional - educational techniques. The recent anatomy literature is replaced with articles explaining the advantages of digitization and replacing dissecting classes with classes based on modern information technologies [7, 8, 34].

However, the results obtained here clearly indicate the necessity of great caution in implementing new digital technologies and abandoning the traditional form of anatomy classes. The qualitative advantage of typical dissecting classes over online classes in anatomy teaching has been proven, demonstrating the importance of contact with the specimen in gaining a better understanding of human morphology, as demonstrated in this publication.

It is worth noting that the high usefulness of workshops co-delivered by students from higher years of study - (NPT) has already been demonstrated [5].

The hybrid workshop based on NPT and experienced teachers used in the present study therefore meets the recommendations from scientific papers. [36]. The form of classes conducted in the relationship between a student of first year and a student of the senior years, allows diversity in methods of acquiring knowledge, supports the development and broadens the scientific horizons of students interested in teaching, and also constitutes a certain facilitation for academic teachers. It is worth highlighting that this type of assistance takes place in European countries on a paid basis (Bugaj et al., 2019). The effectiveness of the so-called peer-assisted learning can be evidenced, among other things, by the fact that this solution is an academic everyday feature of many universities across Europe, including Germany [20].

The high effectiveness of NPT in anatomy teaching demonstrated in current work can be attributed to the fact that, students who have recently studied a subject may have a better understanding of the difficulties in learning the given subject and therefore may be better equipped to help students overcome these difficulties [18, 25].

The creation of a positive atmosphere is important for students who are beginning their studies in combination with higher level of teaching would give rise to considerations of introducing peer student assistance from older colleagues permanently into the medical school

curriculum.

It has been proven that NPT is perceived positively by educated students. It offers the opportunity to improve educational outcomes while reducing the teaching load of teachers. Therefore, when integrated with other teaching methods, peer teaching can be a viable resource in the pursuit of excellence in future teaching of anatomy [1].

CONCLUSIONS

It has been shown that retaking the exam in a similar format increases the chances of passing the learned anatomical material. It has been also proved that the introduction of workshops based on the demonstration of anatomical structures by NPT significantly affects the results obtained by trainees. In conclusion, this project has confirmed the important role of student contact with the anatomical specimen. Additionally, the usefulness of NPT as a support in the didactic process carried out by experts – University employees – was confirmed. The study indirectly suggests that weeks of restricted access to dissection-based teaching or even anatomical demonstration may have a negative impact on the development of future physicians.

LIMITATIONS OF THE STUDY

The study has some important limitations:

1. Covid-19 pandemic constraints contributed to the need to limit the study and control groups.
2. Time constraints contributed to limiting the scope of the material discussed and the duration of the workshop.
3. the nature of the study was related to only one anatomical topic.
4. only selected topics from the anatomy course were discussed.
5. the theoretical knowledge of the students was not assessed

ETHICAL STATEMENT

Approval from the local bioethics committee was obtained for the purpose of the study.

ACKNOWLEDGMENTS

The authors of the study would like to thank Mr Andrzej Mrozek for his selfless work and knowledge,

with which he supported the realization of the project. Thanks to the members of the Clinical and Dissecting Anatomy Students Scientific Club and the members of “Vertex” Scientific Club for organizing the workshop for younger colleagues.

According to the new recommendations [21] all authors sincerely thank those who donated their bodies to the science so that anatomical research could be performed. Results from such research can potentially increase mankind/s overall knowledge that can then improve patient care. Therefore, these donors and their families deserve our highest gratitude.

REFERENCES

1. Agius A, Calleja N, Camenzuli C, et al. Perceptions of first-year medical students towards learning anatomy using cadaveric specimens through peer teaching. *Anatomical Sciences Education*. 2018; 11(4): 346–357, doi: 10.1002/ase.1751.
2. Bajor G, Likus W, Kuszewski P, et al. “Mortui vivos docent” or who gives his body to science? The analysis of the personal questionnaires of Polish donors in the conscious body donation program. *PLoS ONE*. 2015; 10(3), doi: 10.1371/journal.pone.0121061.
3. Berman AC. Anatomy of curriculum: Digging to the core. *Anatomical Sciences Education*. 2014; 7: 326–328, doi: 10.1002/ase.1474.
4. Bonnel F, Lavabre-Bertrand T, Bonnel C. The teaching of anatomy in Montpellier University during VIII centuries (1220–2020). *Surgical and Radiologic Anatomy*. 2019; 41(10): 1119–1128, doi: 10.1007/s00276-019-02289-6.
5. Ten Cate O, Durning S. Peer teaching in medical education: Twelve reasons to move from theory to practice. *Medical Teacher*. 2007; 29(6): 591–599, doi: 10.1080/01421590701606799.
6. Davis CR, Bates AS, Ellis H, et al. Human anatomy: Let the students tell us how to teach. *Anatomical Sciences Education*. 2014; 7(4): 262–272, doi: 10.1002/ase.1424.
7. Du YC, Fan SC, Yang LC. The impact of multi-person virtual reality competitive learning on anatomy education: a randomized controlled study. *BMC Medical Education*. 2020; 20(1), doi: 10.1186/s12909-020-02155-9.
8. Duarte ML, Santos LR, Guimarães Júnior JB, et al. Learning anatomy by virtual reality and augmented reality. A scope review. *Morphologie*. 2020; 104(347): 254–266, doi: 10.1016/j.morpho.2020.08.004.
9. Durán CEP, Bahena EN, Rodríguez M de los ÁG, et al. Near-peer teaching in an anatomy course with a low faculty-to-student ratio. *Anatomical Sciences Education*. 2012; 5(3): 171–176, doi: 10.1002/ase.1269.
10. Ellis H. Andreas Vesalius: father of modern anatomy. *British journal of hospital medicine (London, England : 2005)*. 2014; 75(12): 711, doi: 10.12968/hmed.2014.75.12.711.
11. Engels D, Haupt C, Kugelmann D, et al. The peer teachers’ perception of intrinsic motivation and rewards. *Advances in Physiology Education*. 2021; 45(4): 758–768, doi: 10.1152/ADVAN.00023.2021.
12. Evans DJR, Cuffe T. Near-peer teaching in anatomy: An approach for deeper learning. *Anatomical Sciences Education*. 2009; 2(5): 227–233, doi: 10.1002/ase.110.
13. Flynn W, Kumar N, Donovan R, et al. Delivering online alternatives to the anatomy laboratory: Early experience during the COVID-19 pandemic. *Clinical Anatomy*. 2021; 34(5): 757–765, doi: 10.1002/ca.23722.
14. Garrett Grolemond, Hadley Wickham. *R for Data Science Release*. O’Reilly Media, Inc., Sonoma, California, USA 2016.
15. George R, Mathew S. Anatomy lessons. *Christian Journal for Global Health*. 2017; 4(3): 96–101, doi: 10.15566/cjgh.v4i3.198.
16. Ghosh SK. Paying respect to human cadavers: We owe this to the first teacher in anatomy. *Annals of Anatomy*. 2017; 211: 129–134, doi: 10.1016/j.aanat.2017.02.004.
17. Gongola AB, Gowen JT, Reif RJ, et al. Anatomy Scholars Program for Medical Students Entering a Surgical Residency. *Medical Science Educator*. 2021; 31(5): 1581–1585, doi: 10.1007/s40670-021-01352-5.
18. Hall S, Stephens J, Andrade T, et al. Perceptions of junior doctors and undergraduate medical students as anatomy teachers: Investigating distance along the near-peer teaching spectrum. *Anatomical Sciences Education*. 2014; 7(3): 242–247, doi: 10.1002/ase.1419.
19. Van Hee R, Wells FC, Ballestriero R, et al. The art of human anatomy: Renaissance to 21st century. *Vesalius : acta internationales historiae medicinae*. 2014; 20(1): 25–29.
20. Herrmann-Werner A, Gramer R, Erschens R, et al. Peer-Assisted Learning (PAL) im medizinischen Grundstudium: eine Übersicht. *Zeitschrift für Evidenz, Fortbildung und Qualität im Gesundheitswesen*. 2017; 121: 74–81, doi: 10.1016/j.zefq.2017.01.001.
21. Iwanaga J, Singh V, Ohtsuka A, et al. Acknowledging the use of human cadaveric tissues in research papers: Recommendations from anatomical journal

- editors. *Clinical Anatomy*. 2021; 34(1), doi: 10.1002/ca.23671.
22. Johansson E, Holmin TE, Johansson BR, et al. Improving near-peer teaching quality in anatomy by educating teaching assistants: An example from Sweden. *Anatomical Sciences Education*. 2018; 11(4): 403–409, doi: 10.1002/ase.1775.
 23. Jones DG. Anatomy in a Post-Covid-19 World: Tracing a New Trajectory. *Anatomical Sciences Education* . 2021, 14: 148–153, doi: 10.1002/ase.2054.
 24. Kelsey AHCM, McCulloch V, Gillingwater TH, et al. Anatomical sciences at the University of Edinburgh: Initial experiences of teaching anatomy online. *Translational Research in Anatomy*. 2020; 19, doi: 10.1016/j.tria.2020.100065.
 25. Lachman N, Christensen KN, Pawlina W. Anatomy teaching assistants: Facilitating teaching skills for medical students through apprenticeship and mentoring. *Medical Teacher*. 2013; 35(1): e919–e925, doi: 10.3109/0142159X.2012.714880.
 26. Limbrecht K, Brinkmann A, Lamp C, et al. Mortui vivos docent? - Subjektives Belastungserleben von Studierenden im Kursus Makroskopische Anatomie. *PPmP Psychotherapie Psychosomatik Medizinische Psychologie*. 2013; 63(8): 327–333, doi: 10.1055/s-0032-1329977.
 27. Raftery AT. Anatomy teaching in the UK. *Surgery* . 2007, 25: 1–2, doi: 10.1016/j.mpsur.2006.11.002.
 28. Rhodes D, Fogg QA, Lazarus MD. Dissecting the role of sessional anatomy teachers: A systematic literature review. *Anatomical Sciences Education* . 2018, 11: 410–426, doi: 10.1002/ase.1753.
 29. Sokołowska-Pituchowa J. [The 400th Anatomy Department of Cracow (1602-2002)] 400 lat Katedry Anatomii w Krakowie (1602-2002). 2002.
 30. Splavski B, Rotim K, Lakičević G, et al. Andreas Vesalius, the Predecessor of Neurosurgery: How his Progressive Scientific Achievements Affected his Professional Life and Destiny. *World Neurosurgery* . 2019, 129: 202–209, doi: 10.1016/j.wneu.2019.06.008.
 31. The President of the Republic of Poland DA. USTAWA z dnia 3 lipca 2018 r. Przepisy wprowadzające ustawę – Prawo o szkolnictwie wyższym i nauce. [The Act - Law on Higher Education and Science]. *Dziennik Ustaw*. 2018; 1669: 1–107.
 32. Topping KJ. The effectiveness of peer tutoring in further and higher education: A typology and review of the literature. *Higher Education*. 1996; 32(3): 321–345, doi: 10.1007/BF00138870.
 33. Totlis T, Tishukov M, Piagkou M, et al. Online educational methods vs. traditional teaching of anatomy during the COVID-19 pandemic. *Anatomy and Cell Biology*. 2021; 54(3): 332–339, doi: 10.5115/acb.21.006.
 34. Triepels CPR, Smeets CFA, Notten KJB, et al. Does three-dimensional anatomy improve student understanding? *Clinical Anatomy* . 2020, 33: 25–33, doi: 10.1002/ca.23405.
 35. Tubbs RS, Salter EG. Charles Estienne (Carolus Stephanus) (ca.1504-1564): physician and anatomist. *Clinical anatomy (New York, NY)*. 2006; 19(1): 4–7, doi: 10.1002/ca.20180.
 36. Walser J, Horneffer A, Oechsner W, et al. Quantitative and qualitative analysis of student tutors as near-peer teachers in the gross anatomy course. *Annals of Anatomy*. 2017; 210: 147–154, doi: 10.1016/j.aanat.2016.10.007.
 37. Yoo H, Kim D, Lee YM, et al. Adaptations in Anatomy Education during COVID-19. *Journal of Korean Medical Science*. 2021; 36(1): 1–12, doi: 10.3346/jkms.2021.36.e13.



Citation: Zygmunt Domagała, Agnieszka Pinkowska, Aleksandra Piotrowska, Jurand Domański, Victoria Tarkowski, Aleksandra Zimmer-Stelmach, Jakub Śliwa (2022) Utility of the Movat pentachrome stain technique in the microanatomical analysis of the human placenta. *Italian Journal of Anatomy and Embryology* 126(2): 25-32. doi: 10.36253/ijae-13882

Copyright: © 2022 Zygmunt Domagała, Agnieszka Pinkowska, Aleksandra Piotrowska, Jurand Domański, Victoria Tarkowski, Aleksandra Zimmer-Stelmach, Jakub Śliwa. This is an open access, peer-reviewed article published by Firenze University Press (<http://www.fupress.com/ijae>) and distributed under the terms of the Creative Commons Attribution License, which permits unrestricted use, distribution, and reproduction in any medium, provided the original author and source are credited.

Data Availability Statement: All relevant data are within the paper and its Supporting Information files.

Competing Interests: The Author(s) declare(s) no conflict of interest.

ORCID

ZD: 0000-0002-2317-1932
APin: 0000-0002-8918-0129
APio: 0000-0003-4093-7386
JD: 0000-0003-2416-8062
AZ-S: 0000-0003-1114-6980
JS: 0000-0001-5343-0707

Utility of the Movat pentachrome stain technique in the microanatomical analysis of the human placenta

ZYGMUNT DOMAGAŁA¹, AGNIESZKA PINKOWSKA¹, ALEKSANDRA PIOTROWSKA², JURAND DOMAŃSKI^{3,*}, VICTORIA TARKOWSKI³, ALEKSANDRA ZIMMER-STELMACH⁴, JAKUB ŚLIWA⁴

¹ Division of Anatomy, Department of Human Morphology and Embryology, Wrocław Medical University, Wrocław, Poland

² Division of Histology and Embryology, Department of Human Morphology and Embryology, Wrocław Medical University, Wrocław, Poland

³ Clinical and Dissecting Anatomy Students Scientific Club, Wrocław Medical University, Wrocław, Poland

⁴ II Department of Obstetrics and Gynaecology, Wrocław Medical University, Wrocław, Poland

*Corresponding author. E-mail: jurand.dom@gmail.com

Abstract. The efficacy and utility of pentachrome staining has been demonstrated in many studies on diverse human body tissues. Movat pentachrome technique is used for multicolor staining of tissue sections and vascular and stroma visualization. So far, the utility of this method for microanatomical evaluation of placental structures has not been demonstrated. The aim of this study is to evaluate the image of normal placenta and to develop some reference images for future evaluation of pathological tissues based on this technique. *Material and method.* The study was carried out on 21 paraffin slices taken from seven mature human placenta of single pregnant women without significant pathology and completed with a planned, elective Caesarean section. All paraffin slices were used for preparation of tissue microarrays and then performing a histochemical staining (HE and Movat). *Results.* On the basis of the collected material, microscopic analysis enabled the identification of normal placental villi - terminal villi, mature intermediate villi and stem villi. Moreover the maternal part of placenta was visualized. It is worth emphasizing that in each case not only the trophoblast but also the stroma structures were visualized. *Conclusions.* This study proved the effectiveness and usefulness of Movat imaging of placenta especially in visualization of the stroma.

Keywords: microanatomy, pentachrome staining, placenta.

INTRODUCTION

The placenta is an organ with a unique function and composition for the human body. The anatomical structure is relatively simple, consisting of two surfaces: fetal and maternal. On the fetal surface, which is covered by the amniotic membrane, there is the separation of the umbilical cord (Rome-

ro 2015). It is usually located in the central part of the placenta, but can be found marginally or eccentrically. There are vessels branching from the umbilical cord, which usually spread radially (Huppertz 2008). Underneath the fetal surface, there is a chorionic plate consisting of a fibrous mass and a thick layer of connective tissue in which various calibre blood vessels run: veins and chorionic arteries. From the plate, villous arteries descend deep into the placenta towards the intervillous space (Domagała et al. 2020). Small vessels diverge into the placental villi from the villous arteries. The villi tree itself grows from the chorionic plate starting from the broad stem villi, and is formed at a very early stage of placental development (Huppertz 2008). From the villi tree, successive generations of villi descend, which at the very end of the tree produce the intervillous space floating villi. Together the described elements form the structural unit of the placenta - the cotyledon (Otake et al. 2019) (Figure 1). There is a basal plate on the other side of the placenta on the maternal surface, which is a partially artificial structure created by the separation of the placenta from the uterus at birth (Kay, Nelson, and Wang 2011). It is therefore composed of maternal tis-

sues including the uterine arterial vessels. A thin layer of trophoblast separates it from the intervillous space, and is connected to the individual cotyledons by the anchoring villi (Salaria et al. 2005). Adequate, proper placental structure is critical for fetal welfare. Any disturbance of this structure translates into significant clinical abnormalities of both the fetus and the mother, e.g. pregnancy-related hypertension. Detailed knowledge of the placenta structure is important, not only from a cognitive perspective but also that of a clinical one (Kay, Nelson, and Wang 2011).

The understanding of the placenta microstructure requires, apart from *in vivo* and macroscopic analysis, a microscopic analysis. Immunohistochemical techniques, i.e. mono- or polyclonally labelled antibodies are most commonly used to visualise components of the examined tissue. In spite of this, modern diagnostics and scientific research still uses histochemical methods for research as the immunohistochemical technique is based mainly on the use of two primary colours: blue and brown. This is a stark contrast to the ability of dye-based methods to produce multi-coloured images. This type of staining allows for the simultaneous identification of

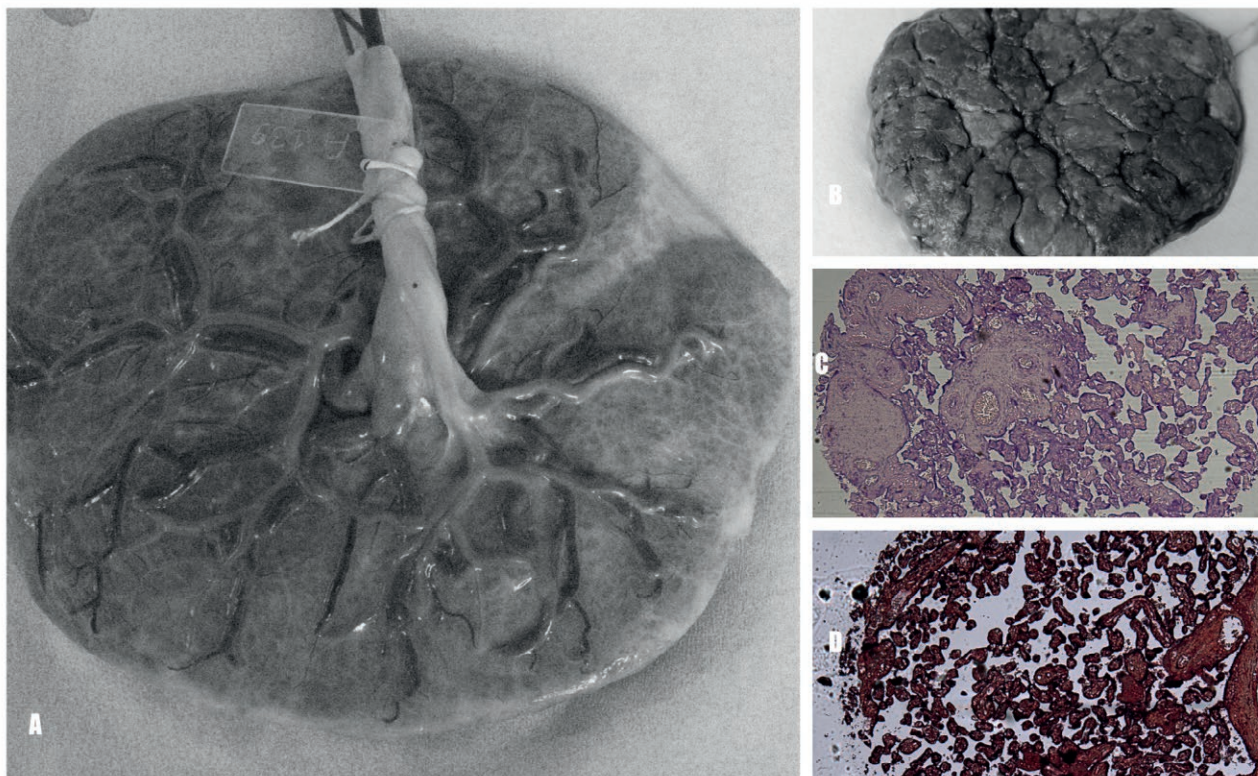


Figure 1. Human placenta (A – fetal side B – maternal side C – HE view of exemplary histospot, D – Pentachrome staining of exemplary histospot).

many tissue structures in order to provide a microscopic analysis of their coexisting morphological-functional interactions (Petrovic et al. 2011).

One such histochemical technique is Movat pentachrome staining (Felföldi et al. 2021; MOVAT 1955). In the case of the placenta, the authors believe that this technique can be useful to visualise parenchyma and stroma structures and, by simultaneously staining epithelia, also allow assessment of the interaction between trophoblast, stroma, and fetal vessels. The analysis of the available literature did not reveal the presence of any scientific work investigating the pentachrome staining image of normal placental tissues. Therefore, the aim of this study is to evaluate the normal microscopic analysis of the placenta using Movat staining. The definition of normal morphological images will then enable comparative studies comparing normal and pathological images to definitively confirm the usefulness of the histochemical technique in the diagnosis of placental pathology.

MATERIAL AND METHODS

The study was carried out on 21 paraffin slices taken from seven mature human placenta of single pregnant women without significant pathology and completed with a planned, elective Caesarean section (38-40 weeks of pregnancy).

The mean age of the mothers was 31.62 years, and mean neonatal weight was 3702 g, with a mean APGAR score of 9.86 points at the first minute after birth and 10 points at subsequent minutes (Table 1). All eligible mothers were healthy and the newborns did not show any abnormalities during the 24-hour clinical follow-up. Antenatal and postnatal assessment of the mothers and medical evaluation of the newborns were performed

Table 1. Basic clinical data and general characteristics of the material. SD – data in brackets, c-child/children; M- males, F-females; AG -Apgar points; BMI – body mass index; w – woman/women

Neonatus mass	Neonatus AG 1 min	Maternal BMI	Maternal parity	Maternal age
3702 (320.4) [g]	9,86	26.9 (2.4)	0c – 5 w 1c – 1 w 2c – 1 w	30,57 (1.6) [years]
Placenta mass	Placenta vertical diameter	Placenta horizontal diameter	Gestational age	Neonatus gender
560 (56) [g]	17.0(1.4) [cm]	18.5 (2.0) [cm]	40 (1.2) [weeks]	F-4 M-3

according to Polish medical standards (Zdrowia 2018). Material was collected from three placental sites (umbilical cord attachment area, paracentral zone and marginal zone of placenta) based on the technique proposed by Kay et al. (Kay, Nelson, and Wang 2011) using surgical clamps and dissecting forceps.

After sampling, the material was preserved in 4% buffered formalin. The paraffin blots were prepared from the obtained material in a typical manner. Hematoxylin and eosin stained slides were then made and, after initial evaluation in a Leica LD 5000HL light microscope (Leica Microsystems, Wetzlar, Germany), scanned using a Panoramic MIDI histology scanner (3DHistotech, Budapest, Hungary) to create virtual slides.

Based on these, representative 1.5mm histospots were selected for tissue microarrays using the automated TMA Gran Master system (3D Histtech, Budapest, Hungary).

Pentachrome Movat staining was carried out following a standard procedure. In the first step, staining was carried out in Alcian blue solution (20 minutes). This step was performed to buffer the basic substance. Next, the slides were rinsed under running water and then placed in alkaline alcohol. This part of the procedure was done to convert the Alcian blue into the insoluble pigment Monastral fast blue.

The next step was to rinse the material again with running water and then distilled water. Afterwards, staining in Verheoffs' haematoxylin solution was carried out to stain the cell nuclei and elastic fibres. This step was again followed by rinsing the material several times in distilled water. The next step was differentiation in a 2% aqueous solution of ferric trichloride. The differentiation process was interrupted by rinsing the preparation again. At this stage a microscopic check of the staining of the slide was carried out. If the result was satisfactory, the slides were placed in sodium trisulfate solution (1 min) and then rinsed again under running and distilled water.

The material was then stained in crocein scarlet acid fuchsin solution to stain fibrin and muscle. Slides were then washed in distilled water and, in the final step, in 0.5% ice-cold acetic acid. The washing was necessary to differentiate the slide in 5% hydrated phosphotungstic acid solution. Differentiation time was a maximum of 10 minutes. The staining effects were evaluated under the microscope. The slide was then rinsed again in acetic acid solution to remove phosphotungstic acid and the material was rinsed three times in 100% alcohol to prepare it for staining in alcoholic saffron solution. This staining took approximately 15-20 minutes to stain the collagen and reticulin fibres.

Finally, the slide was rinsed in alcohol solutions of decreasing concentrations, and covered with a coverslip.

The expression of the studied markers was evaluated independently by two independent observers (ZD, JD) using the Leica LD 5000HL light microscope. Identification of tissue types was based on colour evaluation of stained tissues derived from the available literature (Chu et al. 2009; Felföldi et al. 2021; Kajbafzadeh et al. 2017; Willershausen et al. 2019). Due to the small size of the material, statistical analysis was omitted and the results were presented as observational data.

RESULTS

Microscopic analysis based on the obtained material allowed us to identify normal villi of the placenta: terminal villi (Figure 2a), mature intermediate villi (Figure 3a,b), and stem villi (Figure 4a). Moreover, the maternal part of the placenta was visualised (Figure 5). Microscopic evaluation was conducted based on the acquired histospots. Qualification of tissue types was carried out independently based on the evaluation of the obtained multicolour image.

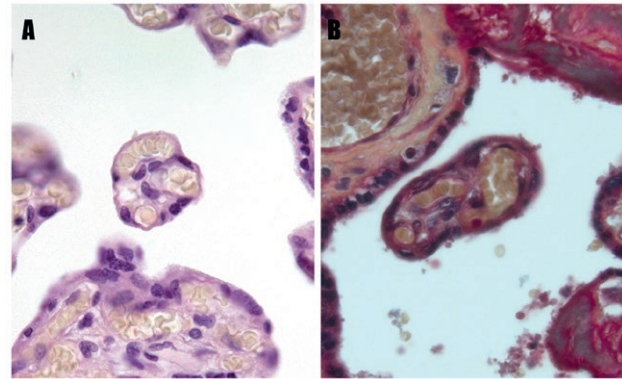


Figure 2. Terminal villus in HE (A) and MOVAT(B) staining (magnification 400x).

The evaluation of the terminal villi (Figure 2b) showed the presence of intensely black stained nuclei of trophoblast cells building the outer structure of the villi. The purplish-black colour is due to elastin fibres, which are present within the trophoblast, but also build the capillary walls and are found in the stroma. Inside the terminal villus, collagen fibres can also be seen (yellowish coloured tissue fragments).

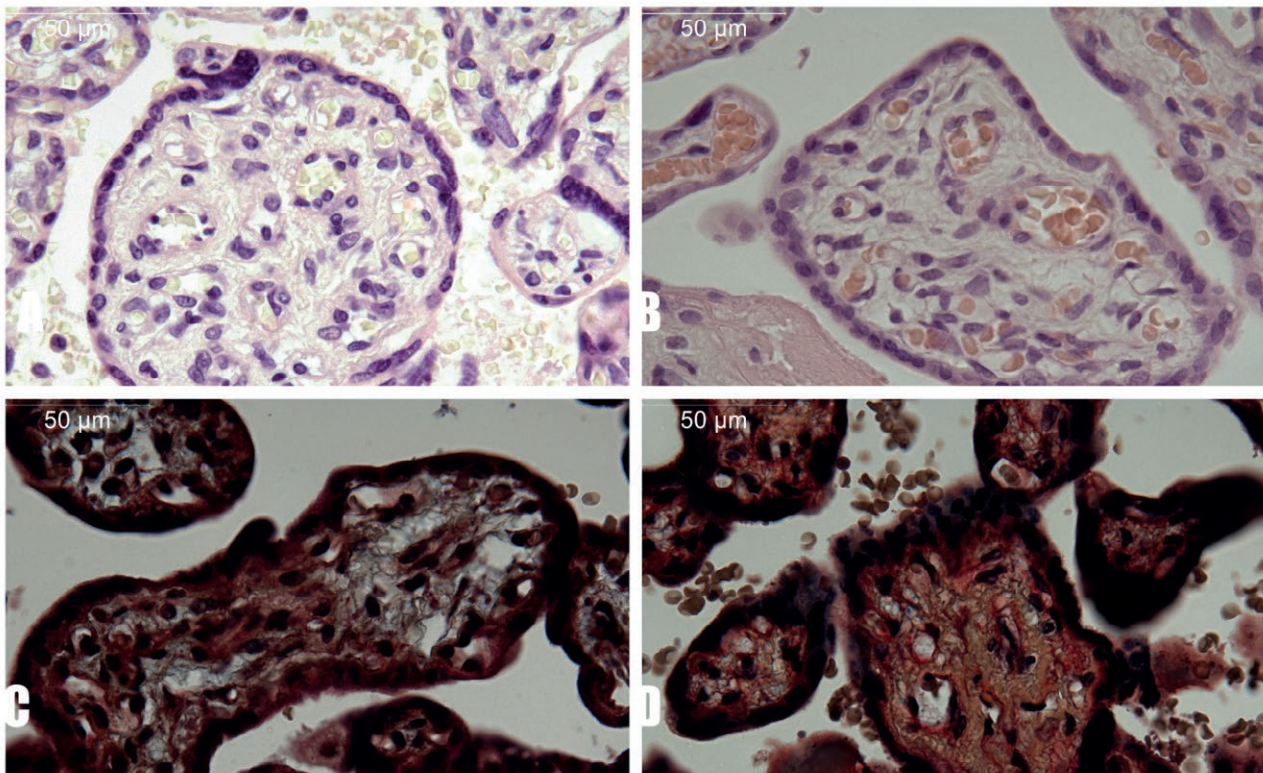


Figure 3. Human intermediate villus in HE(A,B) and MOVAT (C,D) staining.

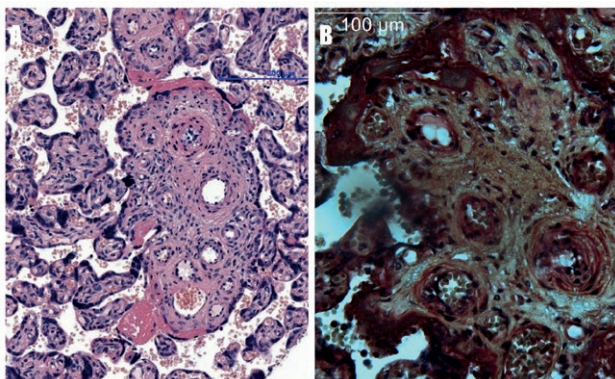


Figure 4. Human stem villus in HE (A) and Movat (B) staining.

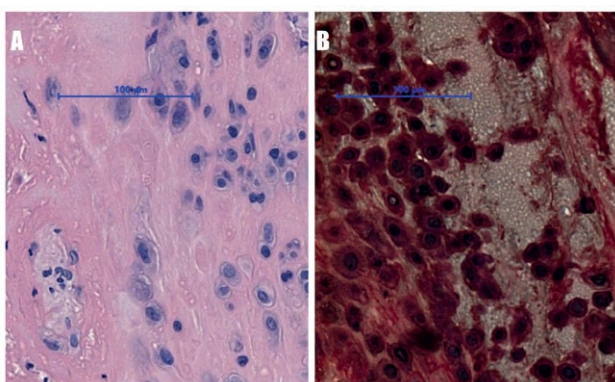


Figure 5. Extravillous trophoblast in HE (A) and Movat (B) staining.

In the case of the intermediate villi (Figure 3c,d), the presence of black-stained cell nuclei and black-purple elastin fibres present within the trophoblast and the central part is also demonstrated. In the central part of the villi, yellowish collagen fibres are visible. Around the few vessels red or orange coloured muscle fibres and in some places blue coloured reticular fibres can be seen.

In the case of stem villi (Figure 4), black stained cell nuclei and trophoblast cells were visualised. Around the vessels, reddish-brown stained muscle fibres were visualised and in the stroma blue stained collagen and brownish-yellow and brown proteoglycans and reticular fibres were visualised.

Assessment of maternal tissues stained with Movat demonstrated intense black colouration of villous and extravillous trophoblasts, red colouration of tissue surrounding villi and beige-yellow colouration of tissues in the stroma. Bluish staining was also found in limited areas corresponding to tissues containing large amounts of collagen and reticular fibres.

DISCUSSION

The reported data demonstrates the advantages of imaging the human placenta with Movat pentachrome staining techniques. Histochemical techniques (trichrome or pentachrome stain) are used relatively often for histochemical evaluation of tissues (Kara et al. 2020; Klećkowska-Nawrot et al. 2015; Skonieczna et al. 2021; Zaki and Youssef 2013). Despite its complexity, the Movat technique allows for simultaneous visualisation of multiple tissue structures such as muscles, cell nuclei or tissues containing elastin fibres or glycosaminoglycans (Wilson et al. 2021).

Its attractiveness lies primarily in the acquisition of a multicoloured image, which greatly facilitates the assessment and differentiation of individual placental structures by the consulting pathologist at a reasonable cost limit. Presently, most placentas in the postpartum period are not evaluated histopathologically. Reasons for this situation include staff shortages as well as the limitations associated with the high cost of histopathological examination (Hadravská et al. 2017).

In our opinion, a detailed microscopic evaluation of the placenta should be considered because the results may present clinically relevant data. Such data may indicate an association between certain placental features, assessed macroscopically and microscopically, and pathologies associated with the later development of the child as an independent organism from the mother (Barker et al. 2010; Barker et al. 2012; Cirillo and Cohn 2020; Hodyl et al. 2017). The human placenta is an organ that exists only during the developmental period and supports the growth and development of the fetus (Hupertz 2008). Its growth is associated with rapid proliferation of cytotrophoblast cells. This is accompanied by multistage differentiation into several subpopulations of cells with different anatomical localisation and function (Aplin et al. 2020). One such subpopulation, the syncytiotrophoblast, covers the outer side of the chorionic villi. It comes into direct contact with maternal blood and thus defines the nutritional, endocrine, and immunological interface between mother and fetus (Pijnenborg et al. 1981). Some trophoblast cells leave the placenta and enter the tissues of the mother; they are defined as extravillous trophoblasts. These cells penetrate the walls of the spiral arteries in such a way that they replace the endothelial cells of the mother's vessels. In addition, there is displacement of smooth muscle cells and breakdown of the associated extracellular matrix. This process induces remodelling of the spiral arteries, resulting in a change in vessel characteristics. The artery transforms from a narrow vasoreactive vessel into a wider low-

pressure tube that supplies the placenta and fetus with nutrient- and oxygen-rich maternal blood (Pijnenborg et al. 1981). The phenomenon described earlier defines placental tissues as “pseudomalignant tissue” because of the numerous similarities of trophoblast cells to tumour cells. Both cell types are characterised by a high tendency to proliferation and invasion (Wilczyński 2006). Scientific data suggest that, in their development, cancer cells revert to primitive developmental processes representative of trophoblast cells by taking over genes used by these cells to achieve metastatic potential (Koslowski et al. 2007). For example, the epithelial-mesenchymal transition (EMT) that is characteristic for neoplastic invasion occurs during early implantation/placentation (Roldán et al. 2020). Movat’s pentachrome technique is a useful tool in assisting physicians in the diagnosis of cancer. It supports the physician in assessing the degree of invasion of the proliferative process, and has been proven to confirm venous invasion in oesophageal adenocarcinoma (Castonguay, Li-Chang, and Driman 2014). It is also used to evaluate the stroma of tumours (Haeberle et al. 2018). For example, in pancreatic cancer, Movat’s method allows the probability of a successful tumour response to neoadjuvant chemotherapy to be determined (Haeberle et al. 2021). It is worth emphasizing that the assessment of the cell stroma is not only important in neoplastic diseases but also in the assessment of the physiology and pathology of the human placenta (Ji et al. 2021; Wang et al. 2011).

Pentachrome staining has also proven to be of value in the assessment of vascular remodelling associated with damage in the course of atherosclerosis. It allows a reliable qualitative and quantitative assessment of glycosaminoglycans, elastic fibres, proteoglycans, or collagen in tissues forming a blood vessel. For example, it has been shown that it can be used to assess the risk of cardiovascular events in patients after carotid endarterectomy.

In sum, the placenta is an organ whose main purpose is to ensure the exchange of nutrients between the developing fetus and its mother. This exchange is possible thanks to the characteristic structure of the organ, in which the blood vessels are a crucial element. The placenta is therefore characterised by a dynamic cellular development based on mechanisms typical for neoplastic tissues; simultaneously, it is an unusual “vascular” organ. The present work demonstrates that the use of histochemical techniques for tissue visualisation allows for a more comprehensive assessment of placental tissue in contrast to standard histochemical staining, and may be useful for both clinical and scientific evaluation of this tissue. In the future, it is planned to use this tool to assess placental tissue in health and disease research.

ETHICAL STATEMENT

The study was made according to the Declaration of Helsinki and approved by the Local Bioethics Committee.

ACKNOWLEDGEMENTS

This work was funded by grant SUB.A351.19.032.

REFERENCES

- Aplin, John D., Jenny E. Myers, Kate Timms, and Melissa Westwood. 2020. “Tracking Placental Development in Health and Disease.” *Nature Reviews Endocrinology*. doi:10.1038/s41574-020-0372-6.
- Barker, David J.P., Gail Larsen, Clive Osmond, Kent L. Thornburg, Eero Kajantie, and Johan G. Eriksson. 2012. “The Placental Origins of Sudden Cardiac Death.” *International Journal of Epidemiology* 41 (5): 1394–1399. doi:10.1093/ije/dys116.
- Barker, David J.P., Kent L. Thornburg, Clive Osmond, Eero Kajantie, and Johan G. Eriksson. 2010. “The Surface Area of the Placenta and Hypertension in the Offspring in Later Life.” *International Journal of Developmental Biology* 54 (2–3): 525–530. doi:10.1387/ijdb.082760db.
- Castonguay, Mathieu C., Hector H. Li-Chang, and David K. Driman. 2014. “Venous Invasion in Oesophageal Adenocarcinoma: Enhanced Detection Using Elastic Stain and Association with Adverse Histological Features and Clinical Outcomes.” *Histopathology* 64 (5): 693–700. doi:10.1111/his.12308.
- Chu, Kim E., Bettina G. Papouchado, Zhaoli Lane, and Mary P. Bronner. 2009. “The Role of Movat Pentachrome Stain and Immunoglobulin G4 Immunostaining in the Diagnosis of Autoimmune Pancreatitis.” *Modern Pathology* 22 (3): 351–358. doi:10.1038/modpathol.2008.196.
- Cirillo, Piera M., and Barbara A. Cohn. 2020. “Gestational Biomarkers of Daughter’s Breast Cancer in the Child Health and Development Studies.” *Reproductive Toxicology* 92: 105–111. doi:10.1016/j.reprotox.2019.05.057.
- Domagała, Zygmunt, Jurand Domański, Aleksandra Zimmer, Anna Tarczyska, Jakub Sliwa, and Bohdan Gworys. 2020. “Methodology of Preparation of Corrosive Specimens from Human Placenta — A Technical Note.” *Annals of Anatomy* 228 (March): 151436. doi:10.1016/j.aanat.2019.151436.

- Felföldi, Balázs, Ildikó Bódi, Krisztina Minkó, Zsófia Benyeda, Nándor Nagy, Attila Magyar, and Imre Oláh. 2021. "Infection of Bursal Disease Virus Abrogates the Extracellular Glycoprotein in the Follicular Medulla." *Poultry Science* 100 (4). doi:10.1016/j.psj.2021.01.023.
- Hadravská, Šárka, M. Dubová, P. Mukenšnabl, and O. Daum. 2017. "Complications Arising out of Insufficient Reporting of Clinical Data to the Pathologist Investigating Placentas." *Ceska Gynekologie* 82 (3): 197–201.
- Haerberle, Lena, Andrea Cacciato Insilla, Anne-Christine Kapp, Katja Steiger, Anna Melissa Schlitter, Björn Konukiewicz, Ihsan Ekin Demir, Helmut Friess, and Irene Esposito. 2021. "Stroma Composition and Proliferative Activity Are Related to Therapy Response in Neoadjuvant Treated Pancreatic Ductal Adenocarcinoma." *Histology and Histopathology*, 18332. doi:10.14670/HH-18-332.
- Haerberle, Lena, Katja Steiger, Anna Melissa Schlitter, Sami Alexander Safi, Wolfram Trudo Knoefel, Mert Erkan, and Irene Esposito. 2018. "Stromal Heterogeneity in Pancreatic Cancer and Chronic Pancreatitis." *Pancreatology* 18 (5): 536–549. doi:10.1016/j.pan.2018.05.004.
- Hodyl, Nicolette A., Natalie Aboustate, Tina Bianco-Miotto, Claire T. Roberts, Vicki L. Clifton, and Michael J. Stark. 2017. "Child Neurodevelopmental Outcomes Following Preterm and Term Birth: What Can the Placenta Tell Us?" *Placenta*. doi:10.1016/j.placenta.2017.06.009.
- Huppertz, B. 2008. "The Anatomy of the Normal Placenta." *Journal of Clinical Pathology*. doi:10.1136/jcp.2008.055277.
- Ji, Shuhan, Diane Gumina, Kathryn McPeak, Radu Moldovan, Miriam D. Post, and Emily J. Su. 2021. "Human Placental Villous Stromal Extracellular Matrix Regulates Fetoplacental Angiogenesis in Severe Fetal Growth Restriction." *Clinical Science* 135 (9): 1127–1143. doi:10.1042/CS20201533.
- Kajbafzadeh, Abdol Mohammad, Reza Khorramirouz, Seyede Maryam Kameli, Javad Hashemi, and Amin Bagheri. 2017. "Decellularization of Human Internal Mammary Artery: Biomechanical Properties and Histopathological Evaluation." *BioResearch Open Access* 6 (1): 74–84. doi:10.1089/biores.2016.0040.
- Kara, H., S. Gedikli, Z. Özudogru, D. Özdemir, and H. Balkaya. 2020. "A Morphological, Morphometrical and Histological Investigation of the Interdigital Gland in Hasmer and Hasak Sheep." *Folia Morphologica (Poland)* 74 (9): 742–747. doi:10.5603/FM.A2020.0014.
- Kay, Helen H., D. Michael Nelson, and Yuping Wang. 2011. *The Placenta: From Development to Disease. The Placenta: From Development to Disease*. doi:10.1002/9781444393927.
- Klećkowska-Nawrot, J., R. Nowaczyk, K. Goździewska-Harłajczuk, K. Krasucki, and M. Janeczek. 2015. "Histological, Histochemical and Fine Structure Studies of the Lacrimal Gland and Superficial Gland of the Third Eyelid and Their Significance on the Proper Function of the Eyeball in Alpaca (Vicugna Pacos)." *Folia Morphologica (Poland)* 74 (2): 195–205. doi:10.5603/FM.2015.0001.
- Kosłowski, Michael, Ugur Sahin, Rita Mitnacht-Kraus, Gerhard Seitz, Christoph Huber, and Özlem Türeci. 2007. "A Placenta-Specific Gene Ectopically Activated in Many Human Cancers Is Essentially Involved in Malignant Cell Processes." *Cancer Research* 67 (19): 9528–9534. doi:10.1158/0008-5472.CAN-07-1350.
- MOVAT, H. Z. 1955. "Demonstration of All Connective Tissue Elements in a Single Section; Pentachrome Stains." *A. M. A. Archives of Pathology* 60 (3): 289–295.
- Otake, Yuko, Hidenori Kanazawa, Hironori Takahashi, Shigeki Matsubara, and Hideharu Sugimoto. 2019. "Magnetic Resonance Imaging of the Human Placental Cotyledon: Proposal of a Novel Cotyledon Appearance Score." *European Journal of Obstetrics and Gynecology and Reproductive Biology* 232. doi:10.1016/j.ejogrb.2018.11.011.
- Petrovic, A., M. Abramovic, D. Mihailovic, J. Gligorijevic, V. Zivkovic, M. Mojsilovic, and I. Ilic. 2011. "Multi-color Counterstaining for Immunohistochemistry a Modified Movat's Pentachrome." *Biotechnic and Histochemistry* 86 (6): 429–435. doi:10.3109/10520295.2010.528026.
- Pijnenborg, R., W. B. Robertson, I. Brosens, and G. Dixon. 1981. "Review Article: Trophoblast Invasion and the Establishment of Haemochorial Placentation in Man and Laboratory Animals." *Placenta*. doi:10.1016/S0143-4004(81)80042-2.
- Roldán, Diana Barea, Matthias Grimmler, Christoph Hartmann, Stefanie Hubich-Rau, Tim Beißert, Claudia Paret, Giuseppe Cagna, et al. 2020. "PLAC1 Is Essential for FGF7/FGFR3b-Induced Akt-Mediated Cancer Cell Proliferation." *Oncotarget* 11 (20): 1862–1875. doi:10.18632/oncotarget.27582.
- Romero, Roberto. 2015. "Images of the Human Placenta." *American Journal of Obstetrics and Gynecology*. doi:10.1016/j.ajog.2015.08.039.
- Salaria, Carolyn M., John C. Pezzullo, Adrian K. Charles, Linda M. Ernst, Elizabeth M. Maas, Benita Gross, and Robert Pijnenborg. 2005. "Morphometry of the

- Basal Plate Superficial Uteroplacental Vasculature in Normal Midtrimester and at Term.” *Pediatric and Developmental Pathology* 8 (6): 639–646. doi:10.1007/s10024-005-0409-9.
- Skonieczna, Joanna, Jan P. Madej, Agnieszka Kaczmarek-Pawelska, and Romuald Będziński. 2021. “Histological and Morphometric Evaluation of the Urethra and Penis in Male New Zealand White Rabbits.” *Journal of Veterinary Medicine Series C: Anatomia Histologia Embryologia* 50 (1): 136–143. doi:10.1111/ah.12611.
- Wang, Y., J. Sun, Y. Gu, S. Zhao, L. J. Groome, and J. S. Alexander. 2011. “D2-40/Podoplanin Expression in the Human Placenta.” *Placenta* 32 (1): 27–32. doi:10.1016/j.placenta.2010.10.014.
- Wilczyński, Jacek R. 2006. “Cancer and Pregnancy Share Similar Mechanisms of Immunological Escape.” *Chemotherapy*. doi:10.1159/000092537.
- Willershausen, Ines, Christina Erbe, Sarah Al-Maawi, Anna Orłowska, Heiner Wehrbein, and Shahram Ghanaati. 2019. “Development of a Novel Histological and Histomorphometric Evaluation Protocol for a Standardized Description of the Mid-Palatal Suture – An Ex Vivo Study.” *Journal of Anatomy* 235 (1): 180–188. doi:10.1111/joa.12985.
- Wilson, Susan J., Jonathan A. Ward, Helen M. Pickett, Simonetta Baldi, Ana R. Sousa, Peter J. Sterk, Kian Fan Chung, et al. 2021. “Airway Elastin Is Increased in Severe Asthma and Relates to Proximal Wall Area: Histological and Computed Tomography Findings from the U-BIOPRED Severe Asthma Study.” *Clinical and Experimental Allergy* 51 (2): 296–304. doi:10.1111/cea.13813.
- Zaki, S. M., and M. F. Youssef. 2013. “Thyroid Hormone Dysfunctions Affect the Structure of Rat Thoracic Aorta: A Histological and Morphometric Study.” *Folia Morphologica (Poland)* 72 (4): 333–339. doi:10.5603/FM.2013.0056.
- Ministerstwo Zdrowia. 2018. “Rozporządzenie Ministra Zdrowia z Dnia 16 Sierpnia 2018 r. w Sprawie Standardu Organizacyjnego Opieki Okołoporodowej.” [Ministry of Health. 2018. “Decree of the Minister of Health dated August 16, 2018 on the Organizational Standard of Perinatal Care”] *Dziennik Ustaw*, poz. 1756.



Citation: Oriana Trubiani (2022) Special issue on Innovative Technologies in Clinical Medicine & Dentistry (InTEchMed). *Italian Journal of Anatomy and Embryology* 126(2): 33-33. doi: 10.36253/ijae-14165

Copyright: © 2022 Oriana Trubiani. This is an open access, peer-reviewed article published by Firenze University Press (<http://www.fupress.com/ijae>) and distributed under the terms of the Creative Commons Attribution License, which permits unrestricted use, distribution, and reproduction in any medium, provided the original author and source are credited.

Data Availability Statement: All relevant data are within the paper and its Supporting Information files.

Competing Interests: The Author(s) declare(s) no conflict of interest.

Special issue on Innovative Technologies in Clinical Medicine & Dentistry (InTEchMed)

PREFACE

The PhD course in Innovative Technologies in Clinical Medicine & Dentistry (InTEchMed) of the University “G. d’Annunzio” of Chieti-Pescara, is a newly instituted course that brings together professors and researchers belonging to scientific-disciplinary sectors that are homogeneous and coherent with a scientific project that has as its objective “ the pursuit of multidisciplinary research” by finalizing the research, in terms of content and applicability, as a priority to satisfying the growing demands for a medicine of excellence with particular reference to spheres of interest of great relevance and considerable impact social responsibility attributable to the areas of specialization identified by the National Research Plan.

The PhD course in InTEchMED incorporates and processes technological and scientific innovations in the context of the skills that characterize it and, with a synergistic work, seeks to interface with the national and international scientific community with a constructive and innovative spirit. To this end, to promote the research activity of their PhD students, the First PhD InTEchMED Conference was organized, where the students presented the preliminary data of the research carried out and these oral presentations were collected to be published in the special issue of the Italian Journal of Anatomy and Embryology.

Professor Oriana Trubiani
Coordinator of PhD InTEchMed Course



Citation: Ylenia Della Rocca, Jacopo Pizzicannella, Guya Diletta Marconi, Luigia Fonticoli, Oriana Trubiani, Francesca Diomedede (2022) Role of extracellular vesicles derived by human gingival mesenchymal stem cells in cardiomyocytes acute hypoxia. *Italian Journal of Anatomy and Embryology* 126(2): 35-38. doi: 10.36253/ijae-13785

Copyright: © 2022 Ylenia Della Rocca, Jacopo Pizzicannella, Guya Diletta Marconi, Luigia Fonticoli, Oriana Trubiani, Francesca Diomedede. This is an open access, peer-reviewed article published by Firenze University Press (<http://www.fupress.com/ijae>) and distributed under the terms of the Creative Commons Attribution License, which permits unrestricted use, distribution, and reproduction in any medium, provided the original author and source are credited.

Data Availability Statement: All relevant data are within the paper and its Supporting Information files.

Competing Interests: The Author(s) declare(s) no conflict of interest.

Role of extracellular vesicles derived by human gingival mesenchymal stem cells in cardiomyocytes acute hypoxia

YLENIA DELLA ROCCA^{1,*}, JACOPO PIZZICANNELLA², GUYA DILETTA MARCONI³, LUIGIA FONTICOLI¹, ORIANA TRUBIANI¹, FRANCESCA DIOMEDE¹

¹ Department of Innovative Technologies in Medicine & Dentistry, University "G. d'Annunzio" Chieti-Pescara, Via dei Vestini, 31, 66100 Chieti, Italy

² Ss. Annunziata" Hospital, ASL 02 Lanciano-Vasto-Chieti, 66100 Chieti, Italy

³ Department of Medical, Oral and Biotechnological Sciences, University "G. d'Annunzio" Chieti-Pescara, Via dei Vestini, 31, 66100 Chieti, Italy

*Corresponding author. E-mail: Dr. Ylenia Della Rocca, ylenia.dellarocca@unich.it

Abstract. Hypoxia has an impact on pathological conditions of different tissues and especially on the heart where it can have different consequences depending on the duration of exposure to the hypoxic state. Acute hypoxic exposure can result in reversible acclimatization in heart tissue, maintaining a good systemic oxygen supply, while chronic hypoxic exposure leads to tissue damage exacerbating hypoxia-induced cardiac dysfunction. Extracellular vesicles (EVs) are small membrane vesicles, of the order of nanometers, secreted by different cell types. EVs are mediators of intercellular communication in both physiological and pathological conditions. EVs produced by oral-cavity-derived Mesenchymal Stem Cells (MSCs), including human gingival mesenchymal stem cells, have pro-angiogenic and anti-inflammatory effects. For this reason, the EVs can be identified as a new therapeutic potential for tissue regeneration. The aim of the present work was to evaluate the effect of treatment with EVs produced by human gingival mesenchymal stem cells (hGMSCs) on an in vitro model of HL-1 cardiomyocytes cultured under acute hypoxia state (0,2% hypoxia) followed by normoxia conditions. The HIF-1 α expression was downregulated with EVs treatment. EVs could represent an innovative platform to prevent the hypoxic damages.

Keywords: extracellular vesicles, human gingival mesenchymal stem cells, cardiomyocytes, acute hypoxia.

INTRODUCTION

The heart is one of the tissues most affected by variations in oxygen levels and therefore in the hypoxic state, mainly due to phenomena such as nitric oxide (NO) and reactive oxygen species (ROS) formation and increased superoxide formation through NADPH, which lead respectively to an alteration of cardiac contractility, mitochondrial damage, and formation of atherosclerosis [1-3]. Therefore hypoxia-inducible factor (HIF), key molecule of the

hypoxic pathway activation [4], has an impact on several cardiac phenotypes including heart failure [5].

A mild exposure to hypoxia can provoke a reversible physiological acclimatization in the heart tissue as happens following an acute and systemic hypoxic exposure in which there is an immediate increase in heart rate and lung function maintaining a good supply of systemic oxygen, while the prolonged exposure to hypoxia (chronic hypoxia) leads to tissue damage [6,7]. Furthermore, oxygenation after acute or prolonged exposure has been shown to cause oxidative damage exacerbating hypoxia-induced cardiac dysfunction [8].

Extracellular vesicles (EVs) are nanometer-sized vesicles containing lipid, proteins and different types of nucleic acids, enclosed by lipid membranes. These are secreted by different cell types and act as important mediators of intercellular communication in both physiological and pathological conditions [9,10]. EVs isolated from oral-cavity-derived Mesenchymal Stem Cells (MSCs) have been shown to carry pro-angiogenic and anti-inflammatory factors showing themselves as therapeutic potential for tissue regeneration [11,12].

The aim of the present work is to evaluate the effect of EVs produced by human gingival mesenchymal stem cells (hGMSCs) on an in vitro model of HL-1 cardiomyocytes cultured under 0.2% hypoxia (acute hypoxia) followed by normoxia evaluating the HIF-1 α expression.

MATERIALS AND METHOD

Hypoxic culture

The HL-1 cells (Sigma-Aldrich, Milan, Italy) were cultured in Claycomb medium completed with 10% fetal bovine serum (Euroclone, Milan, Italy), 2 mM l-glutamine, 0,1 mM norepinephrine, and 100 μ g/mL penicillin/streptomycin (Lonza, Basel, Switzerland) under hypoxia 0,2% for 24h and then in normoxia at 37 °C in a humidified atmosphere of 5% of CO₂ in air for 24h. The hypoxia state was performed using ProOx Model P110 (BioSpherix, 25 Union Street, Parish, NY 13131) hypoxia chamber, and following the referred Manual.

EVs isolation

EVs were isolated starting from supernatants (10mL) of hGMSCs culture after 48 hours of culture using ExoQuick-TC (System Biosciences, Euroclone SpA, Milan, Italy) following the manufacturer's protocol. The mixture was placed at 4 °C overnight and the following day was centrifuged 1500 \times g for 30 minutes

to settle the EVs and the pellets were resuspended in 200 μ L of PBS [13].

Experimental study design

The study design is reported as follows:

- (i) HL-1, used as a negative control (CTRL), were kept in hypoxia at 0,2% for 24 h and successively in normoxia for 24 h;
- (ii) HL-1 were kept in hypoxia at 0,2% for 24 h and treated with hGMSCs EVs in normoxia for successively 24 h (EVs Post-hypoxia);
- (iii) HL-1 treated with with hGMSCs EVs in hypoxia at 0,2% for 24 h and then in normoxia for successively 24 h (EVs Pre-hypoxia).

Confocal microscopy analysis

The HL-1 cells were seeded at 8500/well on 8-well culture glass slides (Corning, Glendale, Arizona, USA), under hypoxia state and treated with hGMSCs EVs as described in ii) and iii). The Confocal Microscopy analysis was performed as previously described [14] using HIF-1 α as primary mouse monoclonal antibody (1:200, Santa Cruz Biotechnology) and Alexa Fluor 568 red fluorescence conjugated goat anti-mouse antibody (1:200; Molecular Probes, Invitrogen, Eugene, OR, United States) as secondary antibody. The microscope used is Zeiss LSM800 confocal system (Zeiss, Jena, Germany).

Western Blotting Analysis

The proteins derived from cell cultures of the three experimental points were used at the concentration of 50 μ g for the electrophoresis and subsequent transfer on the membrane of polyvinyl-denifluoride (PVDF) as previously described [15]. The primary monoclonal antibody used (mouse, 1:500, Santa Cruz Biotechnology) is HIF-1 α . β -actin has been used as housekeeping protein. The ECL method was used to visualize the bands with an image documenter Alliance 2.7 (Uvitec, Cambridge, UK). The data were normalized with β -actin.

RESULTS

Under the light microscope, the cells show the typical morphology of the HL-1 mouse heart muscle cell line (Figure 1).

The immunofluorescence showed that the levels of HIF-1 α was significantly downregulated in HL-1 EVs

HL-1

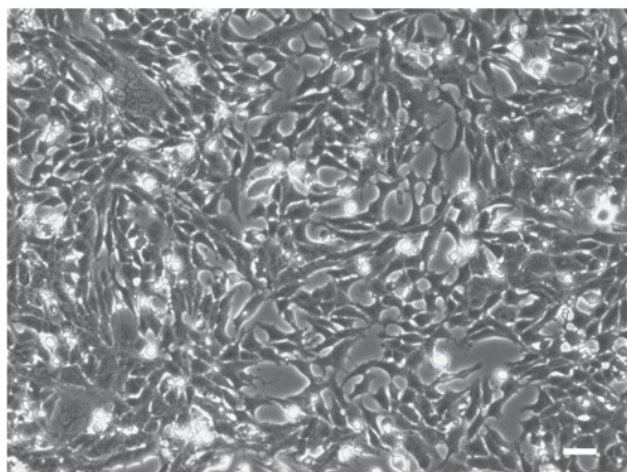


Figure 1. HL-1 Morphological features. Representative image of HL-1 maintained under normoxia conditions observed under inverted light microscopy. Scale bar: 20 μ m.

Post-hypoxia and EVs Pre-hypoxia groups.

On the other hand, HL-1 CTRL group HIF-1 α showed an high expression levels when compared to the other sample groups (Figure 2). The Western blot analysis confirmed the obtained results (Figure 3).

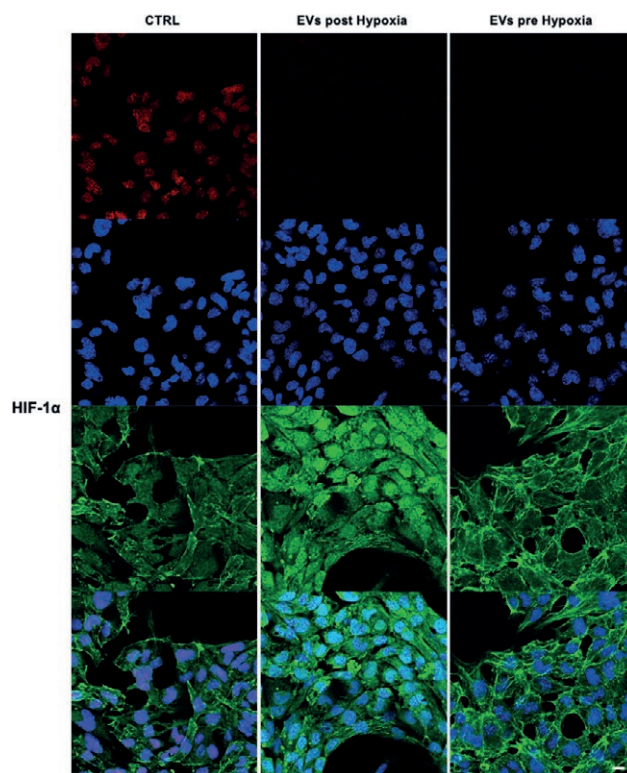


Figure 2. HIF-1 α expression in HL-1 at Confocal Microscopy in CTRL, post hypoxia and pre hypoxia. HIF-1 α is highly expressed in the CTRL while it decreases with EVs treatment both in post Hypoxia and pre hypoxia. Scale bar: 20 μ m.

DISCUSSION

The principal mechanism of response to hypoxia is that involves hypoxia inducible factors (HIFs)[16]. HIF-1 α proteins is continuously synthesized, but under normoxic

conditions they are rapidly degraded by the ubiquitin-proteasome system [17]. HIF-1 α is stabilized by low oxygen availability controlling the expression of a multitude of genes involved in different processes like angiogenesis,

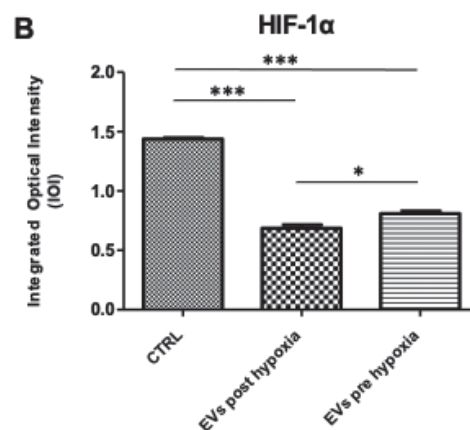
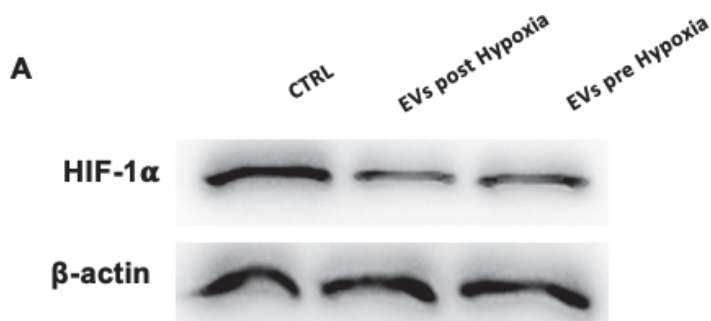


Figure 3. HIF-1 α protein expression in HL-1 in CTRL, post hypoxia and pre hypoxia. (A) HIF-1 α specific band protein expression. (B) Densitometric analysis of HIF-1 α normalized with β -actin. *** p <0.001; * p <0.05.

cell survival, metabolism, and metastasis [18]. Hypoxia, in which HIF-1 α is stabilized, can involve the heart following various pathological conditions leading to cardiomyopathies [19]. Even in vivo, an increase in HIF-1 α protein levels was detected in heart samples from patients with cardiomyopathy, indicating that the HIF pathway is activated during the progression of the disease [20]. The results obtained show that HIF-1 α protein levels decrease with EVs treatment both in post-hypoxia and pre-hypoxia conditions. These data indicate a protective effect against hypoxia from EVs at this molecular level.

ACKNOWLEDGMENTS

This paper is supported by OT and FD research funds (OT60/2020 and FD60/2020).

REFERENCES

- Balligand, J.L., et al. (1992) Control of Cardiac-Muscle Cell-Function by an Endogenous Nitric-Oxide Signaling System. *Clin Res.* 40:A200-A200. doi:10.1097/FJC.0000000000001037.
- Suematsu, N., et al. (2003) Oxidative stress mediates tumor necrosis factor-alpha-induced mitochondrial DNA damage and dysfunction in cardiac myocytes. *Circulation.* 107:1418-1423. doi:10.1161/01.cir.0000055318.09997.1f.
- Babior, B.M. (2000) Phagocytes and oxidative stress. *Am J Med.* 109:33-44. doi:10.1016/s0002-9343(00)00481-2.
- Nakayama, K., Kataoka, N. (2019) Regulation of Gene Expression under Hypoxic Conditions. *Int J Mol Sci.* 20:3278. doi:10.3390/ijms20133278.
- Murry C.E., Jennings R.B., Reimer K.A. (1986) Preconditioning with ischemia: a delay of lethal cell injury in ischemic myocardium. *Circulation* 74:1124-1136. doi:10.1161/01.cir.74.5.1124
- Zarndt, R., et al. (2015) Cardiac responses to hypoxia and reoxygenation in *Drosophila*. *Am J Physiol Regul Integr Comp Physiol.* 309:R1347-57. doi:10.1152/ajpregu.00164.2015.
- Lu, L., et al. (2015) Myocardial Infarction: Symptoms and Treatments. *Cell Biochem Biophys.* 72:865-867. doi:10.1007/s12013-015-0553-4.
- Prabhakar, N.R., Semenza, G.L. (2012) Adaptive and maladaptive cardiorespiratory responses to continuous and intermittent hypoxia mediated by hypoxia-inducible factors 1 and 2. *Physiol Rev.* 92: 967-1003. doi:10.1152/physrev.00030.2011.
- Raposo, G., Stoorvogel, W. (2013) Extracellular vesicles: exosomes, microvesicles, and friends. *J Cell Biol.* 200(4):373-83. doi:10.1083/jcb.201211138.
- Wiklander, O.P.B., et al. (2019) Advances in therapeutic applications of extracellular vesicles. *Sci Transl Med.* 11(492):eaav8521. doi:10.1126/scitranslmed.aav8521.
- Fonticoli, L., et al. (2022) A Narrative Review: Gingival Stem Cells as a Limitless Reservoir for Regenerative Medicine. *Int J Mol Sci.* 23:4135. doi:10.3390/ijms23084135.
- Diomede, F., et al. (2022) Decellularized Dental Pulp, Extracellular Vesicles, and 5-Azacytidine: A New Tool for Endodontic Regeneration. *Biomedicines.* 10:403. doi:10.3390/biomedicines10020403.
- Silvestro, S., et al. (2020) Extracellular Vesicles Derived from Human Gingival Mesenchymal Stem Cells: A Transcriptomic Analysis. *Genes.* 11:118. doi:10.3390/genes11020118
- Marconi, G.D., et al. (2022) The Beneficial Effect of Carvacrol in HL-1 Cardiomyocytes Treated with LPS-G: Anti-Inflammatory Pathway Investigations. *Antioxidants (Basel).* 11(2):386. doi:10.3390/antiox11020386.
- Marconi, G.D., et al. (2021) Transforming Growth Factor-Beta1 and Human Gingival Fibroblast-to-Myofibroblast Differentiation: Molecular and Morphological Modifications. *Front Physiol.* 21:676512. doi:10.3389/fphys.2021.676512.
- Salceda, S., Caro, J. (1997) Hypoxia-inducible factor 1alpha (HIF-1alpha) protein is rapidly degraded by the ubiquitin-proteasome system under normoxic conditions. Its stabilization by hypoxia depends on redox-induced changes. *J Biol Chem.* 272(36):22642-7. doi:10.1074/jbc.272.36.22642.
- Srinivas, V., et al. (1999) Characterization of an oxygen/redox-dependent degradation domain of hypoxia-inducible factor alpha (HIF-alpha) proteins. *Biochem Biophys Res Commun.* 260(2):557-61. doi:10.1006/bbrc.1999.0878.
- Salceda, S., Caro, J. (1997) Hypoxia-inducible factor 1alpha (HIF-1alpha) protein is rapidly degraded by the ubiquitin-proteasome system under normoxic conditions. Its stabilization by hypoxia depends on redox-induced changes. *J Biol Chem.* 272:22642-22647. doi:10.1074/jbc.272.36.22642.
- Davies, S.W., Wedzicha, J.A. (1993) Hypoxia and the heart. *Br Heart J.* 69(1):3-5. doi:10.1136/hrt.69.1.3.
- Hölscher, M. et al. (2012) Unfavourable consequences of chronic cardiac HIF-1 α stabilization. *Cardiovasc Res.* 94(1):77-86 doi:10.1093/cvr/cvs014.



Citation: Francesco Valente, Oriana Trubiani, Tonino Traini (2022) The role of the applied load in bone homeostasis and its implications in implant dentistry: a mini-review. *Italian Journal of Anatomy and Embryology* 126(2): 39-42. doi: 10.36253/ijae13786

Copyright: © 2022 Francesco Valente, Oriana Trubiani, Tonino Traini. This is an open access, peer-reviewed article published by Firenze University Press (<http://www.fupress.com/ijae>) and distributed under the terms of the Creative Commons Attribution License, which permits unrestricted use, distribution, and reproduction in any medium, provided the original author and source are credited.

Data Availability Statement: All relevant data are within the paper and its Supporting Information files.

Competing Interests: The Author(s) declare(s) no conflict of interest.

The role of the applied load in bone homeostasis and its implications in implant dentistry: a mini-review

FRANCESCO VALENTE^{1,2,*}, ORIANA TRUBIANI^{1,2}, TONINO TRAINI^{1,2}

¹ Department of Innovative Technologies in Medicine & Dentistry, University “G. d’Annunzio” of Chieti-Pescara, Via dei Vestini 31, 66100 Chieti, Italy; tonino.traini@unich.it (T.T.); oriana.trubiani@unich.it (O.T.)

² Electron Microscopy Laboratory, University “G. d’Annunzio” of Chieti-Pescara, Via dei Vestini 31, 66100 Chieti, Italy

*Corresponding author. E-mail: francesco.valente@unich.it

Abstract. The aim of this work is to carry out a review about the role of applied load on bone development and homeostasis and its implications in dental implantology. The history of theoretical bone physiology has been evaluated in detail. The modern theory of bone physiology is consistent with the integration among regional acceleratory phenomenon, Utah paradigm, and mechanostat hypothesis: bone modelling and remodelling respond to pleiotropic stimuli. To date, several histologic, in silico and in vitro studies in implant dentistry corroborate the theories about bone physiology. However, each evaluation method has pros and cons, providing analytical data that can only be used to esteem the in vivo behaviour of the bone-implant system. There is the need of further research with highly validated methods and improved measurement devices, to better integrate data from different research types. This would progressively lead to more structured comprehension of the in vivo performance of dental implants and their surrounding bone, and hopefully to a clear definition of the impact of loading on implant failure.

Keywords: applied load, bone homeostasis, bone physiology, bone adaptation, dental implants, mechanical factors.

INTRODUCTION

Mainly three kinds of factors control the bone tissue development and morphology: genetic, epigenetic, and environmental factors (Frost 2001). Among the environmental, it has always been studied if the mechanical agents (applied load), could be considered paramount factors affecting the bone homeostasis. In dentistry field, it might be an enormous advantage to predict the bone response and adaptation to the applied load, in both qualitative and quantitative manner. This because of every dentistry procedure is finalized to comply with the occlusal load, most of all in the implantology field, where achieving an adequate osteointegration is mandatory for a suc-

successful treatment. The purpose of this mini-review is therefore to outline a historical overview about the role of loading on bone development and homeostasis, to highlight its key implications in implant dentistry and to establish whether the current knowledge is able to predict the bone response to the applied load.

HISTORY AND CURRENT KNOWLEDGE OF BONE HOMEOSTASIS

In 1892, Julius Wolff argued that mathematical laws are the major controllers of the process of bone remodelling, and that it results from mechanical load (Wolff 1892). Beginning in 1930, however, it was argued that osteoblasts and osteoclasts, the effector cells of bone, were responsible for the health or disease of the tissue and that they act under the control of non-mechanical agents. In 1960, all these laws and theories were summoned into the theory of bone physiology called “the paradigm of 1960”. The modern theory of bone physiology called “the Utah paradigm” was born. In 1964, during a historic workshop at the University of Utah. A new element in bone physiology was introduced: the biomechanical mechanisms, acting on a tissue level (Frost 2000). It replaced and integrated Wolff’s law and the paradigm of 1960. Remodelling, modelling, and repair

were identified as biological mechanisms which directly act on bone tissue. The bone acquired a mechanical competence. In 1987, Frost introduced the concept of dynamic interaction between form and function of the bone with the “mechanostatic theory” (Frost 1987). Frost argued that remodelling, modelling and repair determine the structural adaptation of the bone to different demands. This happens in the general context of four levels (windows) of ascending mechanical stress. The transition from one window to another is established threshold values of microstrain. The activation of each adaptive process requires the attainment of a threshold value of microstrain, defined as minimum effective strain (MES) (Figure 1). In association with loading, Frost described the Regional Accelerating Phenomenon (RAP) as a biological local factor for the control of bone adaptation. It is an acceleration of the physiological process of tissue healing (both soft and hard tissues), localized in the site insulted by a micro-damage (Frost 1983).

Mechanostatic theory considers load as the main actor on bone adaptation, producing different effects depending on function of the peak level of microstrain. The frequency of load can play an equally important role. The entity of load determines the number of activated cells, while the level of strain is responsible for the strength of osteoblastic activity (Forwood and Turner 1995). After, Turner formulated the following mathematical equation (1):

$$E = K_1 \sum_{i=1}^n \varepsilon_i f_i \quad (1)$$

where the strain stimulus E , with a proportionality constant K_1 , depends on the entity of the strain and its frequency of the load application f . When the frequency of application of the load is zero ($f = 0$) the stimulus is absent ($E = 0$) (Turner 1998). Figure 2 summarizes the current knowledge about bone homeostasis.

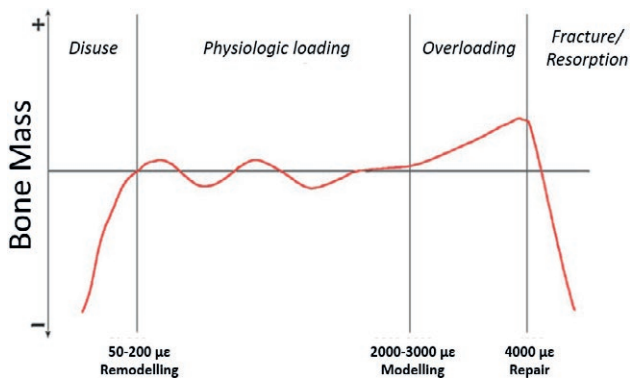


Figure 1. Bone response to applied load following the mechanostat theory. *Window of disuse:* bone exposed to low or without load has very low or zero deformation and undergoes resorption, until reaching a new equilibrium between load and strain. *Window of physiologic load:* the bone exposed to physiologic load presents a continuous remodelling with the achievement of mass balance between resorption and apposition, with a preservation of the bone mass. *Window of overload:* the bone exposed to a load greater than the physiologic limit presents a high deformation and gets a mass gain (corticalization) until reaching a new balance between load and deformation. *Window of fracture:* the bone exposed to a load greater than the limit of the overload fractures and resorbs. Y axis: generic bone mass; x axis: microstrain (ε).

APPLIED LOAD ON THE BONE-IMPLANT SYSTEM: HISTOLOGICAL AND MECHANICAL FINDINGS

Dental implants transmit loading forces from the dental arches to the jaw bones. Bone stability around the margins of fixtures is one of the key factors for long-term implant success. However, the biomechanical mechanisms related to implant failure remains unknown (Pesqueira et al. 2014). The main factors that determine the mechanical properties of bone are the collagen fibres orientation (BCFO) and the matrix mineralization

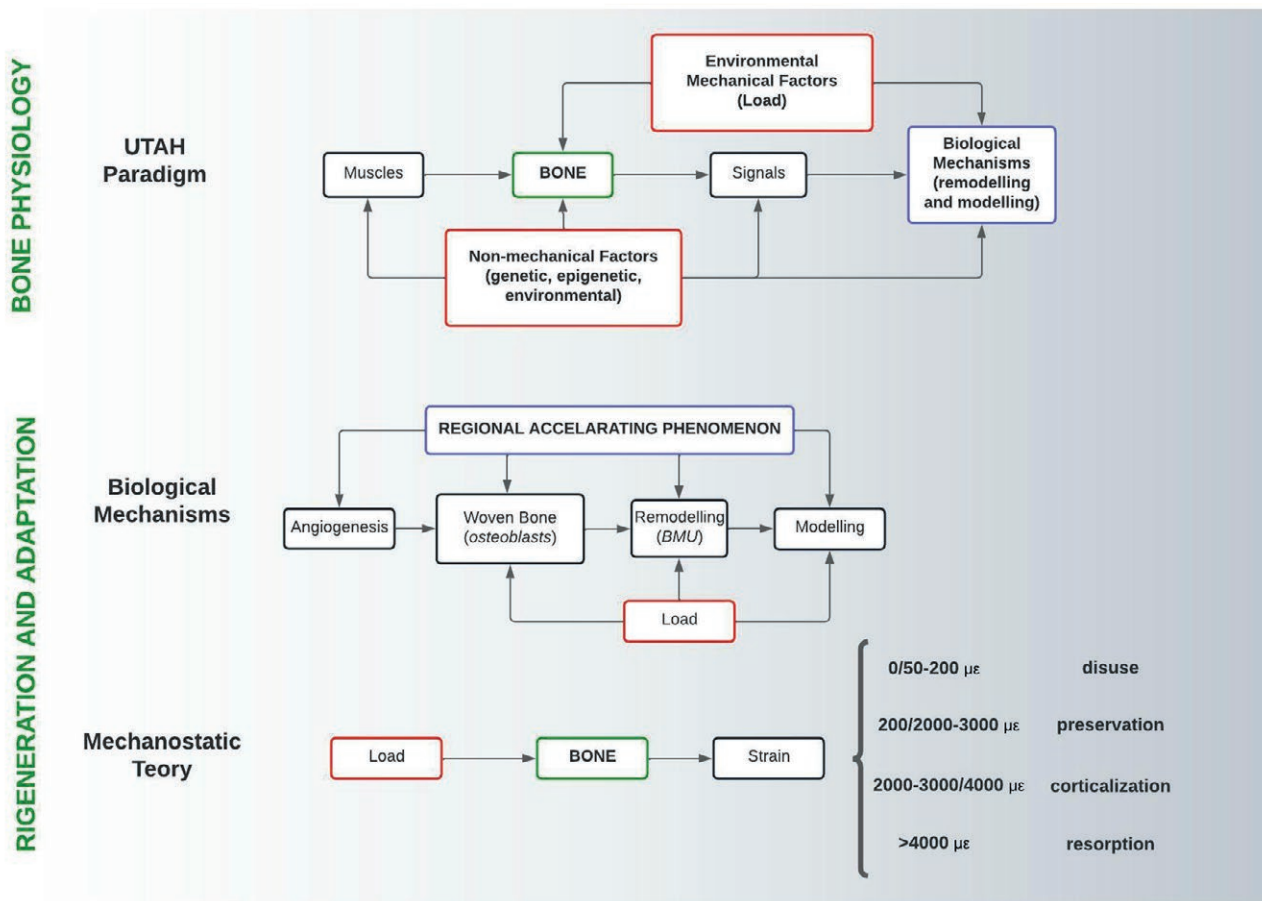


Figure 2. Schematic representation of current knowledge about bone homeostasis. The Utah paradigm gives an important role to both non-mechanical and mechanical factors in determining the balance between bone health and disease with the action of biological mechanisms of modelling and remodelling. This basic mechanism has got continuous feedback modulations. Their maximum expressions are the regenerative and adaptive processes through secondary interactions operated by RAP and mechanisms from mechanostatic theory. RAP: Regional Accelerating Phenomenon; BMU: Bone Multicellular Unit.

degree (Wang et al. 2001). Applied load has a profound effect on BCFO: transversely oriented collagen fibres show the best resistance to compression strength, while longitudinally oriented collagen fibres show the best resistance to shear and traction strengths (Riggs et al. 1993). The predominance of transverse BCFO was noted around an overloaded fractured dental implant after 5 years of function (Traini et al. 2006). In contrast, around unloaded dental implants, there was a predominance of longitudinal BCFO (Traini et al. 2007), along with low mineral density (Traini et al. 2007). These histological findings are consistent with in silico studies (Alemayehu and Jeng 2021). However, high-level validation of Finite Element Analysis using in vivo experiments is still rare in the dental implant field, therefore the precision and accuracy of this kind of studies are still questionable (Chang et al. 2018). In vitro studies concerning

the use of strain gauges to evaluate the mechanical stress on bone have been performed. However, when complex geometry is involved in the analysis, it is difficult to determine the analytical solution (Pesqueira et al. 2014). Finally, due to the anisotropic property of the bone, the multitude of factor influencing bone homeostasis, and the inherent limitation of each analysis' method, to date it is difficult to have an in vivo appraisal of the weight of each factor and of the clear impact of masticatory function on periimplant bone adaptation. Further research is needed in this intent.

CONCLUSIONS

The conclusion of this mini-review can be summarized as follows:

1. Applied load is an environmental factor influencing bone homeostasis, in terms of both entity and frequency of application.
2. Experimental findings on bone surrounding dental implants confirms point 1.
3. In dentistry there is lack of findings to clinically predict the periimplant bone adaptation.
4. To date, the major drawback of the in silico, in vitro and in vivo studies available is the difficulty to interconnect their findings for a thorough comprehension of the bone-implant system response to the applied load.
5. Stated the above, it would be highly desirable to have a continuous quantitative control of occlusal loading on dental implants. This would make us able to modulate the mechanical stress in order to build a mechanically competent bone.

ACKNOWLEDGMENTS

This research received no external funding.

BIBLIOGRAPHY

- Alemayehu D-B, Jeng Y-R. 2021. Three-Dimensional Finite Element Investigation into Effects of Implant Thread Design and Loading Rate on Stress Distribution in Dental Implants and Anisotropic Bone. *Materials*. 14(22):6974.
- Chang Y, Tambe AA, Maeda Y, Wada M, Gonda T. 2018. Finite element analysis of dental implants with validation: to what extent can we expect the model to predict biological phenomena? A literature review and proposal for classification of a validation process. *Int J Implant Dent*. 4(1):7.
- Forwood MR, Turner CH. 1995. Skeletal adaptations to mechanical usage: results from tibial loading studies in rats. *Bone*. 17(4 Suppl):197S-205S.
- Frost H. 1983. The Regional Acceleratory Phenomenon: A Review. *Henry Ford Hospital Medical Journal*. 31(1):3-9.
- Frost HM. 1987. Bone "mass" and the "mechanostat": a proposal. *Anat Rec*. 219(1):1-9.
- Frost HM. 2000. The Utah paradigm of skeletal physiology: an overview of its insights for bone, cartilage and collagenous tissue organs. *J Bone Miner Metab*. 18(6):305-316.
- Frost HM. 2001. From Wolff's law to the Utah paradigm: Insights about bone physiology and its clinical applications. *Anat Rec*. 262(4):398-419.
- Pesqueira AA, Goiato MC, Filho HG, Monteiro DR, Santos DM dos, Haddad MF, Pellizzer EP. 2014. Use of Stress Analysis Methods to Evaluate the Biomechanics of Oral Rehabilitation With Implants. *Journal of Oral Implantology*. 40(2):217-228.
- Riggs CM, Lanyon LE, Boyde A. 1993. Functional associations between collagen fibre orientation and locomotor strain direction in cortical bone of the equine radius. *Anatomy and Embryology*. 187(3). [accessed 2020 Aug 21]. <http://wblldb.lievers.net/10189855.html>.
- Traini T, De Paoli S, Caputi S, Iezzi G, Piattelli A. 2006. Collagen fiber orientation near a fractured dental implant after a 5-year loading period: case report. *Implant Dent*. 15(1):70-76.
- Traini Tonino, Degidi M, Iezzi G, Artese L, Piattelli A. 2007. Comparative evaluation of the peri-implant bone tissue mineral density around unloaded titanium dental implants. *J Dent*. 35(1):84-92.
- Traini T., Degidi M, Murmura G, Piattelli A, Caputi S. 2007. Bone microstructure evaluation near unloaded dental implants combining confocal scanning laser microscopy, circularly polarized light microscopy, and SEM backscattered electrons imaging. *Int J Immunopathol Pharmacol*. 20(1 Suppl 1):37-41.
- Turner CH. 1998. Three rules for bone adaptation to mechanical stimuli. *Bone*. 23(5):399-407.
- Wang X, Bank RA, TeKoppele JM, Agrawal CM. 2001. The role of collagen in determining bone mechanical properties. *J Orthop Res*. 19(6):1021-1026.
- Wolff J. 1892. *Das Gesetz der Transformation der Knochen*. Reprint der Ausg. Berlin, Hirschwald, 1892. Wessinghage D, editor. Stuttgart: Schattauer (Reihe: "Reprints medizinhistorischer Schriften").



Citation: Valentina Botondi, Ebe D'Adamo, Oriana Trubiani, Diego Gazzolo (2022) Presepsin: a biomarker of early-onset neonatal sepsis. *Italian Journal of Anatomy and Embryology* 126(2): 43-45. doi: 10.36253/ijae-13787

Copyright: © 2022 Valentina Botondi, Ebe D'Adamo, Oriana Trubiani, Diego Gazzolo. This is an open access, peer-reviewed article published by Firenze University Press (<http://www.fupress.com/ijae>) and distributed under the terms of the Creative Commons Attribution License, which permits unrestricted use, distribution, and reproduction in any medium, provided the original author and source are credited.

Data Availability Statement: All relevant data are within the paper and its Supporting Information files.

Competing Interests: The Author(s) declare(s) no conflict of interest.

Presepsin: a biomarker of early-onset neonatal sepsis

VALENTINA BOTONDI^{1,*}, EBE D'ADAMO¹, ORIANA TRUBIANI², DIEGO GAZZOLO¹

¹ Neonatal Intensive Care Unit, G. d'Annunzio University, Chieti, Italy

² Department of Innovative Technologies in Medicine & Dentistry, University "G. D'Annunzio", Chieti, Italy

*Corresponding author. E-mail: valentina.botondi.91@gmail.com

Abstract. Neonatal early-onset sepsis represents one of the most common diseases leading to morbidity and mortality in preterm infants. A prompt diagnosis is still a challenge in the clinical practice due to several biases affecting the current standard of care performance. In this regard, the soluble cluster of differentiation CD14 subtype, namely Presepsin, has been shown to be a promising diagnostic biomarker of sepsis in newborns. Although Presepsin provides high accuracy and short results output, its reliability in daily clinical practice is still an issue that needs further investigation. Therefore, in the present review we offer an overview of Presepsin role as diagnostic tool of early-neonatal onset sepsis.

Keywords: presepsin, newborns, early onset sepsis.

1. INTRODUCTION

Neonatal sepsis is still a major cause of morbidity and mortality in NICUs (Shah BA and Padbury JF) with an incidence of 12–17% in very low birth weight infants (Shane AL et al).

The definition of early-onset sepsis (EOS) is still debated since symptoms are non-specific. However, among several EOS classification the one commonly accepted is “a bacterial infection occurring in the first 3 days of life” (Ahmed AM et al).

At present, EOS diagnosis is mainly based on blood culture, C-reactive protein (CRP) and Procalcitonin (PCT) blood assessment although their poor performance in terms of accuracy and diagnostic value (Poggi C et al). Nonetheless, several bias such as gestational age and hypoxia have been shown to affect CRP and PCT reliability suggesting the need of new diagnostic tools (Van Maldeghem I et al). Recently, presepsin (P-SEP), the soluble cluster of differentiation CD14 subtype (sCD14-ST), has been shown to be an early diagnostic tool of sepsis in adults, children and newborns (Montaldo P et al; Botondi V et al).

In the present review we offer an update of recent advances in the use of P-SEP as a biomarker of EOS in newborns.

2. RESEARCH STRATEGY

We searched in the PubMed database for the period 2011 to 2022 all records matching the terms “Newborns”, “Presepsin” and “Early onset sepsis”. We found 6 records in whom P-SEP was assessed specifically as an early onset sepsis diagnosis biomarker.

3. CONTENT

3.1 P-SEP molecule

P-SEP can be defined as a truncated form of CD14 that is a cell surface glycoprotein expressed by various innate immunity cells, like monocytic and neutrophils. CD14 receptor has a high-affinity for bacterial lipopolysaccharides and activates the toll-like receptor 4-specific proinflammatory signaling cascade. At the end of the process, P-SEP is released in the blood stream (Mussap M et al).

3.2 P-SEP accuracy

The P-SEP sensitivity and specificity as predictor of EOS are shown in Table 1. In detail, a wide heterogeneity among the studies has been found. In particular P-SEP: i) sensitivity ranged from 66 to 97% and specificity from 75 to 100%, ii) cut-off references values ranged from 304.5 ng/L to 1442 ng/L. Nonetheless, a series of limitations have been also reported affecting its accuracy such as: i) the different monitoring time points (from birth to 72h); ii) different studied populations (preterm and term), and iii) different measurement techniques. In

particular, 4 out of 6 studies used CLEIA assay that is to date the main assessment technique providing results output within 15' (Seliem W and Sultan AM). Moreover, 2 out of 6 series performed P-SEP measurement by ELISA assay, that can provide results output about 1-h (Alhadj M and Farhana A). Another issue deserving further consideration resides in the possibility that, similarly to CRP and PCT, perinatal asphyxia (PA) and gestational age could somewhat affect P-SEP reliability as early biomarker of EOS (Botondi V et al). Recently, P-SEP blood and urine levels of PA newborns have been found not to be affected by PA and/or multiorgan failure.

4. DISCUSSION

Despite recent advances in EOS management the early mortality rate is still high (about 50%) particularly in preterm infants (Maddaloni C et al). The main weakness points regard EOS non-specific symptoms, the low predictive value of diagnostic parameters to date standard of care suggesting a pivotal role for new diagnostic markers (Poggi C et al; Van Maldeghem I et al). On this scenario, the need of new tools able to early provide useful information to frontline physicians on the occurrence of EOS is of utmost relevance. In this respect, P-SEP *pros* and *cons* need to be considered (Poggi C et al). From one hand *pros* regard its: i) measurability in non-invasive biological fluids (i.e. saliva and urine) (Biria M et al; Koh J et al), ii) speed activation and early peak of concentration after 3h from EOS occurrence (Maddaloni C et al) iii) results output in 15 minutes (Maddaloni C et al). On the other hand, *cons* regard the: i) small number of patients enrolled in the studies, ii) lack of consensus on a valuable P-SEP cut-off value, iii) studies heterogeneity in inclusion and exclusion cri-

Table 1. Available studies of Presepsin as predictor of early onset sepsis.

Population	Fluid	Assay	Time-points	P-SEP cut-off (ng/L)	SE (%)	SP (%)	Ref.
T	PB	C	birth	539.0	80.0	75.0	16
T	PB	C	48-72h	672.0	97.0	98.0	9
PT	CB	E	birth	1442.0	NA	NA	12
PT	PB	C	birth	453.0	66.0	84.0	6
PT	PB	C	12h	653.0	88.0	94.0	6
PT	PB	C	24h	788.0	93.0	100.0	6
PT	PB	C	48h	744.0	79.0	92.0	6
T	PB	C	T*	304.5	95.8	84.9	17
T	PB	E	24h	480.0	96.77	95.0	18

Abbreviations: T, term; PT, preterm; PB, peripheral blood; CB, cord blood; C, CLEIA; E, ELISA; d, days; NA, not available; SE, sensitivity; SP, specificity; Ref, references; T*, before and after therapy.

teria, monitoring time-points and assay used for P-SEP measurement (CLEIA vs ELISA), and iv) potential biases due to associated adverse perinatal conditions (maternal diseases, acute/chronic hypoxia, prematurity) (Botondi V et al; Poggi C et al). Altogether, despite today P-SEP constitutes a promising early biomarker of EOS its inclusion in clinical guidelines requires the fulfilment of the aforementioned critical points.

ACKNOWLEDGMENTS

This research received no external funding.

REFERENCES

- Ahmed A. M., Mohammed A. T., Bastawy S., Attalla H. A., Yousef A. A., Abdelrazek M. S., Fransawy Alkomos M., & Ghareeb A. (2019) Serum Biomarkers for the Early Detection of the Early-Onset Neonatal Sepsis: A Single-Center Prospective Study. *Adv neonatal care*. 19(5):E26–E32.
- Alhadj M., & Farhana A. (2022). Enzyme Linked Immunosorbent Assay. In *StatPearls*. StatPearls Publishing.
- Biria M., Sattari M., Vahid Golpayegani M., & Kooshki F. (2010) Association of salivary sCD14 concentration levels with early childhood caries. *Iran J immunol*. 7(3):193–197.
- Botondi V., D'Adamo E., Plebani M., Trubiani O., Perrotta M., Di Ricco L., Spagnuolo C., De Sanctis S., Barbante E., Strozzi M. C., Maconi A., Gazzolo F., Betti M., Roveta A., Levantini G., & Gazzolo D. (2022) Perinatal presepsin assessment: a new sepsis diagnostic tool?. *Clin Chem Lab Med*. 60(8):1136–1144.
- Botondi V., Pirra A., Strozzi M., Perrotta M., Gavilanes D., Di Ricco L., Spagnuolo C., Maconi A., Rocchetti A., Mazzucco L., Balbo V., Schena F., Stelitano G., Oddi A., Dotta A., Bersani I., Sannia A., Peila C., Bertino E., Bianco I., Gazzolo D. (2022) Perinatal asphyxia partly affects presepsin urine levels in non-infected term infants. *Clin Chem Lab Med*. 60(5):793–799.
- Chen L., Xiao T., Luo Y., Qiu Q., Que R., Huang X., & Wu D. (2017) Soluble CD14 subtype (sCD14-ST) is a biomarker for neonatal sepsis. *Int J Clin Exp Pathol*. 10(9):9718–9724.
- Gad G. I., Shinkar D. M., Kamel El-Din M. M., & Nagi H. M. (2020) The Utility of Soluble CD14 Subtype in Early Diagnosis of Culture-Proven Early-Onset Neonatal Sepsis and Prediction of Outcome. *Am J perinatal*. 37(5):497–502.
- Koh J. H., Lee S., Kim H. S., Lee K., Lee C. S., Yoo S. A., Lee N., & Kim W. U. (2020) Development of Monitoring System for Assessing Rheumatoid Arthritis within 5 Minutes Using a Drop of Bio-Fluids. *J Clin Med*. 9(11):3499.
- Maddaloni C., De Rose D. U., Santisi A., Martini L., Caoci S., Bersani I., Ronchetti M. P., & Auriti C. (2021) The Emerging Role of Presepsin (P-SEP) in the Diagnosis of Sepsis in the Critically Ill Infant: A Literature Review. *Int J Mol Sci*. 22(22):12154.
- Montaldo P., Rosso R., Santantonio A., Chello G., & Giliberti P. (2017) Presepsin for the detection of early-onset sepsis in preterm newborns. *Pediatr res*. 81(2):329–334.
- Motalib T.A., Khalaf F.A., Hendawy G.R., Kotb S.E., Ali A.M., & Sharnoby A.E. (2015) Soluble CD 14-subtype (Presepsin) and Hcpicidin as Diagnostic and Prognostic markers in Early Onset Neonatal Sepsis.
- Mussap M., Noto A., Fravega M., & Fanos V. (2011) Soluble CD14 subtype presepsin (sCD14-ST) and lipopolysaccharide binding protein (LBP) in neonatal sepsis: new clinical and analytical perspectives for two old biomarkers. *J Matern Fetal Neonatal Med*. 24(2):12–14.
- Ozdemir A. A., & Elgormus Y. (2017) Diagnostic Value of Presepsin in Detection of Early-Onset Neonatal Sepsis. *Am J perinatol*. 34(6):550–556.
- Poggi C., Lucenteforte E., Petri D., De Masi S., & Dani C. (2022). Presepsin for the Diagnosis of Neonatal Early-Onset Sepsis: A Systematic Review and Meta-analysis. *AMA Pediatr*. e221647.
- Poggi C., Vasarri M. V., Boni L., Pugni L., Mosca F., & Dani C. (2020) Reference ranges of Presepsin in preterm infants in the first 48 h of life: A multicenter observational study. *Clin Chim Acta*. 508:191–196.
- Seliem W., & Sultan A. M. (2018) Presepsin as a predictor of early onset neonatal sepsis in the umbilical cord blood of premature infants with premature rupture of membranes. *Pediatr Int*. 60(5):428–432.
- Shah B. A., & Padbury J. F. (2014) Neonatal sepsis: an old problem with new insights. *Virulence*. 5(1):170–178.
- Shane A. L., Sánchez P. J., & Stoll B. J. (2017) Neonatal sepsis. *Lancet*. 390(10104):1770–1780.
- Van Maldeghem I., Nusman C. M., & Visser D. H. (2019) Soluble CD14 subtype (sCD14-ST) as biomarker in neonatal early-onset sepsis and late-onset sepsis: a systematic review and meta-analysis. *BMC immunol*. 20(1):17.



Citation: Martina Ceci, Manuela Iezzi, Marco Trerotola (2022) Autophagy inhibitors in the treatment of colorectal cancer: a brief review. *Italian Journal of Anatomy and Embryology* 126(2): 47-49. doi: 10.36253/ijae-13788

Copyright: ©2022 Martina Ceci, Manuela Iezzi, Marco Trerotola. This is an open access, peer-reviewed article published by Firenze University Press (<http://www.fupress.com/ijae>) and distributed under the terms of the Creative Commons Attribution License, which permits unrestricted use, distribution, and reproduction in any medium, provided the original author and source are credited.

Data Availability Statement: All relevant data are within the paper and its Supporting Information files.

Competing Interests: The Author(s) declare(s) no conflict of interest.

Autophagy inhibitors in the treatment of colorectal cancer: a brief review

MARTINA CECI^{1,2,*}, MANUELA IEZZI^{1,2}, MARCO TREROTOLA^{1,3}

¹ Center for Advanced Studies and Technology (CAST), University "G. d'Annunzio", 66100 Chieti, Italy

² Department of Neurosciences, Imaging and Clinical Sciences, University "G. d'Annunzio", 66100 Chieti, Italy

³ Department of Medical, Oral and Biotechnological Sciences, University "G. d'Annunzio", 66100 Chieti, Italy

*Corresponding author. E-mail: martina.ceci@unich.it

Abstract. Colorectal cancer (CRC) is the third most frequent cancer. The first-line adjuvant or neoadjuvant chemotherapy is represented by 5-fluorouracil (5-FU) but its application is limited due to induction of chemoresistance. Recent studies showed that the 5-FU resistance in CRC is closely related to the activation of autophagy. During human carcinogenesis, autophagy has been demonstrated to play opposite roles of inhibitor or promoter of malignant progression depending on initial or advanced stages of growth. Currently, the autophagy inhibitor chloroquine (CQ) and its derivate, hydroxychloroquine (HCQ), are the only Food and Drug Administration (FDA)-approved drugs for clinical use. This review summarizes recent findings on the possible employment of autophagy inhibitors to overcome chemoresistance engaged in the CRC.

Keywords: colorectal cancer, chemotherapy, chemoresistance, autophagy, chloroquine.

INTRODUCTION

Colorectal cancer (CRC) is the third most frequent cancer and the second most common cause of cancer-related deaths worldwide (Sung *et al.*, 2021). In the clinical practice, surgery is the primary option followed by chemotherapy. 5-fluorouracil (5-FU) is utilized for treatment of patients with stage II/III CRC (Blondy *et al.*, 2020), thus representing the best first-line adjuvant or neoadjuvant chemotherapeutic choice.

The clinical applications of 5-FU have been significantly limited due to the development of innate or acquired chemoresistance in most patients with metastatic CRC. To enhance the efficacy and reduce the adverse effects of 5-FU, novel combination treatments are being currently employed, such as FOLFOX (5-FU, Leucovorin with Oxaliplatin) or FOLFIRI (5-FU, Leucovorin with Irinotecan), which improved both efficacy and survival rate in CRC patients (Alnuqaydan *et al.*, 2020).

Despite the impact of the chemoresistance on CRC patients survival, the mechanisms underlying chemoresistance to 5-FU remain poorly understood. Recent studies have shown that the 5-fluorouracil resistance in CRC is closely related to the activation of cancer cell autophagy (Alnuqaydan *et al.*, 2020; Mulcahy Levy *et al.*, 2017).

Finding effective chemotherapeutic drugs for CRC remains one of the greatest challenges in long-term management of metastatic CRC patients. This review describes the most recent findings that demonstrated the complex mechanisms underlying chemoresistance in CRC patients. Among these mechanisms, several studies have shown that autophagy plays a vital role in the resistance to tumor chemotherapeutic treatments.

THE DUAL ROLE OF AUTOPHAGY IN CRC

Autophagy protects cancer cells from stress-induced damage, promoting resistance and reducing the efficiency of anti-cancer drugs. Therefore, identifying the mechanisms underlying autophagy modulation during malignant progression might provide new approaches in the pharmacological treatment of CRC (Yang *et al.*, 2015)

Autophagy is an evolutionarily conserved catabolic process by which the cells degrade and recycle their internal components. Autophagy is accomplished through the formation of autophagosomes, double-membraned vesicles that engulf cellular proteins and organelles for delivery to the lysosomes and following degradation. The formation and turnover of the autophagosomes is divided into five stages: initiation, nucleation of the autophagosome, elongation of the autophagosome membrane, fusion with the lysosome for cargo degradation (Boya *et al.*, 2013).

A large number of studies have demonstrated that autophagy plays a dual role in cancer progression. In early stages of tumorigenesis autophagy maintains cellular homeostasis by degrading damaged and toxic cellular components. On the other hand, autophagy facilitates malignant progression at later stages by promoting cancer cell growth under stressful stimuli such as hypoxia and nutrient deprivation (Singh *et al.*, 2017).

Despite the complex interplay between the tumor suppressive and promoting role in cancer, autophagy is a novel and promising target for CRC therapy. The use of various autophagy inhibitors has been recently proposed as a novel strategy to sensitize CRC cells to chemotherapy and overcome drug resistance.

AUTOPHAGY IN CLINICAL PRACTICE

Recently, several extensive studies on autophagy clarified the possible molecular mechanisms engaged in the CRC progression, in order to hypothesize and develop novel targeted drugs. Currently, chloroquine (CQ) and its derivate, hydroxychloroquine (HCQ), are the only Food and Drug Administration (FDA)-approved drugs for clinical use. These drugs inhibit the last step of the autophagic flux, by deacidifying the lysosomes and compromising the activity of most lysosomal proteases (Mulcahy Levy *et al.*, 2017). This results in the accumulation of late endosomes and redirection of their content to the extracellular space.

The SOX2/ β -catenin/Beclin1/autophagy signaling axis has been shown to be able to regulate chemo-resistance, cancer stem cells properties, and epithelial-mesenchymal transition in CRC (Zhu *et al.*, 2021). This is particularly important in clinical contexts, as inhibition of cancer autophagy could lead to strong reduction of metastatic spreading.

Another study reported that targeting ERK leads to the production of high concentrations of reactive oxygen species (ROS) which turn on autophagy by activating ROS/p53. The combination of autophagy and ERK inhibition was shown to have a strong additive antitumor effect in CRC treatment (Mi *et al.*, 2021).

Wang *et al.* recently suggested a novel potential therapeutic strategy for CRC by combined inhibition of PI3K/Akt/mTOR signaling and autophagy. This combination therapy was demonstrated to lead to a significant increase of apoptosis (Wang *et al.*, 2021).

Several experimental evidence is now accumulating that provides insight in the molecular mechanisms underlying autophagy and chemoresistance in CRC. One of these studies conducted by Chen and colleagues identified serine hydroxymethyltransferase-2 (SHMT2) as a critical regulator of 5-FU chemoresistance in CRC. The authors showed that patients with CRC that expressed low levels of SHMT2 exhibited resistance to 5-FU and suffered of worse prognosis compared with patients with CRC expressing high levels of SHMT2 (Chen *et al.*, 2021). Under 5-FU treatment, SHMT2 depletion promotes autophagy and inhibits apoptosis, thus suggesting that the lethality of 5-FU treatment to CRC cells was enhanced by treatment with CQ *in vitro* and *in vivo* (Chen *et al.*, 2021).

Other mechanisms involved in 5-FU resistance of CRC have been described. Among them, Sun and colleagues performed a series of *in vitro* and *in vivo* experiments and found that ubiquitin-specific protease 11 could induce resistance to 5-FU activating autophagy

through AMPK/Akt/mTOR pathway via stabilization of valosin-containing protein (Sun *et al.*, 2021). Although the clinical outcome of using autophagy inhibitors for treatment of CRC patients is still under assessment (Mohsen *et al.*, 2022) and clinical trials are now in progress (<https://clinicaltrials.gov/ct2/results?cond=Colorectal+Cancer&term=Autophagy>), there is strong experimental evidence that these agents should be employed in combination with specific signaling modulators in order to maximize their potential.

CONCLUSIONS

We summarized here the most recent findings of the involvement of autophagy in the chemoresistance in CRC. CQ and HCQ appear to represent efficient inhibitors of autophagy both *in vitro* and *in vivo*, making them potential targets for future cancer therapies.

Taken together, these findings contribute to improving our understanding of the molecular mechanisms of chemotherapy resistance in CRC. The signaling targets described here may contribute to the development of novel combined therapeutic strategies for treatment of CRC based on modulation of cell autophagy, providing a potentially novel window of intervention to reduce chemoresistance.

REFERENCES

- Sung H, Ferlay J, Siegel RL, et al. (2021) Global Cancer Statistics 2020: GLOBOCAN Estimates of Incidence and Mortality Worldwide for 36 Cancers in 185 Countries. *CA Cancer J Clin.* 71(3):209–249.
- Blondy S, David V, Verdier M, Mathonnet M, Perraud A, Christou N (2020) 5-Fluorouracil resistance mechanisms in colorectal cancer: From classical pathways to promising processes. *Cancer Science.* 111:3142–3154.
- Alnuqaydan Am, Rah B, Almutary Ag, Chauhan SS (2020) Synergistic antitumor effect of 5-fluorouracil and withaferin-A induces endoplasmic reticulum stress-mediated autophagy and apoptosis in colorectal cancer cells. *Am J Cancer Res.* 10(3):799-815
- Mulcahy Levy JM, Towers CG, Thorburn AN (2017) Targeting autophagy in cancer. *Nat Rev Cancer.* 17:528-542.
- Yang X, Yu D, Yan F, et al. (2015) The role of autophagy induced by tumor microenvironment in different cells and stages of cancer. *Cell & Bioscience.* 5(14):1-11.
- Boya P, Reggiori F, Codogno P (2013) Emerging regulation and functions of autophagy. *Nat Cell Biology.* 15(7):713-721.
- Singh Ss, Vats S, Yi-Qian Chia A, et al. (2017) Dual role of autophagy in hallmarks of cancer. *Oncogene.* 37:1142–1158.
- Zhu Y, Huang S, Chen S, et al. (2021) SOX2 promotes chemoresistance, cancer stem cells properties, and epithelial–mesenchymal transition by β -catenin and Beclin1/autophagy signaling in colorectal cancer. *Cell Death and Disease.* 12:1-16.
- Mi W, Wang C, Luo G, et al. (2021) Targeting ERK induced cell death and p53/ROS-dependent protective autophagy in colorectal cancer. *Cell Death Discovery.* 7:1-11.
- Wang J, Liang D, Zhang X, et al. (2021) Novel PI3K/Akt/mTOR signaling inhibitor, W922, prevents colorectal cancer growth via the regulation of autophagy. *Int J Oncol.* 58:70-82.
- Chen J, Na R, Xiao C, et al. (2021) The loss of SHMT2 mediates 5-fluorouracil chemoresistance in colorectal cancer by upregulating autophagy. *Oncogene.* 40:3974-3988.
- Sun H, Wang R, Liu Y, Mei H, Liu X, Peng Z (2021) USP11 induce resistance to 5-Fluorouracil in Colorectal Cancer through activating autophagy by stabilizing VCP. *J Cancer.* 12:2317-2325.
- Mohsen S, Sobash Pt, Algwaiz GF, et al. (2022) Autophagy agents in clinical trials for cancer therapy: a brief review. *Curr. Oncol.* 29:1695-1708.



Citation: Stefano Oliva, Antonio Scarano, Oriana Trubiani, Bruna Sinjari, Maurizio Piattelli (2022) A prospective, blinded, randomized-controlled study on regressive bone modeling around dental implants with different machined coronal portion. *Italian Journal of Anatomy and Embryology* 126(2): 51-54. doi: 10.36253/ijae-13789

Copyright: ©2022 Stefano Oliva, Antonio Scarano, Oriana Trubiani, Bruna Sinjari, Maurizio Piattelli. This is an open access, peer-reviewed article published by Firenze University Press (<http://www.fupress.com/ijae>) and distributed under the terms of the Creative Commons Attribution License, which permits unrestricted use, distribution, and reproduction in any medium, provided the original author and source are credited.

Data Availability Statement: All relevant data are within the paper and its Supporting Information files.

Competing Interests: The Author(s) declare(s) no conflict of interest.

A prospective, blinded, randomized-controlled study on regressive bone modeling around dental implants with different machined coronal portion

STEFANO OLIVA*, ANTONIO SCARANO, ORIANA TRUBIANI, BRUNA SINJARI, MAURIZIO PIATTELLI

Department of Innovative Technologies in Medicine and Dentistry, University "G. d'Annunzio" Chieti-Pescara, 66100 Chieti, Italy

*Corresponding author. E-mail: oliva.stefano@hotmail.com

Abstract. Scientific evidence showed variable degree of marginal bone loss around dental implants both during integration process and during function. Among the different factors that seem to influence this process, a crucial role is up to the crestal module of dental implant. In order to reduce marginal bone loss, different configurations of crestal module have been proposed. The aim of this study was to evaluate the efficacy of half treatment dental implants with a coronal smooth portion of 3.5 mm compared to rough surfaced implants with a smooth coronal portion of 0.5mm, to reduce peri-implant marginal bone resorption. The degree of marginal bone loss was assessed through radiological measures. In addition, soft tissues healing was evaluated through plaque index and gingival index. The results demonstrated a significantly ($p= 0.03$) lower value of MBL (mean 0.7mm), than HT implants (mean 1.03mm) after 1year functional loading. In conclusion, use of FT implants could be determine better results in order to reduce MBL.

Keywords: marginal bone loss, osteointegration, implants surface treatment.

INTRODUCTION

The clinical success of titanium dental implants is based on a high percentage of bone/implant contact, and for this purpose, dental implants surfaces have been treated in order to trigger cellular actions and enhance the proper integration of the implant with the surrounding bone. (Scarano et al., 2007) (Shin et al., 2006) The crest module of an implant is defined as the active part of the implant and serves as the region which receives the crestal stresses after loading. (Hermann et al., 2000) Some studies have demonstrated that peak stress, especially shear stress, was concentrated at the crestal bone area. (Hansson, 1999) for example a rough surface of suitable micro-architecture and/or a micro-thread. It is furthermore suggested that retention elements at the implant neck will counteract marginal bone resorption in

accordance with Wolff's law. This paper is a revision of: Hansson, S. (1997).

Others claimed that a smooth, parallel-sided crest module may result in shear stresses in this region and described a positive correlation between surface roughness parameters and interfacial shear strength and suggested that microthreads at implant neck may counteract marginal bone resorption. (Oh et al., 2002; Jung et al., 1996)

On the other side, Iezzi et al (Iezzi et al., 2012), showed that machined implants present higher bone-implant-contact percentage (92.7%) than sandblasted implants (85%). Thus, if on one hand, rough implant surfaces enhance initial bone formation and osteointegration, on the other hand they seem to increase adhesion and colonization of oral plaque. (Quirynen et al., 2006) split-mouth, single-blind study followed the colonization of 'pristine' sulci created in 42 partially edentulous patients during implant surgery (e.g. abutment connection

Implants with a shorter polished smooth collar have proven to be more effective in decreasing marginal bone loss. Nowadays, gold standard is represented by rough surface implants. Thus, the aim of the present study was to radiographically analyze MBL on HT and FT implants after 1 year follow-up.

MATERIAL AND METHODS

Three partially edentulous patients who needed two single implant supported restorations afferent to department of "Oral Surgery" at University of studies "G.D'Annunzio" Chieti-Pescara, Abruzzo, Italy, were recruited for this study.

Inclusion criteria

Patients between 21 and 75 years old of both sexes; partially edentulous who needed at least 2 single implant rehabilitations on both the upper and lower jaws;

Exclusion criteria

General contraindications to implant surgery; smoking more than 10 cigarettes per day; patients irradiated to the head or neck during preceding 2 years; patients undergoing chemotherapy during preceding 1 year; patients with uncontrolled diabetes; post-extraction sites with acute or purulent infections; patients with uncontrolled systemic or metabolic disease; patients with periodontal disease.

Patients were randomised according to a split-mouth design to receive one half treatment implant (HT) (Group I) and one full-treatment implant (FT) (Group II). Two different titanium dental implants surface (Resista, Omegna, VB, Italy) have been used:

- Full treatment implants (Fig 1, A):

Micro-Nano Dae surface treatment speeds up bone recovery processes, removing the manufacturing organic residuals along with Argon Plasma Cleaning. It increases surface and wettability improving the first fibrin bridges adhesion, protein adhesion and cellular adhesion through the nano-micrometric roughness suitable for actine filaments anchoring. Finally, it changes the chemical surface increasing cellular proliferation and vitality. (Giordano et al., 2006) (Morra et al., 2006) (Cassinelli et al., 2003) (Park and Davies, 2000) (Neugebauer et al., 2009) four different implants were used for immediate loading. The following implants were placed 3 months after tooth extraction: screw with low thread profile and anodic oxidized surface (LPAOS

- Half treatment implants, also named hybrid surface, present 3,5mm machined neck in order to reduce bacteria adhesion and plaque colonization. (Fig 1, B)

In order to evaluate radiographic change of the peri-implant bone, intraoral radiograph, applying the parallel ray technique, was realized at T0 and at 1-year follow-up. The mean value between mesial and distal region was used as the primary outcome measure for this study and indicated as marginal bone loss (MBL). The commercially available Rinn film holders, used for intraoral radiographs applying the parallel X-ray technique, were customized using a silicone key for the exact reposition in every subject, in order to obtain a highly reproducible and faithful radiograph. To evaluate the difference between the groups, Student's- test was used. Significance was set at $p < 0.05$.

Evaluation of soft tissues comprehended:

- Plaque index (PI)
- Gingival index (GI)

Probing depth of peri-implants pocket (PPD). (L e, 1967)

RESULTS

All implants were perfectly osseointegrated and clinically stable. No implant fractures occurred.

FT implants presented a significantly ($p=0.03$) lower value of MBL (mean 0.7mm), than HT implants (mean 1.03mm) after 1 year functional loading.

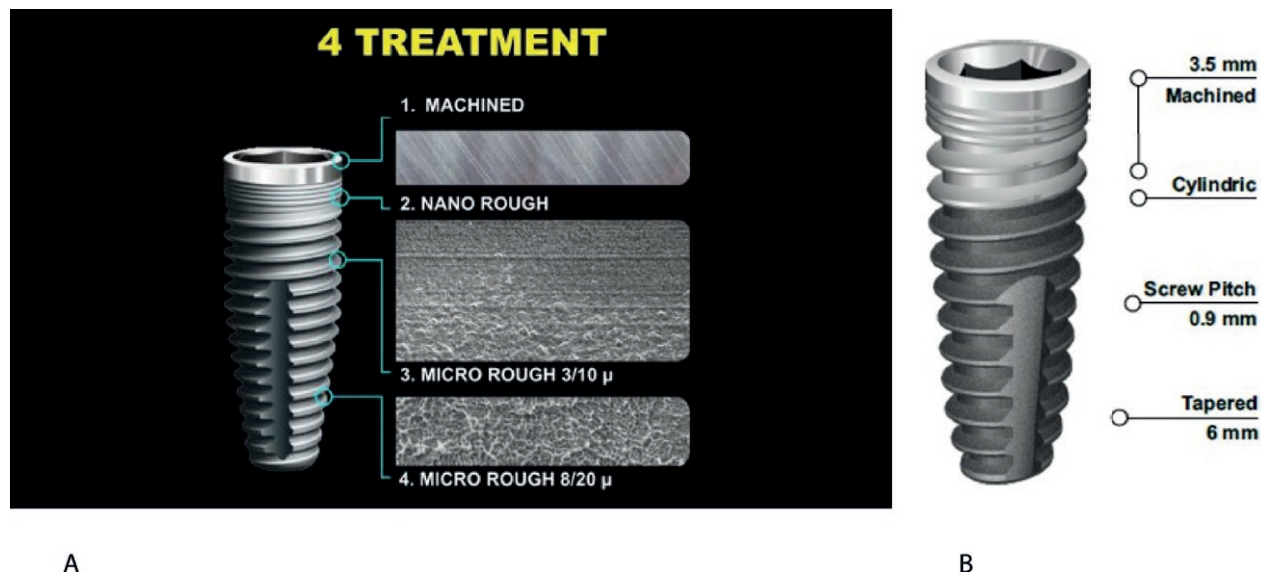


Figure 1. Full treatment implant (A) and Half treatment implant (B).

Table 1. Values of marginal bone loss (MBL) in one half treatment implant (HT) and one full-treatment implant (FT) at 1 year follow-up.

Pz	MBL 1Y	
	HT	FT
1	1	0.7
2	1.2	0.8
3	0.9	0.6

Table 2. Clinical parameters, Gingival index (GI), Plaque index (PI), Probing depth of peri-implants pocket (PPD) of soft tissues.

	GI	PI	PPD
HT	0.66	0.66	2.91mm
FT	1	1	2.33mm

DISCUSSION

Success of endosseous implants treatment is strictly related to maintaining of hard and soft tissues health and stability, in order to obtain osseointegration. Surface topography and roughness influence the early healing stages of bone integration. Also, surface properties such as wettability, topography, and charge are known to affect endothelial cells attachment and growth, likely by altering the rate of the amount of adsorbed proteins and their conformational change (Scarano et al., 2017).

In this study comparison were made between two different implants neck designs on soft and hard tissue responses. Results showed how after 1 year of functional loading, there is a largest share of MBL to hybrid surface implants than rough surfaced implants. As regards soft tissues health, HT implants revealed better results than FT implants. Results analysis confirmed literature scores. Presence of surface roughness on implants neck seems to reduce MBL. Soft tissues seem to benefice to smooth surface on implants neck, confirming the reduction of bacterial adhesion and plaque colonization.

This study can be intended as a pilot study since the small size patients examined does not allow to draw definite conclusions.

FUNDING

This research receives no external funding.

REFERENCES

Cassinelli, C., Morra, M., Bruzzone, G., Carpi, A., Di Santi, G., Giardino, R., Fini, M., 2003. Surface chemistry effects of topographic modification of titanium dental implant surfaces: 2. In vitro experiments. *Int. J. Oral Maxillofac. Implants* 18, 46–52.

Giordano, C., Sandrini, E., Busini, V., Chiesa, R., Fumagalli, G., Giavaresi, G., Fini, M., Giardino, R., Cigada, A., 2006. A new chemical etching pro-

- cess to improve endosseous implant osseointegration: in vitro evaluation on human osteoblast-like cells. *Int. J. Artif. Organs* 29, 772–780. <https://doi.org/10.1177/039139880602900807>
- Hansson, S., 1999. The implant neck: smooth or provided with retention elements. A biomechanical approach. *Clin. Oral Implants Res.* 10, 394–405. <https://doi.org/10.1034/j.1600-0501.1999.100506.x>
- Hermann, J.S., Buser, D., Schenk, R.K., Higginbottom, F.L., Cochran, D.L., 2000. Biologic width around titanium implants. A physiologically formed and stable dimension over time. *Clin. Oral Implants Res.* 11, 1–11. <https://doi.org/10.1034/j.1600-0501.2000.011001001.x>
- Iezzi, G., Vantaggiato, G., Shibli, J.A., Fiera, E., Falco, A., Piattelli, A., Perrotti, V., 2012. Machined and sandblasted human dental implants retrieved after 5 years: a histologic and histomorphometric analysis of three cases. *Quintessence Int. Berl. Ger.* 1985 43, 287–292.
- Jung, Y.C., Han, C.H., Lee, K.W., 1996. A 1-year radiographic evaluation of marginal bone around dental implants. *Int. J. Oral Maxillofac. Implants* 11, 811–818.
- Löe, H., 1967. The Gingival Index, the Plaque Index and the Retention Index Systems. *J. Periodontol.* 38, Suppl:610-616. <https://doi.org/10.1902/jop.1967.38.6.610>
- Morra, M., Volpe, C.D., Siboni, S., 2006. Comment to the paper: Enhancing surface free energy and hydrophilicity through chemical modification of microstructured titanium implant surfaces, by F. Rupp, L. Scheideler, N. Olshanska, M. de Wild, M. Wieland, J. Geis-Gerstorfer. *J. Biomed. Mater. Res. A* 79, 752–754; author reply 755-757. <https://doi.org/10.1002/jbm.a.31044>
- Neugebauer, J., Weinländer, M., Lekovic, V., von Berg, K.-H.L., Zoeller, J.E., 2009. Mechanical stability of immediately loaded implants with various surfaces and designs: a pilot study in dogs. *Int. J. Oral Maxillofac. Implants* 24, 1083–1092.
- Oh, T.-J., Yoon, J., Misch, C.E., Wang, H.-L., 2002. The causes of early implant bone loss: myth or science? *J. Periodontol.* 73, 322–333. <https://doi.org/10.1902/jop.2002.73.3.322>
- Park, J.Y., Davies, J.E., 2000. Red blood cell and platelet interactions with titanium implant surfaces. *Clin. Oral Implants Res.* 11, 530–539. <https://doi.org/10.1034/j.1600-0501.2000.011006530.x>
- Quirynen, M., Vogels, R., Peeters, W., van Steenberghe, D., Naert, I., Haffajee, A., 2006. Dynamics of initial subgingival colonization of “pristine” peri-implant pockets. *Clin. Oral Implants Res.* 17, 25–37. <https://doi.org/10.1111/j.1600-0501.2005.01194.x>
- Scarano, A., Carinci, F., Quaranta, A., Iezzi, G., Piattelli, M., Piattelli, A., 2007. Correlation between implant stability quotient (ISQ) with clinical and histological aspects of dental implants removed for mobility. *Int. J. Immunopathol. Pharmacol.* 20, 33–36. <https://doi.org/10.1177/039463200702001s08>
- Scarano, A., Piattelli, A., Quaranta, A., Lorusso, F., 2017. Bone Response to Two Dental Implants with Different Sandblasted/Acid-Etched Implant Surfaces: A Histological and Histomorphometrical Study in Rabbits. *BioMed Res. Int.* 2017, 8724951. <https://doi.org/10.1155/2017/8724951>
- Shin, Y.-K., Han, C.-H., Heo, S.-J., Kim, S., Chun, H.-J., 2006. Radiographic evaluation of marginal bone level around implants with different neck designs after 1 year. *Int. J. Oral Maxillofac. Implants* 21, 789–794.



Citation: Luigi Falconio, Oriana Trubiani, Diego Gazzolo, Francesco Valente, Tonino Traini (2022) Presepsin assessment in maxillo-facial infections: a new early biomarker of sepsis?. *Italian Journal of Anatomy and Embryology* 126(2):55-58. doi: 10.36253/ijae-13797

Copyright: ©2022 Luigi Falconio, Oriana Trubiani, Diego Gazzolo, Francesco Valente, Tonino Traini. This is an open access, peer-reviewed article published by Firenze University Press (<http://www.fupress.com/ijae>) and distributed under the terms of the Creative Commons Attribution License, which permits unrestricted use, distribution, and reproduction in any medium, provided the original author and source are credited.

Data Availability Statement: All relevant data are within the paper and its Supporting Information files.

Competing Interests: The Author(s) declare(s) no conflict of interest.

Presepsin assessment in maxillo-facial infections: a new early biomarker of sepsis?

LUIGI FALCONIO^{1,*}, ORIANA TRUBIANI¹, DIEGO GAZZOLO², FRANCESCO VALENTE¹, TONINO TRAINI¹

¹ Department of Innovative Technologies in Medicine & Dentistry, University "G. D'Annunzio" of Chieti-Pescara, 66100 Chieti, Italy

² Neonatal Intensive Care Unit, Department of Pediatrics, University G. d'Annunzio, 65100 Chieti, Italy

*Corresponding author. E-mail: luigi.falconio@unich.it

Abstract. Odontogenic infections can cause serious inflammatory problems of the soft and hard tissues in the maxillofacial area up to, albeit in quite remote circumstances, involvement of the brain tissues. In recent years, therefore, a holistic diagnostic-therapeutic approach has been developed in the management of odontogenic infections by carrying out a careful systemic history of the patient who has an infectious condition in the oral cavity. The early detection of systemic sepsis conditions was facilitated using serum biomarkers such as PCR, Procalcitonin (PCT) and Presepsin (PSEP) in hospital emergency rooms. However, even if used in combination, their diagnostic accuracy is such as to suggest the importance of researching new, more specific, and sensitive biomarkers. A total of 9 articles was analyzed to investigate the use of the PSEP as biomarker in the maxillo-facial region infections and including only English-language articles and the electronic search of publications from 1 January 2017 to 31 December 2021. This study aimed to determine the diagnostic value of presepsin in condition of sepsis derived from an odontogenic infection and to evaluate its use in the prognostic evaluation phase of surgical interventions performed in the maxillofacial area.

Keywords: sepsis, dentistry, presepsin, odontology infection.

INTRODUCTION

Odontogenic infection is a type of bacterial infection that can appear in the maxillofacial region (1). When it is affected by the fascial spaces it can cause cavernous sinus thrombosis and sepsis, including facial and cervical necrotizing fasciitis (2). Sepsis (S) can lead to systemic tissue damage, organ failure, and death. Therefore, early S diagnosis can have a significant impact on patient's management and prognosis. On this scenario the assessment in biological fluids of new biomarkers of S can be useful to determine the severity of the patient's inflammatory and infectious conditions (3). More recently, presepsin (PSEP) as an early biomarker of S in adults, pediatric and infant patients has been proposed (4,5).

Table 1. Risk associated with anatomical location.

Risk	Low	Moderate	High	Extreme
Spaces	Vestibular	Submandibular	Lateral pharyngeal	Mediastinum
	Infraorbital	Submental	Retropharyngeal	
	Buccal	Sublingual	Pretracheal	
		Pterygomandibular		
		Submasseteric		
		Temporal		

PSEP or soluble CD14 subtype (sCD14-ST) is a 13kDa fragment derived from the cleavage of CD14, a cell surface antigen cluster marker protein expressed in bone marrow anchored to the membrane of monocytes, macrophages, and polymorphic neutrophils (6,7). CD14 acts as a receptor for lipopolysaccharides complexes (LPS) and for the specific binding protein of LPS (LBP); it can bind to peptidoglycans and other surface structures present in both Gram-Positive and Gram-Negative bacteria. Once bound, the LPS-LBP complex activates the intracellular inflammatory response of the Toll-Like 4 receptor (TLR4) initiating the host inflammatory cascade against the infectious pathogen; phagocytosis and plasma protease activity result in the formation of the sCD14 subtype fragment (8,9).

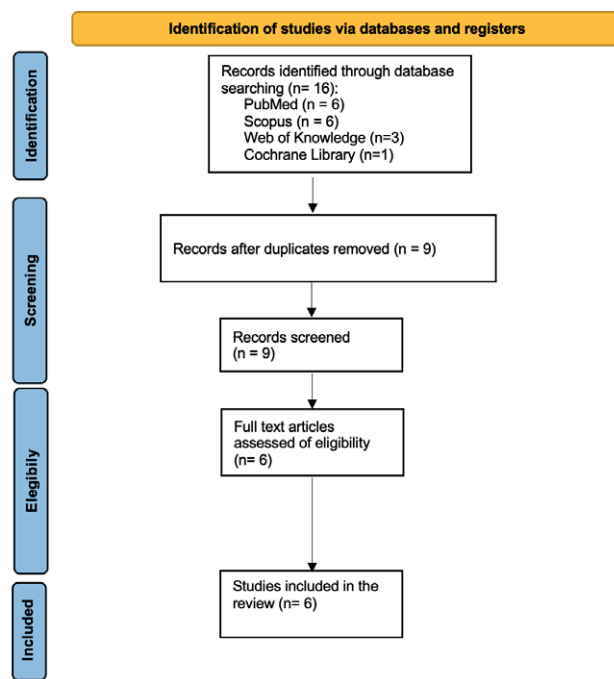
The immune response occurs when various pathogen-associated molecular patterns are into contact with the pathogen, where sCD14 acts as a ubiquitous coreceptor, but sCD14 itself is not a specific factor for sepsis caused by bacterial infection. However, it has been shown that PSEP levels, unlike other inflammatory biomarkers, increase very rapidly (2-4 h) in the presence of systemic infections in adults, children, and newborns, thus determining diagnostic speed and therapeutic possibilities (10,11).

In accordance with previous findings, PSEP has been shown to play a key role in the diagnosis of sepsis caused by various organ infections (12).

The purpose of the present mini review was to offer an update on the potential role of PSEP as an early biomarker of S in patients requiring maxilla facial surgery and/or odontostomathologic care (13,14).

MATERIALS AND METHODS

This mini-review was performed in accordance with the PRISMA (Systematic Reviews and Meta-analyses) statement as shown in Figure 1. Extensive research on the literature and papers related to PSEP used as a diagnostic marker in maxilla-facial infections was performed

**Figure 1.** research method used to identify studies to be included in the review.

on the databases of PubMed (Medline), Scopus, Web of Knowledge, and Cochrane Library. Preferred Reporting Items for the research was performed by using combinations of the following keywords: “sepsis “ AND “dentistry” OR “presepsin “. The search included only English-language articles and the electronic search of publications from 1 January 2017 to 31 December 2021 was conducted. The search strategy

used a combination of free-text words. To exclude duplicates, the references of the identified records were uploaded as Research Information Systems files into Zotero (RRCHNM, Fairfax, Virginia).

RESULTS

The search strategy reported records, including duplicates: **6** from PubMed, **6** from Scopus, **3** from Web of Knowledge, **1** from Cochrane Library. The duplicates were eliminated, thus all the selected databases produced **9** records. Data obtained are the result related to the use of PSEP as a diagnostic marker in the maxillo-facial infections.

DISCUSSION

Odontogenic infections, the most common cause of bacterial infections in the maxillofacial region, rarely progress to sepsis. However, the possibility of progression to sepsis cannot be excluded in cases of moderate or severe infections affected by the fascial spaces (15). According to Kang et al, PSEP can also be useful in determining the severity of odontogenic infection and sepsis, and when combined with existing test methods, it is expected to be better in evaluating patient prognosis. In fact, according to this study, a PSEP level of 671.5 pg/ml or higher for odontogenic infection can be considered an abnormal level (16).

Odontogenic infections can induce the condition of sepsis, caused by the abnormal response of the immune system of our body due to the onset of tissue damage that compromises the functionality of the organs and can lead to death. Furthermore, the COVID-19 pandemic has imposed new difficulties and challenges; for example, the use of tele-dentistry, thus modifying the dental practitioner / patient relationship. Therefore, it would be useful, in dental practice, to introduce the use of markers that can assess the actual risk of sepsis during surgical dental procedures. Several clinical parameters have been used as prognostic indicators for the severity of the infection. C-reactive protein (CRP), Procalcitonin (PCT), fever and anatomical locations have been investigated for the assessment of the extent of odontogenic infections (17). Recently, PSEP was identified as a marker of sepsis, in fact, based on the data collected previously, the sensitivity and specificity of PSEP were 78.95% and 70.83%, respectively. It is reasonable to think that further studies should investigate the use of PSEP as an earlier diagnostic marker of dental infections and as a prognostic tool in the healing processes of oral tissues after surgery, analyzing its concentration not only in serum, but also in other fluids oral such as saliva to reduce the emotional stress of the patients who must undergo the sampling (18).

CONCLUSIONS

Persistent odontogenic infections can be a common cause of sepsis in the head and neck. Infection frequently spreads in a predictable pattern within the fascial spaces of the neck and can result in airway compromise.

The focus of infection was mandibular in 70.1% and maxillary in 29.9%. Further findings regarding biomarkers, including PSEP, would be desirable in the diagnosis of this condition and in the prognosis of oral inflammatory diseases, such as periodontal disease, which can lead to systemic impairment (19,20)

FUNDING

This research received no external funding.

REFERENCES:

1. Kang, E.-S., Lee, J.-H., 2022. Diagnostic value of presepsin in odontogenic infection: a retrospective study. *Maxillofac Plast Reconstr Surg* 44, 22. <https://doi.org/10.1186/s40902-022-00353-7>
2. Abudeev, S.A., Kiselev, K.V., 2018. Cerebrospinal Fluid Presepsin as a Marker of Nosocomial Infections of the Central Nervous System: A Prospective Observational Study. *Front. Neurol.* 9, 58. <https://doi.org/10.3389/fneur.2018.00058>
3. Aliu-Bejta, A., Atelj, 2020. Presepsin values as markers of severity of sepsis. *International Journal of Infectious Diseases* 95, 1–7. <https://doi.org/10.1016>
4. Galliera, E., Massaccesi, L., 2019. Clinical application of presepsin as diagnostic biomarker of infection: overview and updates. *Clinical Chemistry and Laboratory Medicine (CCLM)* 58, 11–17. <https://doi.org/10.1515/cclm-2019-0643>
5. Botondi, V., D'Adamo, E., Plebani, M., 2022. Perinatal presepsin assessment: a new sepsis diagnostic tool? *Clinical Chemistry and Laboratory Medicine (CCLM)* 60, 1136–1144. <https://doi.org/10.1515/cclm-2022-0277>
6. Wu, J., Hu, 2015. Accuracy of Presepsin in Sepsis Diagnosis: A Systematic Review and Meta-Analysis. *PLoS ONE* 10, e0133057. <https://doi.org/10.1371/journal.pone.0133057>
7. Yaegashi, Y., Sato, N., 2005. Evaluation of a newly identified soluble CD14 subtype as a marker for sepsis. *Journal of Infection and Chemotherapy* 11, 234–238. <https://doi.org/10.1007/s10156-005-0400-4>
8. Chenevier-Gobeaux, C., Borderie, 2015. Presepsin (sCD14-ST), an innate immune response marker in

- sepsis. *Clinica Chimica Acta* 450, 97–103. <https://doi.org/10.1016/j.cca.2015.06.026>
9. Memar, M.Y., Baghi, 2019. Presepsin: A promising biomarker for the detection of bacterial infections. *Biomedicine & Pharmacotherapy* 111, 649–656. <https://doi.org/10.1016/j.biopha.2018.12.124>
 10. de Guadiana Romualdo, L.G., Torrella, 2017. Diagnostic accuracy of presepsin (sCD14-ST) as a biomarker of infection and sepsis in the emergency department. *Clinica Chimica Acta* 464, 6–11. <https://doi.org/10.1016/j.cca.2016.11.003>
 11. Yoon, S.H., Kim, 2019. Presepsin as a diagnostic marker of sepsis in children and adolescents: a systematic review and meta-analysis. *BMC Infect Dis* 19, 760. <https://doi.org/10.1186/s12879-019-4397-1>
 12. Koizumi, Y., Sakanashi, 2020. Can presepsin uniformly respond to various pathogens? - an in vitro assay of new sepsis marker -. *BMC Immunol* 21, 33. <https://doi.org/10.1186/s12865-020-00362-z>
 13. Novelli, G., Morabito, 2013. Pathfast Presepsin Assay for Early Diagnosis of Bacterial Infections in Surgical Patients: Preliminary Study. *Transplantation Proceedings* 45, 2750–2753. <https://doi.org/10.1016/j.transproceed.2013.07.021>
 14. Ulla, M., Pizzolato, 2013. Diagnostic and prognostic value of presepsin in the management of sepsis in the emergency department: a multicenter prospective study. *Crit Care* 17, R168. <https://doi.org/10.1186/cc12847>
 15. Marazzi, M.G., Randelli, 2018. Presepsin: A potential biomarker of PJI? A comparative analysis with known and new infection biomarkers. *Int J Immunopathol Pharmacol* 31, 039463201774935. <https://doi.org/10.1177/0394632017749356>
 16. Yang, H.S., Hur, 2018. Prognostic value of presepsin in adult patients with sepsis: Systematic review and meta-analysis. *PLoS ONE* 13, e0191486. <https://doi.org/10.1371/journal.pone.0191486>
 17. Wu, C.-C., Lan, 2017. Comparison of diagnostic accuracy in sepsis between presepsin, procalcitonin, and C-reactive protein: a systematic review and meta-analysis. *Ann. Intensive Care* 7, 91. <https://doi.org/10.1186/s13613-017-0316-z>
 18. Handke, J., Piazza, 2020. Presepsin as a biomarker in perioperative medicine. *Minerva Anestesiol* 86. <https://doi.org/10.23736/S0375-9393.20.14169-5>
 19. Zhang, X., Liu, 2015. The accuracy of presepsin (sCD14-ST) for the diagnosis of sepsis in adults: a meta-analysis. *Crit Care* 19, 323. <https://doi.org/10.1186/s13054-015-1032-4>
 20. Liu, B., Chen, 2013. Diagnostic value and prognostic evaluation of Presepsin for sepsis in an emergency department. *Crit Care* 17, R244. <https://doi.org/10.1186/cc13070>



Citation: Mariangela Mazzone, Maria Carmela Di Marcantonio, Valentina Puca, Beatrice Marinacci, Giulia Nannini, Simone Guarnieri, Amedeo Amedei, Gabriella Mincione, Raffaella Muraro (2022) Effects of *Fusobacterium nucleatum* on migration and cytokines production of ags gastric adenocarcinoma cell line. *Italian Journal of Anatomy and Embryology* 126(2): 59-63. doi: 10.36253/ijae-13798

Copyright: ©2022 Mariangela Mazzone, Maria Carmela Di Marcantonio, Valentina Puca, Beatrice Marinacci, Giulia Nannini, Simone Guarnieri, Amedeo Amedei, Gabriella Mincione, Raffaella Muraro. This is an open access, peer-reviewed article published by Firenze University Press (<http://www.fupress.com/ijae>) and distributed under the terms of the Creative Commons Attribution License, which permits unrestricted use, distribution, and reproduction in any medium, provided the original author and source are credited.

Data Availability Statement: All relevant data are within the paper and its Supporting Information files.

Competing Interests: The Author(s) declare(s) no conflict of interest.

Effects of *Fusobacterium nucleatum* on migration and cytokines production of ags gastric adenocarcinoma cell line

MARIANGELA MAZZONE^{1,*}, MARIA CARMELA DI MARCANTONIO¹, VALENTINA PUCA², BEATRICE MARINACCI², GIULIA NANNINI³, SIMONE GUARNIERI⁴, AMEDEO AMEDEI³, GABRIELLA MINCIONE¹, RAFFAELLA MURARO¹

¹ Department of Innovative Technologies in Medicine & Dentistry, University “G. d’Annunzio Chieti-Pescara, 66100, Chieti, Italy

² Department of Pharmacy, University “G. d’Annunzio” Chieti-Pescara, 66100 Chieti, Italy

³ Department of Experimental and Clinical Medicine, University of Florence, Florence 50134, Italy

⁴ Department of Neuroscience, Center of Advanced Studies and Technology, Imaging and Clinical Sciences, University “G. d’Annunzio” Chieti-Pescara, 66100 Chieti, Italy

*Corresponding author. E-mail: mariangela.mazzone@unich.it

Abstract. Gastric cancer (GC) is the fifth most frequently diagnosed cancer and the third leading cause of cancer death worldwide. *Helicobacter pylori* (*Hp*) infection is an important risk factor for GC. However, the etiology of the tumor is multifactorial, since only 1-3% of infected patients develop cancer. Therefore, attention should be focused on the role of microbiota in gastric tumorigenesis since in some studies an alteration of the microbiota in GC has been shown. *Fusobacterium nucleatum* (*Fn*) has been found in biopsies of patients with GC. However, since its role is not clearly established, this study investigated the effects of *Fn* infection on the human gastric adenocarcinoma cell line AGS. Our results showed that *Fn* co-localized at level of the plasma membrane demonstrating the ability of *Fn* to adhere to AGS cells. In addition, increases in incubation times were associated with its intra-cellular localization with loss of the classic curved rod shape. Interestingly, *Fn* determined a greater capacity of cell migration compared to untreated AGS cells. Moreover, IL-4 expression significantly increased in *Fn* infected GC cells. Since cancer cell migration is an integral component of the metastatic process, additional studies are needed to better understand the mechanisms underlying the *Fn*/host interaction.

Keywords: *Fusobacterium nucleatum*, gastric cancer, IL-4 production.

INTRODUCTION

Gastric cancer (GC) is the third leading cause of cancer deaths worldwide (Ferlay et al., 2021) since most patients are diagnosed with an advanced stage of disease. Thus, great efforts are made on tumor prevention and early diagnosis. *Helicobacter pylori* (*Hp*) infection is the major risk factor for the onset

and evolution of GC, but effectiveness of its eradication by drug therapies is still discussed (Piscione et al., 2021). Actually, it is not clear whether the presence of *Hp* or the imbalanced gastric microbiota generates the conditions for *Hp* or other pathogens colonization. *Fusobacterium nucleatum* (*Fn*), involved in periodontal disease, has been detected also in human tumor samples (Han et al., 2015). Indeed, several studies showed the presence of *Fn* in colorectal adenomas (Gethings-Behncke et al., 2020) and in primary colorectal cancer as compared to healthy tissue (Kim et al., 2020). These data suggest that *Fn* plays a role in the initiation and progression of colorectal tumorigenesis (Abed et al., 2017). *Fn* has also been isolated in esophageal (Yamamura et al., 2017) and gastric cancer (Hsieh et al., 2018). In the intestine *Fn* alters the cellular pathways through FadA, an adhesin that stimulates the proliferation of host cells and regulates inflammatory response (Sahan et al., 2018). Elevated levels of *Fn* were detected in biopsies of patients suffering from GC, associated with low levels of *Hp* (Hsieh et al., 2018). *Hp* colonizes the gastric mucosa through its virulence factors and, by urease enzyme, it raises the gastric pH, making the stomach a more permissive environment towards other pathogens such as *Fn* (Servetas et al., 2016; Hsieh et al., 2018). Periodontal disease has a link with GC (Zhou et al., 2018) and *Fn* could play a key role in making periodontal disease a worsening factor for the development of GC (Flemer et al., 2018; Toma et al., 2018). Therefore, the aim of this study was to evaluate the effects of *Fn* infection on a model of human gastric adenocarcinoma cell line AGS in order to verify whether it affects metastatic behavior.

MATERIALS AND METHODS

Bacterial culture

Fusobacterium nucleatum (ATCC 25586) was cultured as previously reported (Maccelli et al., 2020). Bacteria were harvested by centrifugation at $6000 \times g$ for 10min at 4°C. The bacterial pellets were washed twice, resuspended with phosphate-buffered saline and quantified using a microplate reader.

Cell line culture

Human gastric adenocarcinoma AGS cell line (Cell Lines Services, Eppenheim, Germany) was cultured as previously described (Savino et al., 2022). AGS cells were infected with *Fn* at multiplicity of infection (MOI) of 100-2000. Supernatants were collected after 24h post-infection and used in Luminex Assay.

Confocal microscopy

AGS cells were grown on glass coverslips and infected with *Fn* at different MOI. At the established time they were fixed (2% paraformaldehyde for 10min), treated for 60min with 10% Goat Serum and incubated with primary antibody anti-*Fn* ANT0084 (DIATHEVA, Italy) at 1:100 dilution. Secondary antibody (Alexa Fluor 488 conjugated, Thermo Fisher Scientific, USA) was used at 1:200 dilution. Then, the cells were treated with PHK26 (SIGMA ALDRICH, USA) at 1:1000 dilution to stain AGS cells membrane. Images were obtained using Zeiss LSM800 confocal microscopy and acquired by Zen Blue software (Carl Zeiss, Germany).

Cell migration assay

Cells were infected with *Fn* at a MOI 500-1500 and wound healing scratch assays were performed using noninfected AGS cells as control. Cells were cultured to 95% confluence in 24-well plates and after 24h, a scratch wound was made followed by *Fn* infection. Cellular migration was recorded after 24h and 48h.

Detection and quantification of cytokines with Luminex assay

Expression levels of IFN- γ , IL-1b, IL-4, IL-6, IL-10, IL-17A were determined in AGS cell culture supernatants using Human kits (Milliplex, Merck Millipore, USA) and Luminex MAGPIX detection system following the manufacturer's instructions. The levels of cytokines (pg/ml) were estimated using a 5-parameter polynomial curve (Bio-Plex Manager Software, Bio-Rad, USA).

Statistical analysis

The data are reported as the representative values of three independent experiments.

RESULTS

Localization of Fn after infection of AGS cells by confocal microscopy

Fn localization and its effects on AGS cells morphology were evaluated using a confocal microscope. In Figure 1 orange fluorescence locates AGS cell membrane, while green fluorescence identifies *Fn* as detected using a specific antibody. After 24h, polygonal AGS cells were

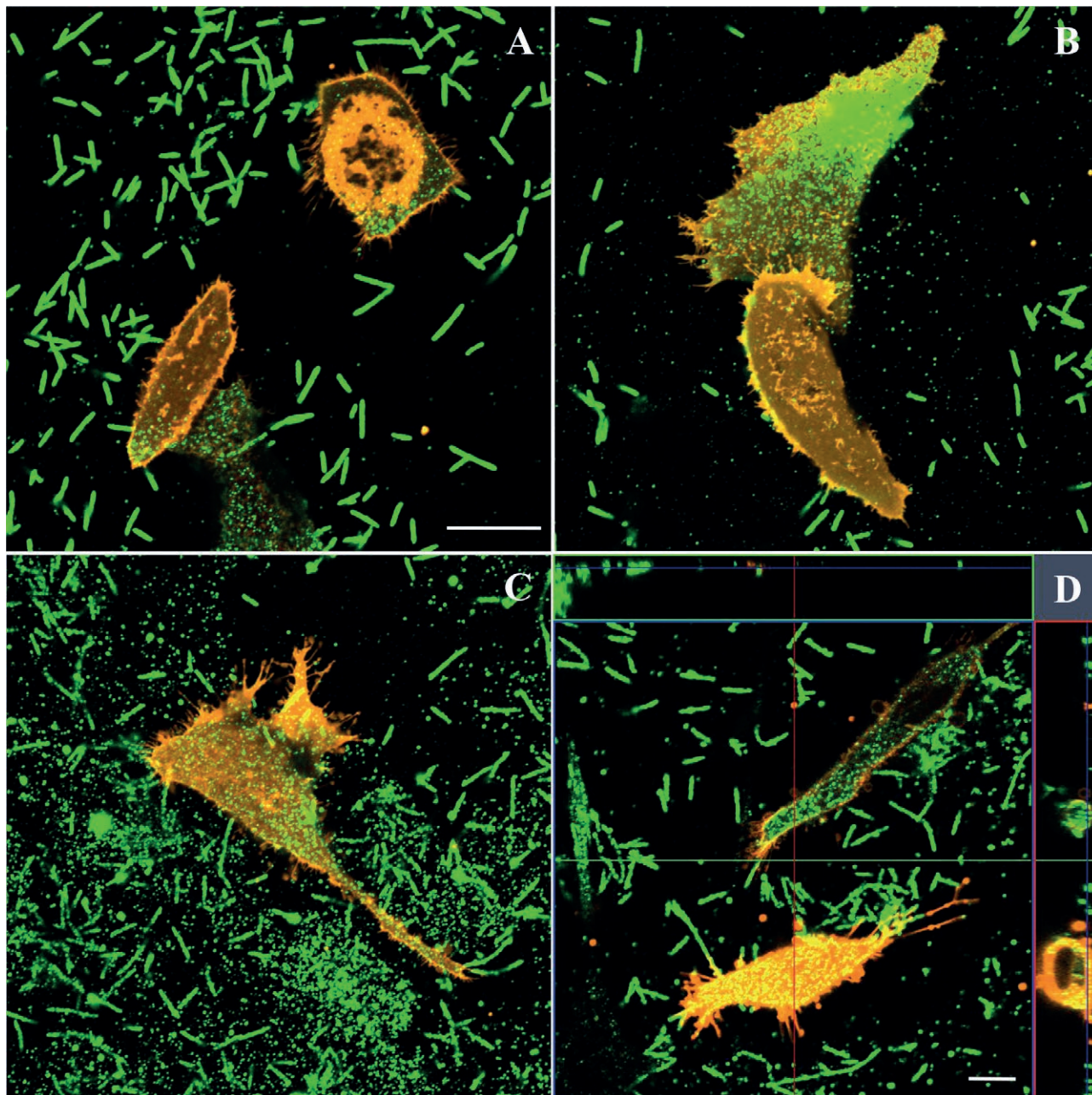


Figure 1. Localization of *Fn* after infection of AGS cells by confocal microscopy. Representative images of co-culture of *Fn* (MOI 100) and AGS cells acquired using confocal microscopy (green and orange fluorescence respectively). Images were captured near the cells contact to coverslip side (A to C) or multiple focal plane (Z stack) to obtain XZ, YZ projection (D). Bar=10 μ m

surrounded by rod shaped bacteria. Interestingly, signals deriving from bacteria in intracellular compartment appeared with a cytoplasmic spotted pattern, (Figure 1A-C). In addition, some AGS cells showed a yellow fluorescence signal, deriving from *Fn* co-localization with AGS cell membrane (Figure 1 B and D).

Effects of Fn infection on migration and cytokine expression in AGS cells

Acquisition of migratory properties is a prerequisite for cancer progression. *Fn* modulates migration and immune cell signaling in colorectal cancer (Casasanta MA et al., 2020).

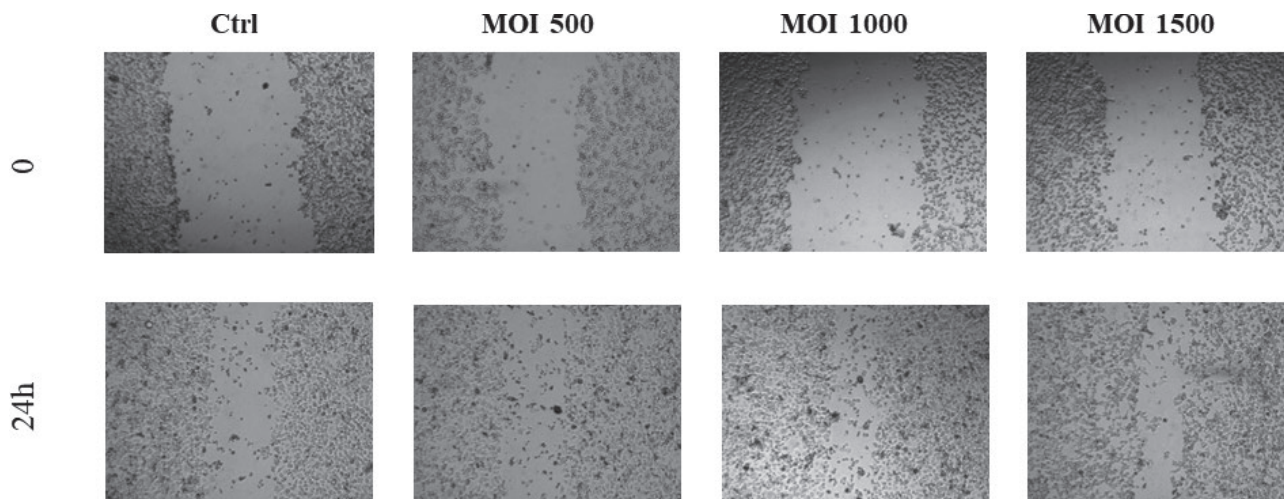


Figure 2. Effects of 24h *Fn* infection at different MOI on migration of AGS cells using a wound healing assay.

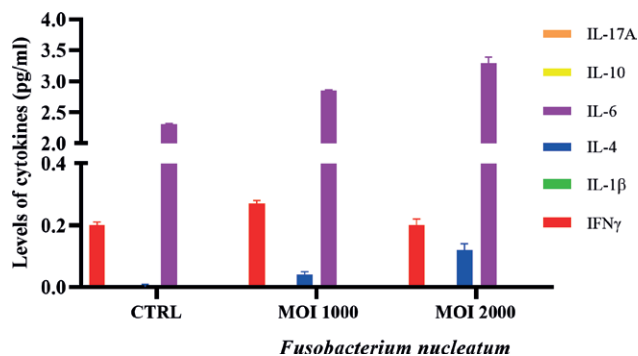


Figure 3. LUMINEX assay to quantify cytokine secretion in cell culture media from AGS cells infected by *Fn*. Infection parameters were MOI 1000 and 2000 *Fn* co-cultured with AGS cells for 24h.

Cell migration of AGS cells was assessed using a wound healing assay after 24h of infection. Our results (Figure 2) demonstrated that *Fn* infection promoted cell migration, as compared to AGS untreated cells.

To find out whether *Fn* was able to induce the secretion of cytokines from these cells, the expressions of IFN- γ , IL-1 β , IL-4, IL-6, IL-10, IL-17A were analyzed in the supernatants of AGS cells collected after 24h of co-culture with *Fn*. Interestingly, while IFN-g showed only a slightly increased at MOI 1000 as compared to control cells, *Fn* infection increased IL-4 and IL-6 from MOI 1000 to MOI 2000, as compared to uninfected cells (Figure 3).

DISCUSSION

The present study showed that *Fn* co-culture of AGS cells caused an increase in cell migration capacity and

induced IL-4 and IL-6 secretion. It is known that IL-4 plays an important role in cancer cell proliferation and migration enhancing the malignant phenotype (Hallett et al., 2012). Moreover, increased plasma IL-4 levels were significantly higher in GC patients than in healthy controls (Cardenas et al., 2018). The preliminary results obtained in this study suggest that IL-4 could increase the migration ability of AGS cells. Further analysis will be needed to verify this hypothesis. Moreover, we demonstrated the adhesion of *Fn* to the plasma membrane of AGS cells and its presence in their cytoplasm. These data are in agreement with the evidence obtained in colorectal adenocarcinoma cells in which the bacterium is internalized by tumor cells (Casasanta et al., 2020). In conclusion, we hypothesize that future studies characterizing how *Fn* influences signaling pathways during cancer development will lead to targeted approaches that could potentially decrease the risk of progression to gastric cancer.

REFERENCES

- Abed J, Maalouf N, Parhi L, Chaushu S, Mandelboim O, Bachrach G. Tumor Targeting by *Fusobacterium nucleatum*: A Pilot Study and Future Perspectives. *Front Cell Infect Microbiol.* 2017 Jun 30;7:295. doi: 10.3389/fcimb.2017.00295
- Cárdenas DM, Sánchez AC, Rosas DA, Rivero E, Papanoni MD, Cruz MA, et al. Preliminary analysis of single-nucleotide polymorphisms in IL-10, IL-4, and IL-4R α genes and profile of circulating cytokines in patients with gastric Cancer. *BMC Gastroenterol.* 2018 Dec 10;18(1):184. doi: 10.1186/s12876-018-0913-9

- Casasanta MA, Yoo CC, Udayasuryan B, Sanders BE, Umaña A, Zhang Y, et al. *Fusobacterium nucleatum* host-cell binding and invasion induces IL-8 and CXCL1 secretion that drives colorectal cancer cell migration. *Sci Signal*. 2020 Jul 21;13(641):eaba9157. doi: 10.1126/scisignal.aba9157
- Ferlay J, Colombet M, Soerjomataram I, Parkin DM, Piñeros M, Znaor A, Bray F. Cancer statistics for the year 2020: An overview. *Int J Cancer*. 2021 Apr 5. doi: 10.1002/ijc.33588
- Flemer B, Warren RD, Barrett MP, Cisek K, Das A, Jeffery IB, et al. The oral microbiota in colorectal cancer is distinctive and predictive. *Gut*. 2018 Aug;67(8):1454-1463. doi: 10.1136/gutjnl-2017-314814
- Gethings-Behncke C, Coleman HG, Jordao HWT, Longley DB, Crawford N, Murray LJ, Kunzmann AT. *Fusobacterium nucleatum* in the Colorectum and Its Association with Cancer Risk and Survival: A Systematic Review and Meta-analysis. *Cancer Epidemiol Biomarkers Prev*. 2020 Mar;29(3):539-548. doi: 10.1158/1055-9965
- Hallett MA, Venmar KT, Fingleton B. Cytokine stimulation of epithelial cancer cells: the similar and divergent functions of IL-4 and IL-13. *Cancer Res*. 2012 Dec 15;72(24):6338-43. doi: 10.1158/0008-5472.CAN-12-3544
- Han YW. *Fusobacterium nucleatum*: a commensal-turned pathogen. *Curr Opin Microbiol*. 2015 Feb;23:141-7. doi: 10.1016/j.mib.2014.11.013
- Hsieh YY, Tung SY, Pan HY, Yen CW, Xu HW, Lin YJ, et al. Increased Abundance of *Clostridium* and *Fusobacterium* in Gastric Microbiota of Patients with Gastric Cancer in Taiwan. *Sci Rep*. 2018 Jan 9;8(1):158. doi: 10.1038/s41598-017-18596-0
- Kim M, Lee ST, Choi S, Lee H, Kwon SS, Byun JH, Kim YA, Rhee KJ, Choi JR, Kim TI, Lee K. *Fusobacterium nucleatum* in biopsied tissues from colorectal cancer patients and alcohol consumption in Korea. *Sci Rep*. 2020 Nov 16;10(1):19915. doi: 10.1038/s41598-020-76467-7
- Maccelli A, Carradori S, Puca V, Sisto F, Lanuti P, Crestoni ME, Lasalvia A, Muraro R, Bysell H, Di Sotto A, Roos S, Grande R. Correlation between the Antimicrobial Activity and Metabolic Profiles of Cell Free Supernatants and Membrane Vesicles Produced by *Lactobacillus reuteri* DSM 17938. *Microorganisms*. 2020 Oct 24;8(11):1653. doi: 10.3390/microorganisms8111653
- Piscione M, Mazzone M, Di Marcantonio MC, Muraro R, Mincione G. Eradication of *Helicobacter pylori* and Gastric Cancer: A Controversial Relationship. *Front Microbiol*. 2021 Feb 4;12:630852. doi: 10.3389/fmicb.2021.630852
- Sahan AZ, Hazra TK, Das S. The Pivotal Role of DNA Repair in Infection Mediated-Inflammation and Cancer. *Front Microbiol*. 2018 Apr 11;9:663. doi: 10.3389/fmicb.2018.00663
- Savino L, Di Marcantonio MC, Moscatello C, Cotellese R, Centurione L, Muraro R, et al. Effects of H₂O₂ Treatment Combined with PI3K Inhibitor and MEK Inhibitor in AGS Cells: Oxidative Stress Outcomes in a Model of Gastric Cancer. *Front Oncol*. 2022 Mar 16;12:860760. doi: 10.3389/fonc.2022.860760
- Servetas SL, Bridge DR, Merrell DS. Molecular mechanisms of gastric cancer initiation and progression by *Helicobacter pylori*. *Curr Opin Infect Dis*. 2016 Jun;29(3):304-10. doi: 10.1097/QCO.0000000000000248
- Toma SC, Ungureanu BS, Patrascu S, Surlin V, Georgescu I. Colorectal Cancer Biomarkers - A New Trend in Early Diagnosis. *Curr Health Sci J*. 2018 Apr-Jun;44(2):140-146. doi: 10.12865/CHSJ.44.02.08
- Yamamura K, Baba Y, Miyake K, Nakamura K, Shigaki H, Mima K, et al. *Fusobacterium nucleatum* in gastroenterological cancer: Evaluation of measurement methods using quantitative polymerase chain reaction and a literature review. *Oncol Lett*. 2017 Dec;14(6):6373-6378. doi: 10.3892/ol.2017.7001
- Zhou Z, Chen J, Yao H, Hu H. *Fusobacterium* and Colorectal Cancer. *Front Oncol*. 2018 Oct 15;8:371. doi: 10.3389/fonc.2018.00371



Citation: Federica De Cecco, Sara Franceschelli, Lorenza Speranza (2022) Inflammatory Bowel Disease (IBD): a novel biological role of saffron petal extracts as a modulator of phlogistic pathway *via* FBW7/NF- κ B in Caco-2 cell line LPS-stimulated. *Italian Journal of Anatomy and Embryology* 126(2): 65-69. doi: 10.36253/ijae-13801

Copyright: © 2022 Federica De Cecco, Sara Franceschelli, Lorenza Speranza. This is an open access, peer-reviewed article published by Firenze University Press (<http://www.fupress.com/ijae>) and distributed under the terms of the Creative Commons Attribution License, which permits unrestricted use, distribution, and reproduction in any medium, provided the original author and source are credited.

Data Availability Statement: All relevant data are within the paper and its Supporting Information files.

Competing Interests: The Author(s) declare(s) no conflict of interest.

Inflammatory Bowel Disease (IBD): a novel biological role of saffron petal extracts as a modulator of phlogistic pathway *via* FBW7/NF- κ B in Caco-2 cell line LPS-stimulated

FEDERICA DE CECCO*, SARA FRANCESCHELLI, LORENZA SPERANZA

Department of Medicine and Aging Sciences, University "G. d'Annunzio" Chieti- Pescara, Via dei Vestini 31, 66100 Chieti, Italy

*Corresponding author. E-mail: federica.dececco@unich.it

Abstract. Inflammatory bowel disease (IBD) is a chronic pathology characterized by extensive inflammation, which causes a functional alteration of the intestinal barrier. Today most of the drugs applied for IBD have adverse consequences. In this scenario, the development of new therapeutic agents for the treatment of IBD is necessary. A new approach to develop effective therapeutic strategies is the study of natural compounds with anti-inflammatory properties. Saffron petals contain flavonolic glycosides (kaempferol), carotenoids (crocin and crocetin) and anthocyanin pigments, with anti-oxidant and anti-inflammatory activity. Recently, kaempferol and crocin identified in Saffron Petal Extract (SPE), has been able to reduce oxidative stress in intestinal epithelial cells. Our aim was to evaluate the therapeutic potential of SPE on inflamed human intestinal Caco2 cells that mimic the intestinal microenvironment. We have demonstrated that SPE, down-regulating the expression of the ubiquitine FBW7, inhibits the degradation of the I κ B- α subunit and keeps NF- κ B in the inactive state. This leads downstream to a reduced activation of inducible molecules (iNOS, COX-2 and HO-1) involved on intestinal inflammatory process. In conclusion, since FBW7 increases in colon tissue of IBD patients, SPE may represent an attractive and promising supplementary treatment for the therapeutic management of IBD with conventional therapies.

Keywords: IBD, inflammation, intestinal epithelial cells, saffron petals extract.

INTRODUCTION

Inflammatory bowel disease (IBD) is a chronic, relapsing inflammatory disorder of the gastrointestinal tract resulting from a loss of homeostasis between the gut immune system and the gut microbiome (Chang JT). The pathophysiology of IBD involves genetic, environmental, epithelial, microbial and immune factors (Hyun CK).

Effective treatment of IBD is one of the most challenging health problems for humans worldwide. New treatment options for IBD are continually

being explored. Chemically synthesized drugs are always accompanied by adverse reactions (Cai Z, et al.). In the search for new pharmacologically active substances, natural ingredients, as saffron and their extracts, are receiving great attention. The *Crocus sativus* plant, saffron, is known for several medicinal uses (Butnariu, et al.). The petals are discarded, but possess flavonolic glycosides (kaempferol), carotenoids (crocin and crocetin), anthocyanin pigments, and other bioactive compounds with anti-inflammatory and other therapeutic effects (Cerdá-Bernad D, et al.). It has been shown that the F-box and WD repeat domain-containing protein 7 (FBW7) was augmented in colon tissues from IBD patients. Whether and how FBW7 participates with IBD remain unknown (Meng Q, et al). Therefore, this study investigated the possible effect of Saffron Petal Extract (SPE) on FBW7 pro-inflammatory pathway using a Caco-2 intestinal epithelial cells that mimic the intestinal microenvironment.

MATERIALS & METHODS

Cell culture

The human colon adenocarcinoma Caco-2 cell line (ATCC® TIB-202™ Rockville, MD, USA) was cultured as previously reported by (Wu XX, et al.).

Cytotoxicity assay

The Methylthiazolyldiphenyl-tetrazolium bromide (MTT) assay (Sigma-Aldrich, St. Louis, MO, USA) was performed, as previously described (Franceschelli S, et al.), to assess the cell viability of Caco-2 cells treated with different concentrations of SPE (from 50ng/ml to 1mg/ml) provided by Hortus Novus (L'Aquila, Abruzzo, Italy) after 24h and 48h.

ROS Detection

An NBT (nitroblue tetrazolium) assay was performed as previously described to detect intracellular ROS levels (Franceschelli, S. et al.).

RNA extraction, reverse transcription, and Real-Time PCR

Cells were collected in 1mL QIAzol lysis reagent (Qiagen, Hilden, Germany), total RNA extraction and Real-Time PCR was performed as previously described (Pesce M, et al.).

Western Blot Analysis

Western blot analysis was performed as described previously (Patruno A et al.) using the following antibodies against ICAM (OTI1E5; 1:700), IKB alpha (NFKBIA) (OTI1D4; 1:400), FBXW7 (OTI6B1; 1:1000), COX-2 (ab52237; 1:500), and β -actin (Santa Cruz Biotechnology).

Statistical analysis

Quantitative variables are summarized as the mean value and standard deviations (SD) in the Tables and Figures. To assess the accuracy of fold change data, the 95% confidence interval (95% CI) and standard error (SE) were determined. A Student's t-test for unpaired data was applied to evaluate the significance of differences. All tests were two-tailed. The threshold of statistical significance was set at $p=0.05$. Data analysis was performed on GraphPad Prism 6 Software, version 6.01, 2012.

RESULTS

SPE does not affect the viability of intestinal cells

To determine the non-toxic concentrations of SPE, we examined the cell viability (at 24h and 48h) on Caco-2 cells treated with different concentrations (see Fig. 1A,B). SPE did not affect the viability cells (Fig. 1A,B). Furthermore, the superoxide anion (O_2^-) radical-scavenging activity was also measured in a non-enzymatic method at 24h. The generation of O_2^- was markedly inhibited (~50%) from the concentration of 50 μ g/ml in respect to cells LPS-stimulated (Fig. 1C). Thus, SPE at 50 μ g/ml was more often used in the following experiments to test its anti-inflammatory activity.

Effect of SPE on inducible proteins

To strengthen our hypothesis about the effect of SPE on intestinal epithelial cells, the expression of inducible proteins, known to be controlled by NF- κ B and up-regulated in the inflammatory state of IBD, were checked. SPE-treatment induces a down-regulation of both mRNA and proteins expression of iNOS (Fig. 2A), COX-2 (Fig. 2B) and HO-1 (Fig. 2C) compared to activated cells.

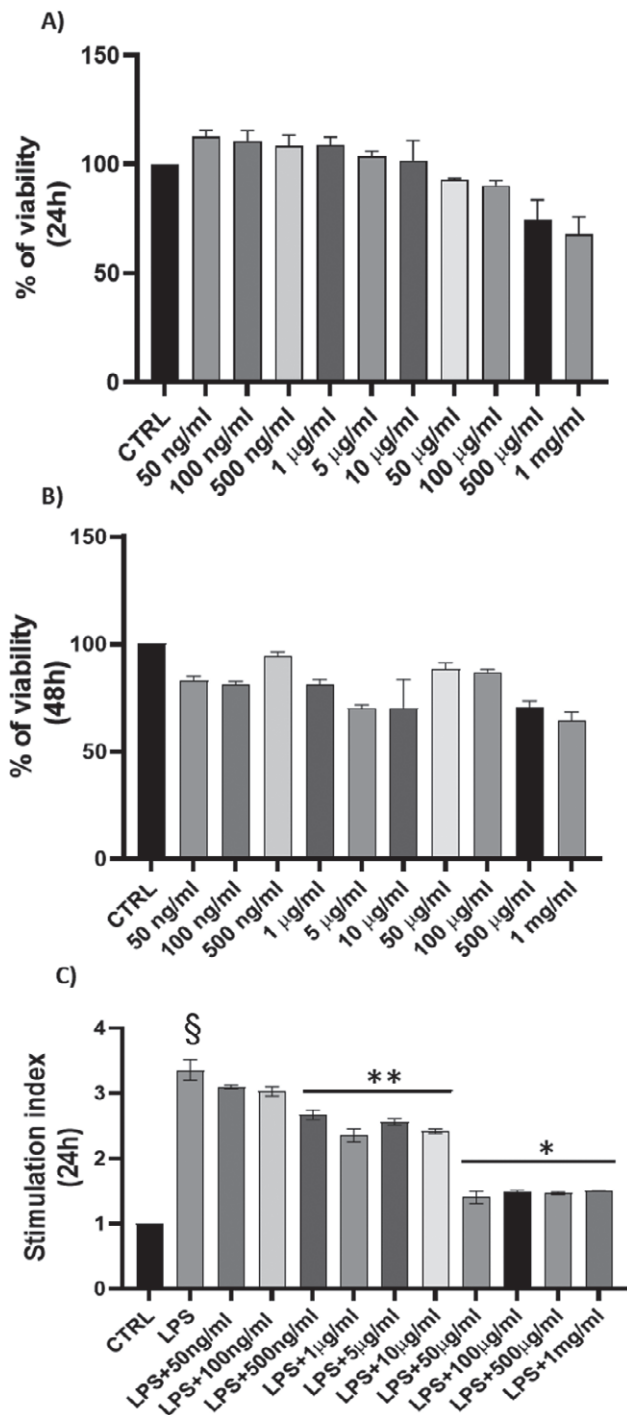


Figure 1. Cytotoxic effect of SPE on Caco-2 cells. Cells were treated with SPE for 24h (A) or 48h (B). Cells viability was measured by MTT assay as reported in Materials and Methods. Data are reported as % of viability in respect to control cells. Each bar represent means \pm SEM (n=3); (C) Antioxidant activity of SPE against oxidative stress LPS-induced measured by NBT test. Results were registered as stimulation index (SI). SI value of 1 was assigned to control cells. Each bar represent means \pm SEM (n=3). \S p<0.005 vs CTRL; **p<0.05 and *p<0.01 vs LPS.

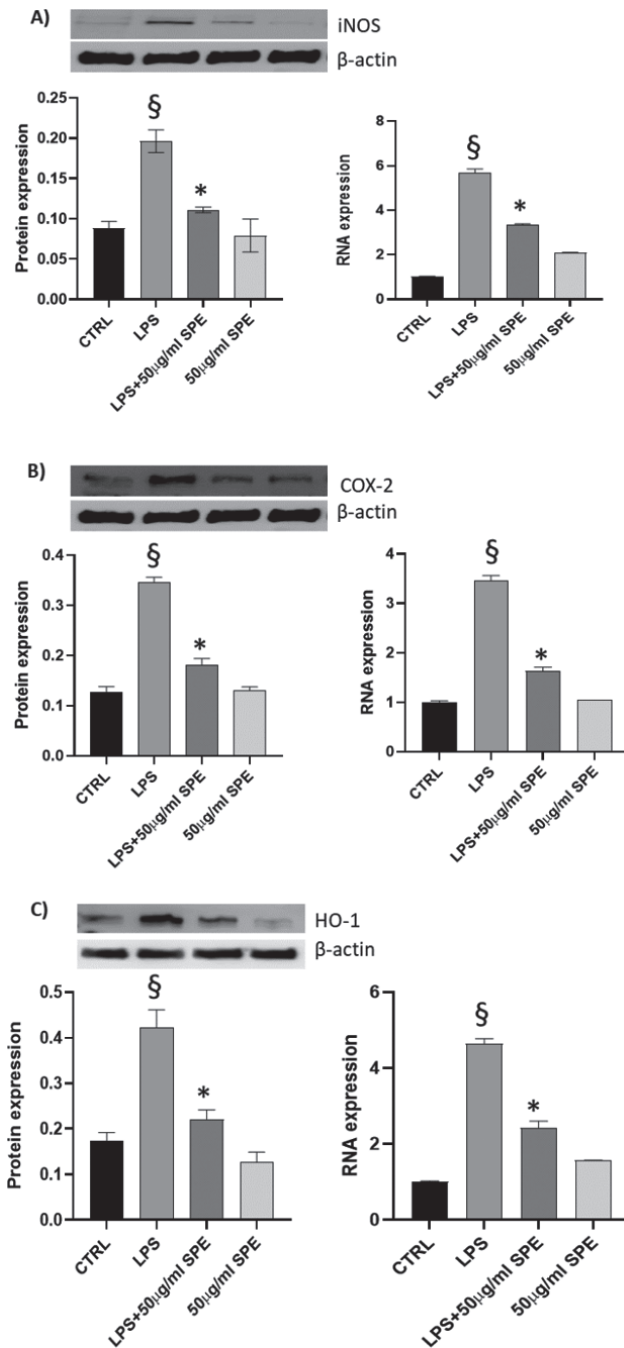


Figure 2. Effect of SPE on inducible molecules in Caco-2 cells. Representative image of Western blot analysis with relative densitometry and real-Time PCR analysis for iNOS (A), COX-2 (B), and HO-1 (C). To the left, in the densitometric analysis (n=3), each bar is reported as the intensity of optical density (IOD) \pm SD. The following primer pair sequence was used: iNOS (F:5'- CATTGCTGTGCTCCATAGTTTC-3', R:5'- CAGGACGTAGTTCAGCATCTC-3'); COX-2 (F:5'-CGATGCTGTGGAGCTGTAT-3'; R:5'-CATTGCTGTGCTCCATAGTTTCG-3'); HO-1 (F:5'- CCAGCAACAAAGTGAAGAT -3'; R: 5'-TCCACCGGACAAA-GTTCAT-3'). \S P<0.05, vs control cells and *P<0.05 vs LPS-stimulated cells.

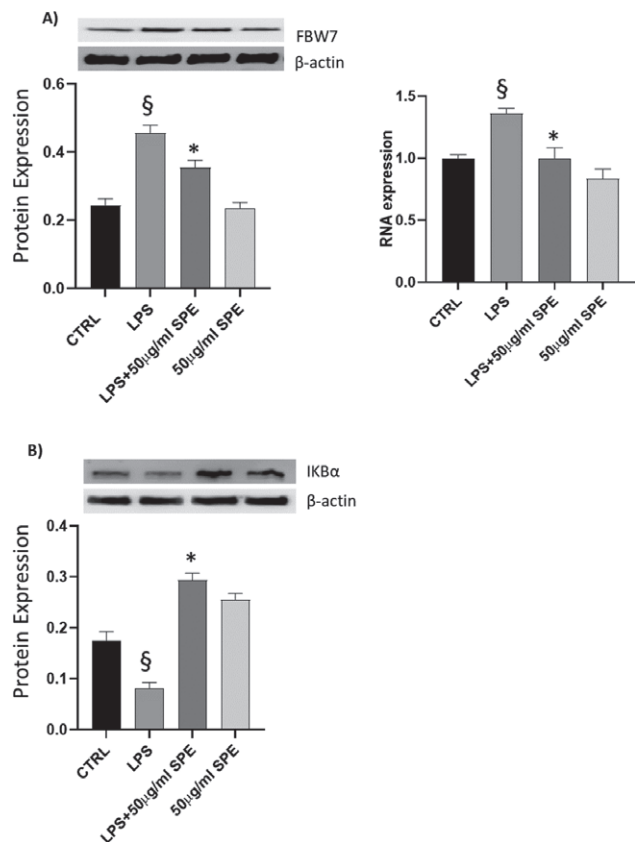


Figure 3. Effects of SPE on FBW7/ IKB- α Signaling in Caco-2 cells. Representative image of Western blot analysis for FBW7 (A) and IKB- α (B). To the left, in the densitometric analysis (n=3), each bar is reported as the intensity of optical density (IOD) \pm SD. §P<0.05, significance vs control cells. For qRT-PCR analysis, the following primer pair sequence was used: FBW7 (F:5'-CAGTC-CGCTGTGTTCAATATG-3', R:5'-GCCCTGTTAACGTGT-GAATG-3'); 18S (F:5'-CTTTGCCATCACTGCCATTAAG-3', R:5'-TCCATCCTTTACATCCTTCTGTC-3'). *P<0.05 significance vs LPS-stimulated cells.

Effect of SPE FBW7/NF- κ B signaling

We study the effect of SPE on FBW7, a novel E3 ubiquitin ligase for IKB α related to NF- κ B activation and intestinal inflammation. Protein and mRNA analysis of FBW7 were significantly up-regulated in cells LPS-stimulated confirming its role in regulating the inflammatory response. SPE-treatment induces a down-regulation of the FBW7 expression. This could make us think of its possible involvement in the negative regulation of a process of inflammation. IKB α level was significantly expressed by SPE-treatment respect to cells LPS-activated, making us hypothesize that SPE exerts its negative effect *via* NF- κ B/FBW7 pathway.

DISCUSSION

IBD is a chronic, relapsing inflammatory disorder of the gastrointestinal tract resulting from a loss of homeostasis between the intestinal immune system and the gut microbiome in genetically predisposed individuals (Chang JT).

Despite the incredible progress of modern medicine, significant obstacles remain in the treatment of IBD. There is high interest in alternative natural agents in the management of IBD (Duan L, et al.). Saffron has been used for health management since ancient times for its several pharmacological effects as well as peptic ulcer and ulcerative colitis (Butnariu M, et al.). Recent studies have demonstrated the efficacy of SPE as a protective agent against several diseases (Maccarone R, et al.). For the first time, we demonstrated that the SPE significantly reduce the expression of FBW7, involved on regulation of inflammatory pathways, in activated Caco-2 cells.

SPE induce a significative reduction of the ROS production (Fig. 1C), as well as the expression of inducible iNOS, COX-2 and HO-1 proteins (Fig. 2). Nuclear factor κ B (NF- κ B), a transcriptional factor, is the hallmark of inflammatory response and several studies have reported that NF- κ B activation contribute to colitis. Upon stimulation with LPS, the inhibitor of κ B (IKB) kinase (IKK) complex activates leading to phosphorylation and ubiquitin-dependent degradation of NF- κ B inhibitory protein IKB α (Franceschelli S, et al.). This allows NF- κ B to translocate into the nucleus and trigger a variety of target genes transcription as iNOS, COX-2 (Pesce M, et al.). FBW7 is a ubiquitin ligase that regulate the development of colorectal cancer and has recently emerged as an important regulator of NF- κ B in intestinal inflammation (Zhang Z, et al.). Our results evidenced that SPE, down-regulating the expression of the ubiquitine FBW7, inhibits the degradation of the IKB α subunit and keeps NF- κ B in the inactive state (Fig. 3). Our findings demonstrate that the SPE inhibited the expression of pro-inflammatory proteins of iNOS, COX-2 and HO-1 in LPS-stimulated Caco-2 cell line by suppressing the NF- κ B activation *via* FBW7. Since proteins degradation plays a critical role in the pathogenesis of human diseases (Hanna J, et al.), the inhibition of FBW7 by the SPE could alleviate a multitude of NF- κ B-driven inflammatory disease as IBD.

FUNDING

This research received no external funding

ACKNOWLEDGMENTS

This work is supported by the Italian Ministry for the University and Research. We thank Paolo Federico (Comune of Navelli, Abruzzo, Italy), the “Cooperativa Altopiano di Navelli” (Abruzzo, Italy) for providing Saffron Petals and Maria Maggi (Hortus Novus, L’Aquila, Abruzzo) for the preparation of SPE used in this study.

REFERENCE

- Butnariu M., Quispe C., Herrera-Bravo J., Sharifi-Rad J., Singh L., Aborehab N.M., Bouyahya A., Venditti A., Sen S., Acharya K., Bashiry M., Ezzat S.M., Setzer W.N., Martorell M., Mileski K.S., Bagiu I.C., Docea A.O., Calina D., Cho W.C. (2022) The Pharmacological Activities of *Crocus sativus* L.: A Review Based on the Mechanisms and Therapeutic Opportunities of its Phytoconstituents. *Oxid Med Cell Longev*. 2022:8214821. doi: 10.1155/2022/8214821.
- Cai Z., Wang S., Li J. (2021) Treatment of Inflammatory Bowel Disease: A Comprehensive Review. *Front Med (Lausanne)*. 8:765474. doi:10.3389/fmed.2021.765474.
- Cerdá-Bernad D., Valero-Cases E., Pastor J.J., Frutos M.J. (2022) Saffron bioactives crocin, crocetin and safranal: effect on oxidative stress and mechanisms of action. *Crit Rev Food Sci Nutr*. 62(12):3232-3249. doi: 10.1080/10408398.2020.1864279.
- Chang J.T. (2020) Pathophysiology of Inflammatory Bowel Diseases. *N Engl J Med*. 383(27):2652-2664. doi: 10.1056/NEJMra2002697.
- Duan L., Cheng S., Li L., Liu Y., Wang D., Liu G. (2021) Natural Anti-Inflammatory Compounds as Drug Candidates for Inflammatory Bowel Disease. *Front Pharmacol*. 12:684486. doi: 10.3389/fphar.2021.684486.
- Franceschelli S., Gatta D.M., Pesce M., Ferrone A., Patruno A., de Lutiis M.A., Grilli A., Felaco M., Croce F., Speranza L. (2016) New Approach in Translational Medicine: Effects of Electrolyzed Reduced Water (ERW) on NF- κ B/iNOS Pathway in U937 Cell Line under Altered Redox State. *Int J Mol Sci*. 17(9):1461. doi: 10.3390/ijms17091461.
- Franceschelli S., Lanuti P., Ferrone A., Gatta D.M.P., Speranza L., Pesce M., Grilli A., Cacciatore I., Ricciotti E., Di Stefano A., Miscia S., Felaco M., Patruno A. (2019) Modulation of Apoptotic Cell Death and Neuroprotective Effects of Glutathione-L-Dopa Codrug Against H₂O₂-Induced Cellular Toxicity. *Antioxidants (Basel)*. 8(8):319. doi: 10.3390/antiox8080319.
- Franceschelli S., Pesce M., Ferrone A., Gatta D.M., Patruno A., De Lutiis M.A., Quiles J.L., Grilli A., Felaco M., Speranza L. (2017) Biological Effect of Licochalcone C on the Regulation of PI3K/Akt/eNOS and NF- κ B/iNOS/NO Signaling Pathways in H9c2 Cells in Response to LPS Stimulation. *Int J Mol Sci*. 18(4):690. doi: 10.3390/ijms18040690.
- Hanna J., Guerra-Moreno A., Ang J., Micoogullari Y. (2019) Protein Degradation and the Pathologic Basis of Disease. *Am J Pathol*. 189(1):94-103. doi: 10.1016/j.ajpath.2018.09.004.
- Hyun C. K. (2021). Molecular and Pathophysiological Links between Metabolic Disorders and Inflammatory Bowel Diseases. *International journal of molecular sciences*, 22(17), 9139. <https://doi.org/10.3390/ijms22179139>.
- Maccarone R., Di Marco S., Bisti S. (2008) Saffron supplement maintains morphology and function after exposure to damaging light in mammalian retina. *Invest. Ophthalmol Vis Sci*. 49, 1254–1261.
- Meng Q., Wu W., Pei T., Xue J., Xiao P., Sun L., Li L., Liang D. (2020) miRNA-129/FBW7/NF- κ B, a Novel Regulatory Pathway in Inflammatory Bowel Disease. *Mol Ther Nucleic Acids*. 19:731-740. doi: 10.1016/j.omtn.2019.10.048.
- Patruno A., Pesce M., Grilli A., Speranza L., Franceschelli S., De Lutiis M.A., Vianale G., Costantini E., Amerio P., Muraro R., Felaco M., Reale M. (2015) mTOR Activation by PI3K/Akt and ERK Signaling in Short ELF-EMF Exposed Human Keratinocytes. *PLoS One*. 10(10): e0139644. doi:10.1371/journal.pone.0139644.
- Pesce M., Ferrone A., Rizzuto A., Tatangelo R., Iezzi I., Ladu S., Franceschelli S., Speranza L., Patruno A., Felaco M., Grilli A. (2014) The SHP-1 expression is associated with cytokines and psychopathological status in unmedicated first episode schizophrenia patients. *Brain Behav Immun*. 41:251-60. doi: 10.1016/j.bbi.2014.04.008.
- Pesce M., Franceschelli S., Ferrone A., De Lutiis M.A., Patruno A., Grilli A., Felaco M., Speranza L. (2015) Verbascoside down-regulates some pro-inflammatory signal transduction pathways by increasing the activity of tyrosine phosphatase SHP-1 in the U937 cell line. *J Cell Mol Med*. 19(7):1548-56. doi: 10.1111/jcmm.12524.
- Wu X.X., Huang X.L., Chen R.R., Li T., Ye H.J., Xie W., Huang Z.M., Cao G.Z. (2019) Paeoniflorin Prevents Intestinal Barrier Disruption and Inhibits Lipopolysaccharide (LPS)-Induced Inflammation in Caco-2 Cell Monolayers. *Inflammation*. 42(6):2215-2225. doi: 10.1007/s10753-019-01085-z.
- Zhang Z., Hu Q., Xu W., Liu W., Liu M., Sun Q., Ye Z., Fan G., Qin Y., Xu X., Yu X., Ji S. (2020) Function and regulation of F-box/WD repeat-containing protein 7. *Oncol Lett*. 20(2):1526-1534. doi: 10.3892/ol.2020.11728.



Citation: Anna Giulia Ruggieri, Michele Sallese (2022) Genotype-phenotype correlation and adaptive proteome reorganization in Marinesco-Sjögren syndrome. *Italian Journal of Anatomy and Embryology* 126(2): 71-75. doi: 10.36253/ijae-13802

Copyright: © 2022 Anna Giulia Ruggieri, Michele Sallese. This is an open access, peer-reviewed article published by Firenze University Press (<http://www.fupress.com/ijae>) and distributed under the terms of the Creative Commons Attribution License, which permits unrestricted use, distribution, and reproduction in any medium, provided the original author and source are credited.

Data Availability Statement: All relevant data are within the paper and its Supporting Information files.

Competing Interests: The Author(s) declare(s) no conflict of interest.

Genotype-phenotype correlation and adaptive proteome reorganization in Marinesco-Sjögren syndrome

ANNA GIULIA RUGGIERI^{1,2}, MICHELE SALLESE^{1,2,*}

¹ Department of Innovative Technologies in Medicine and Dentistry, “G. d’Annunzio” University of Chieti-Pescara, 66100 Chieti, Italy

² Center for Advanced Studies and Technology (CAST), “G. d’Annunzio” University of Chieti-Pescara, 66100 Chieti, Italy

*Corresponding author. E-mail: michele.sallese@unich.it

Abstract. Marinesco-Sjögren Syndrome (MSS) causes cerebellar ataxia, myopathy and congenital cataracts in people carrying *SIL1* mutations. *SIL1* is an ATP exchange factor for BiP, the major endoplasmic reticulum (ER) chaperone involved in protein folding. *SIL1* loss influences BiP activity, leading to ER stress and the activation of unfolded protein response (UPR). Purkinje cells and skeletal muscle fibers are the most sensitive cells to prolonged pathologic UPR, but adverse effects are detectable in other cell types. Currently a clear genotype-phenotype correlation is missing, due to the variable symptomatology and to the discovery of new *SIL1* variants. We decided to focus our attention on two recent works providing different strategies to shed light on the pathophysiology of MSS. In the first one several cellular biomarkers have been evaluated to distinguish between malignant and benign *SIL1* mutations. The other study proposed a proteomic approach to clarify adaptive mechanisms of MSS fibroblasts in response to *SIL1* loss. Further investigations are needed to better understand the pathogenesis of MSS and to simplify the diagnosis in patients.

Keywords: fibroblast, Marinesco-Sjögren syndrome, pathogenic mechanisms, *SIL1*.

INTRODUCTION

Marinesco-Sjögren syndrome (MSS) is described as a rare, early onset, multisystem disorder which is usually characterized by cerebellar ataxia, myopathy, and congenital bilateral cataracts. MSS patients could present additional symptoms including mental retardation, intention tremor, hypergonadotropic hypogonadism, short stature, and skeletal deformities (Anttonen, 2006). Learning disabilities and poor motor coordination are due to cerebellar degeneration, consisting primarily in Purkinje cell loss (Ichhaporia and Hendershot, 2021), while hypotonia occurs because of myopathy associated to gradual substitution of muscle with adipose tissue (Roos et al., 2014). First clear symptoms of the disease manifest after few months from birth, but diagnosis is not so immediate. Regardless, life span appears to be normal (Anttonen, 2006).

In 2005, two different research groups discovered *SIL1* gene mutation in patients affected by MSS (Anttonen et al., 2005; Senderek et al., 2005). In the same year, it was also reported that the spontaneous recessive mutation of *SIL1* (*SIL1^{wz}*) is responsible of Purkinje cells degeneration and myopathy of woozy mice (Zhao et al., 2005). Subsequently, homozygous or compound heterozygous variants of *SIL1* gene have been found in more than 60% of patients. *SIL1* gene encodes for an ATP-exchange factor (SIL1), which is able to bind the endoplasmic reticulum (ER) HSP70 chaperone-binding immunoglobulin protein (BiP). BiP is responsible of protein folding, and SIL1 allows the release of the folded substrate catalyzing the exchange of ADP with a new molecule of ATP (Figure 1). In MSS, mutant *SIL1* generates instable protein that is further degraded, therefore BiP remains associated with the client protein. Consequently, unfolded proteins accumulate in the lumen of ER, inducing the activation of unfolded protein response (UPR) (Chiesa and Sallesse, 2020). The UPR is a complex

cellular mechanism aimed at reestablishing the normal ER proteostasis by improving ER protein-folding potential, degrading unfolded proteins, and reducing protein synthesis. This is achieved through the activation of three distinct ER transmembrane protein effectors: inositol-requiring enzyme 1 (IRE1), activating transcription factor 6 (ATF6), and protein kinase R (PKR)-like endoplasmic reticulum kinase (PERK) (Restelli et al., 2019). Protracted activation of UPR caused by *SIL1* loss induces degeneration of specific cells, namely Purkinje neurons and skeletal muscle fibers. Nevertheless, lack of *SIL1* leads to ER stress and functional injuries in other cellular types (Ichhaporia et al., 2015; Ittner et al., 2014; Potenza et al., 2021).

Consistently with the actual knowledge of MSS, a clear genotype-phenotype correlation is missing, because of the variable symptomatology present in some patients, and the increased number of *SIL1* sequence variants, including a heterozygous missense mutation showing cerebellar ataxia without signs of myopathy or cataract

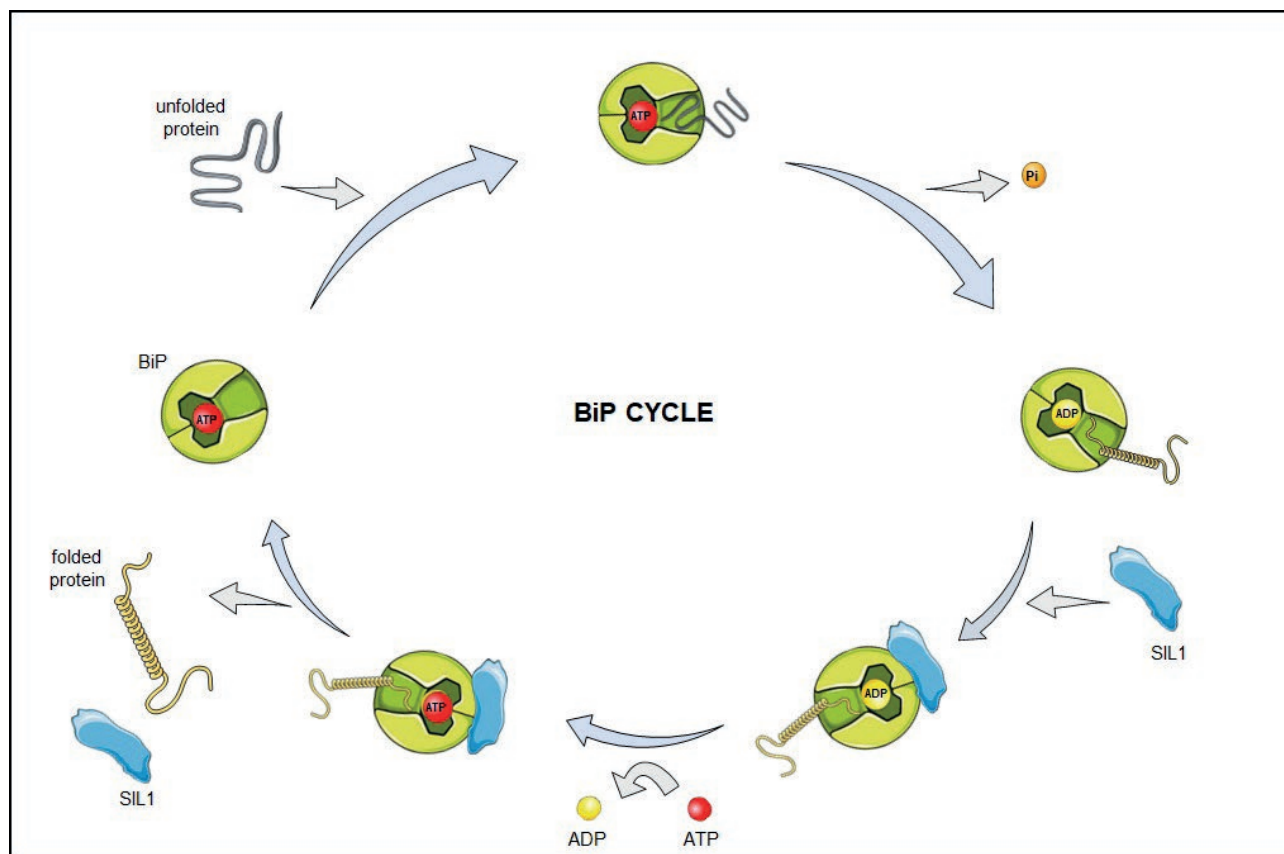


Figure 1. HSP70 chaperone BiP cycle. ATP is needed to bind a new unfolded protein, and its following hydrolysis leads to a conformational change of BiP, which promotes the folding of the client protein. SIL1 protein binds ADP-bound BiP and catalyze the ADP-ATP exchange. Folded protein release occurs in presence of ATP, and then BiP is ready to bind a new unfolded client. When SIL1 protein is missing, BiP remains associated with its client protein, and newly synthesized proteins accumulate in the ER.

(Noreau et al., 2015). In this review we reported two different recent approaches to study cells carrying *SIL1* mutations, with the purpose of clarifying the pathophysiology of MSS.

GENOTYPE-PHENOTYPE CORRELATION ANALYSIS IN MSS

In 2019, Gatz and colleagues examined several cellular biomarkers to evaluate the pathogenicity of *SIL1* mutations in cell models (Gatz et al., 2019). They used Hek293 cells to overexpress 5 different mutant forms of SIL1 protein, including three known malignant mutations (p.V231_I232del, p.G312R, and p.L457P), one missense mutation (p.R92W) with an atypical phenotype (Riazuddin et al., 2009), and one polymorphism as a control (p.K132Q). This work suggested that several read-out measures could be useful to evaluate the pathogenicity of amino acid changes in SIL1 protein. Among them, high molecular weight bands in a native PAGE were signs of aberrant SIL1 protein complexes, along with the presence of SIL1 degradation products. Fur-

thermore, cells with a pathogenic *SIL1* mutation showed reduced metabolic activity and a non-reticular pattern of immunoreactivity. Other distinctive markers were subcellular ultrastructural alterations, such as abnormal mitochondria, vacuoles and protein aggregates, dispersed Golgi, and disintegrated centrosomes (Gatz et al., 2019). In this work SIL1 interactome was also investigated, and this led to the discovery of a disrupted interaction with POC1A (a centriolar protein) and a gain of interaction with DNAJB11/ERj3 (another BiP co-chaperone) by pathogenic *SIL1* mutations. Finally, this study confirmed the increased expression of UPR-/ERAD-related proteins as a common cellular pathogenic biomarker. In conclusion, Gatz and colleagues provided a new approach to distinguish between malignant and benign *SIL1* variants and demonstrated that p.R92W missense mutation could more properly be considered a polymorphism (Gatz et al., 2019).

The importance of defining other read-out measures is becoming more evident for genetic counseling and for characterizing clear genotype-phenotype correlations of MSS patients, especially because of the increasing number of discovered *SIL1* mutations.

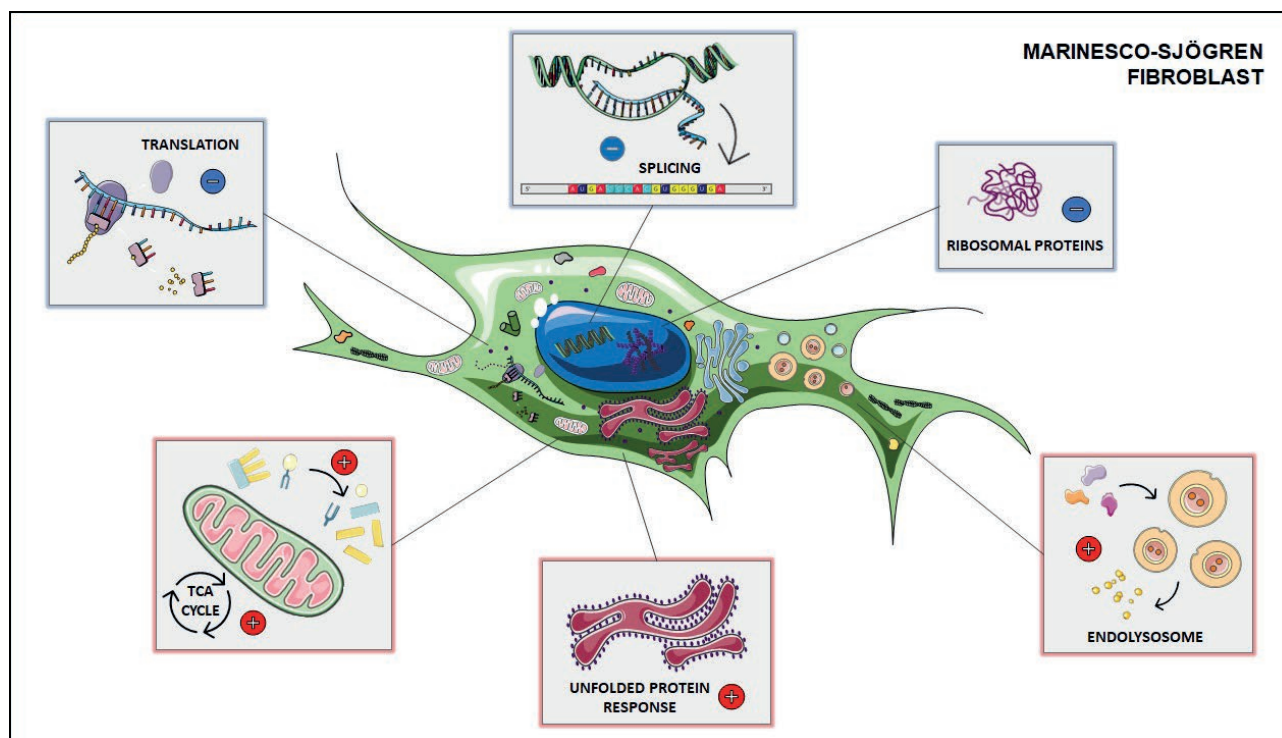


Figure 2. Marinesco-Sjögren fibroblast showing mild signs of UPR. Proteomic analysis revealed downregulation in splicing, ribosome synthesis and translation. TCA cycle is boosted because of enhanced acetyl-CoA production, resulting from increased catabolism of proteins via lysosome-based structure, and reduced biosynthesis of some amino acids. Lipid production is also downregulated, while beta-oxidation is increased.

CELLULAR PROTEOMIC ADAPTATION TO SIL1 LOSS

In 2021 our research group decided to focus on the proteomic adaptation to SIL1 loss in skin fibroblasts collected from a young MSS patient (HF-MSS), affected by *SIL1* R111X mutation (Potenza et al., 2021). Despite fibroblasts are not among the main cellular targets of MSS, mild signs of UPR activation were detected, in addition to an altered cell metabolism. Proteomic analysis on HF-MSS showed differential expression of more than 600 proteins in comparison with control fibroblasts (HF), and after accurate investigations we discovered that these cells reached a senescence-like state to face up to SIL1 loss (Figure 2) (Potenza et al., 2021). In particular, HF-MSS showed an evident downregulation of the spliceosomal complex, as well as ribosomal proteins and RNA translation initiation. Lipids metabolism was also affected with reduced synthesis reactions and increased beta-oxidation. Proteomic analysis also revealed that biochemical pathways leading to acetyl-CoA production were enhanced, resulting in a boosting of TCA cycle and an increased ATP production. ATP, indeed, seems to be more necessary when ER is under stress conditions, and this could explain why MSS fibroblasts undergo metabolic changes when SIL1 protein is mutated (Potenza et al., 2021).

CONCLUSIONS

Marinesco-Sjögren syndrome is not easy to diagnose and there is currently no cure. The detection of new pathogenic cellular biomarkers in addition to a better understanding of the cell reaction to *SIL1* mutation is useful to bring out genotype-phenotype correlations. Further studies with multi-omics approaches will be needed to learn more about the pathogenesis of Marinesco-Sjögren syndrome.

FUNDING

This research was funded by the Italian Telethon ONLUS Foundation, Rome, Italy, grants N° GGP20092 to M.S.

ACKNOWLEDGEMENTS

Figure 1 and figure 2 were partially drawn by using pictures from Servier Medical Art. Servier Medical Art by Servier is licensed under a Creative Commons Attribution 3.0 Unported License (<https://creativecommons.org/licenses/by/3.0/>). We thank Francesca Potenza for her contribution in creating figure 2.

org/licenses/by/3.0/). We thank Francesca Potenza for her contribution in creating figure 2.

REFERENCES

- Anttonen AK, 2006. Marinesco-Sjögren Syndrome. GeneReviews 12.
- Ichhaporia, V.P., Hendershot, L.M., 2021. Role of the HSP70 Co-Chaperone SIL1 in Health and Disease. *Int. J. Mol. Sci.* 22, 1564. <https://doi.org/10.3390/ijms22041564>
- Roos, A., Buchkremer, S., Kollipara, L., et al., 2014. Myopathy in Marinesco-Sjögren syndrome links endoplasmic reticulum chaperone dysfunction to nuclear envelope pathology. *Acta Neuropathol. (Berl.)* 127, 761–777. <https://doi.org/10.1007/s00401-013-1224-4>
- Anttonen, A.-K., Mahjneh, I., Hämäläinen, R.H. et al., 2005. The gene disrupted in Marinesco-Sjögren syndrome encodes SIL1, an HSPA5 cochaperone. *Nat. Genet.* 37, 1309–1311. <https://doi.org/10.1038/ng1677>
- Senderek, J., Krieger, M., Stendel, C., et al., 2005. Mutations in SIL1 cause Marinesco-Sjögren syndrome, a cerebellar ataxia with cataract and myopathy. *Nat. Genet.* 37, 1312–1314. <https://doi.org/10.1038/ng1678>
- Zhao, L., Longo-Guess, C., Harris, B.S., Lee, J.-W., Ackerman, S.L., 2005. Protein accumulation and neurodegeneration in the woozy mutant mouse is caused by disruption of SIL1, a cochaperone of BiP. *Nat. Genet.* 37, 974–979. <https://doi.org/10.1038/ng1620>
- Chiesa, R., Sallese, M., 2020. Review: Protein misfolding diseases – the rare case of Marinesco-Sjögren syndrome. *Neuropathol. Appl. Neurobiol.* 46, 323–343. <https://doi.org/10.1111/nan.12588>
- Restelli, E., Masone, A., Sallese, M., Chiesa, R., 2019. Neuroprotective modulation of the unfolded protein response in Marinesco-Sjögren syndrome: PERK signaling inhibition and beyond. *Neural Regen. Res.* 14, 62–64. <https://doi.org/10.4103/1673-5374.243708>
- Ichhaporia, V.P., Sanford, T., Howes, J., Marion, T.N., Hendershot, L.M., 2015. Sil1, a nucleotide exchange factor for BiP, is not required for antibody assembly or secretion. *Mol. Biol. Cell* 26, 420–429. <https://doi.org/10.1091/mbc.E14-09-1392>
- Ittner, A.A., Bertz, J., Chan, T.Y.B., van Eersel, J., Polly, P., Ittner, L.M., 2014. The nucleotide exchange factor SIL1 is required for glucose-stimulated insulin secretion from mouse pancreatic beta cells in vivo. *Diabetologia* 57, 1410–1419. <https://doi.org/10.1007/s00125-014-3230-z>
- Potenza, F., Cufaro, M.C., Di Biase, L., et al., 2021. Proteomic analysis of marinesco-sjogren syndrome fibro-

blasts indicates pro-survival metabolic adaptation to SIL1 loss. *Int. J. Mol. Sci.* 22. <https://doi.org/10.3390/ijms222212449>

Noreau, A., La Piana, R., Marcoux, et al., FORGE Canada, 2015. Novel SIL1 mutations cause cerebellar ataxia and atrophy in a French-Canadian family. *neurogenetics* 16, 315–318. <https://doi.org/10.1007/s10048-015-0455-z>

Gatz, C., Hathazi, D., Münchberg, U., et al., 2019. Identification of Cellular Pathogenicity Markers for SIL1 Mutations Linked to Marinesco-Sjögren Syndrome. *Front. Neurol.* 10. <https://doi.org/10.3389/fneur.2019.00562>

Riazuddin, S.A., Amiri-Kordestani, L., Kaul, H., et al., 2009. Novel SIL1 mutations in consanguineous Pakistani families mapping to chromosomes 5q31. *Mol. Vis.* 15, 1050–1056.



Citation: Francesca Coccina, Rosa Scurti, Oriana Trubiani, Sante D. Pierdomenico (2022) Left ventricular global longitudinal strain by speckle tracking echocardiography in hypertension: a mini-review. *Italian Journal of Anatomy and Embryology* 126(2): 77-80. doi: 10.36253/ijae-13819

Copyright: © 2022 Francesca Coccina, Rosa Scurti, Oriana Trubiani, Sante D. Pierdomenico. This is an open access, peer-reviewed article published by Firenze University Press (<http://www.fupress.com/ijae>) and distributed under the terms of the Creative Commons Attribution License, which permits unrestricted use, distribution, and reproduction in any medium, provided the original author and source are credited.

Data Availability Statement: All relevant data are within the paper and its Supporting Information files.

Competing Interests: The Author(s) declare(s) no conflict of interest.

Left ventricular global longitudinal strain by speckle tracking echocardiography in hypertension: a mini-review

FRANCESCA COCCINA^{1,3,*}, ROSA SCURTI³, ORIANA TRUBIANI¹, SANTE D. PIERDOMENICO^{1,2}

¹ Department of Innovative Technologies in Medicine & Dentistry, University "Gabriele d'Annunzio", Chieti-Pescara, Chieti, Italy

² Cardiologia Universitaria, Ospedale Clinicizzato Santissima Annunziata, Chieti, Italy

³ UOC Geriatria, Ospedale Civile Santo Spirito, Pescara, Italy

*Corresponding author. E-mail: f.coccina@gmail.com

Abstract. The aim of this mini-review is to report current knowledge about left ventricular systolic function assessed by global longitudinal strain in hypertensive patients with and without left ventricular hypertrophy, that is, stage A and B heart failure. We conducted a literature search through PubMed, Web of science and Cochrane Library by using terms such as myocardial strain, speckle tracking echocardiography, systolic dysfunction, left ventricular hypertrophy, left ventricular geometry, essential hypertension. We identified 2 meta-analyses including 30 studies, 1 review including 8 studies and 5 other studies. The evaluation of published studies suggests that global longitudinal strain is significantly reduced in hypertensive patients than in normotensive subjects, despite normal ejection fraction. This alteration may be present in both patients with and without left ventricular hypertrophy, though it is more relevant in those with left ventricular hypertrophy. Global longitudinal strain is a more sensitive marker for early abnormalities of left ventricular function and can be of greater help than conventional methods in predicting hypertensive disease progression and outcomes. However, the prevalence of left ventricular longitudinal dysfunction in hypertension, its predicting factors and its clinical relevance are not yet completely clear. Thus, other studies are needed to shed further light on this topic.

Keywords: hypertension, left ventricular hypertrophy, global longitudinal strain.

INTRODUCTION

Hypertension is one of the most important factors for the development of heart failure (HF) (Rapsomaniki et al, Williams et al) which is becoming a major public health problem (Roger VL, Ponikowski et al). The population attributable risk of hypertension for HF has been reported to be as high as that of coronary artery disease (Dunlay et al).

According to the American College of Cardiology/American Heart Association guidelines, HF can be divided into different stages (Hunt et al).

Stage A includes patients at high risk for HF (for example hypertension, atherosclerotic disease, diabetes, obesity) but without structural heart disease or signs and symptoms of HF. Stage B includes patients with structural heart disease but without signs or symptoms of HF. Stage C includes symptomatic patients and Stage D includes those with refractory HF.

Historically, left ventricular (LV) systolic function has been assessed by ejection fraction (EF), but this index has some limitations. Strain and strain rate are promising technologies for the evaluation of cardiac function (Geyer et al, Voigt et al). Speckle tracking echocardiography (STE) is now the preferred method for strain measurements and global longitudinal strain (GLS) is the most frequent reported measure (Geyer et al, Voigt et al). Some studies have shown a reduction in myocardial contractile function, despite normal EF and absence of symptoms, in various cardiovascular disorders and measurement of GLS has been reported to provide incremental prognostic information (Stanton et al, Lee et al, Kuznetsova).

Thus, the use of GLS in the evaluation of cardiac function could be helpful in identifying Stage A and B patients at higher risk to develop clinical HF.

The aim of this mini-review is to report current knowledge about LV systolic function as assessed by GLS STE in hypertensive patients with and without LV structural alterations, that is, stage A and B HF, respectively.

METHODS

Search Strategy, inclusion criteria and study selection

We conducted a literature search through PubMed, Web of science and Cochrane Library up to June 28, 2022. The terms used to identify studies were myocardial strain, speckle tracking echocardiography, systolic dysfunction, left ventricular hypertrophy, left ventricular geometry, essential hypertension. Inclusion criteria were: full articles published in peer-reviewed journals; 2D STE echocardiographic studies assessing LV GLS in patients with hypertension with and without LV hypertrophy. Among published studies, we identified 2 recent meta-analyses (Tadic et al a, Tadic et al b), 1 recent review (Oh JK, Park JH) and 5 other studies (Imbalzano et al, Soufi Taleb Bendiab et al, Qingfeng et al, Salas-Pacheco et al, Takahashi et al). The first meta-analysis included 22 studies, the second meta-analysis included 8 studies and the review included 8 studies.

RESULTS

In a meta-analysis (Tadic et al a), 2089 normotensive controls and 2187 hypertensive patients were included. EF was not significantly different between normotensive and hypertensive subjects. GLS was worse in subjects with hypertension (-18.14 ± 0.40) than in those with normotension (-20.58 ± 0.33). The standardized mean difference (SMD) between the groups was 1.07 ± 0.15 , 95% confidence interval (CI) 0.77-1.36, $P < 0.0001$.

In the other meta-analysis (Tadic et al b), 267 normotensive subjects and 712 hypertensive patients (234 normal geometry, 97 LV concentric remodeling, 176 eccentric LVH, 205 concentric LVH) were included. EF was not different between normotensive and hypertensive individuals. GLS was worse in the whole hypertensive group (-18.1 ± 0.73) than in the normotensive one (-20.8 ± 0.7); the SMD between the groups was 0.87 ± 0.25 , 95% CI 0.38-1.37, $P < 0.0001$. When the hypertensive group was analysed separately, compared to patients with normal LV geometry, those with eccentric (SMD 0.49 ± 0.10 , 95% CI 0.29-0.70, $P < 0.0001$) and concentric LVH (SMD 0.90 ± 0.11 , 95% CI 0.68-1.10, $P < 0.0001$) showed altered GLS, but those with LV concentric remodeling (0.18 ± 0.13 , 95% CI - 0.06 to 0.44, $P = 0.15$) did not attain significance.

In the other studies, when compared with normotensive subjects, patients with hypertension had reduced GLS both in the absence and in the presence of LVH, though GLS was more impaired in patients with LVH (Imbalzano et al, Soufi Taleb Bendiab et al, Qingfeng et al, Salas-Pacheco et al, Takahashi et al). A study showed that, beyond LVH, the duration of hypertension, diabetes and increased filling pressures were associated with GLS reduction (Soufi Taleb Bendiab et al). Another study reported that patients with 3 or 4 risk factors, who also had higher LV mass, showed significantly reduced GLS (Takahashi et al).

DISCUSSION

Studies suggest that GLS is lower in hypertensive patients than in normotensive subjects. This alteration may be present in both patients with and without LV hypertrophy. Early impairment of myocardial contractility may be secondary to hemodynamic or biochemical changes. The increased end-systolic wall stress may play a crucial role in leading to longitudinal dysfunction in hypertensive heart disease. During time, chronic increase in end-systolic wall stress promotes progressive increase in LV wall thickness due to myocyte hypertro-

phy and interstitial fibrosis which are associated with LV systolic longitudinal dysfunction. Indeed, GLS gradually reduces from hypertensive patients with normal LV geometry to those with concentric remodelling, eccentric LVH and concentric LVH. A possible explanation for the increased cardiovascular risk in patients with hypertension, and particularly in those with eccentric and concentric LVH, may be related to the subclinical reduction in longitudinal function, which is undetectable by traditional measures of LV systolic function, such as EF. In this context, GLS assessed by 2D STE is a more sensitive marker for early subtle abnormalities of LV myocardial function and can be of greater help than conventional methods in predicting hypertensive disease progression and outcomes. However, the prevalence of LV longitudinal dysfunction in both hypertensive patients with and without LVH, its predicting factors and its relevance for future LV deterioration and cardiovascular outcomes are not yet completely clear. Thus, other studies are needed to shed further light on the pathophysiology, predictors, epidemiology and short- and long-term clinical consequences of impaired longitudinal systolic function identified by GLS assessment.

REFERENCES

- Dunlay SM, Weston SA, Jacobsen SJ, Roger VL. Risk factors for heart failure: a population-based case-control study. *Am J Med* 2009; 122:1023-1028.
- Geyer H, Caracciolo G, Abe H, et al. Assessment of myocardial mechanics using speckle tracking echocardiography: fundamentals and clinical applications. *J Am Soc Echocardiogr*. 2010;23:351-69.
- Hunt SA, Abraham WT, Chin MH, et al. 2009 focused update incorporated into the ACC/AHA 2005 Guidelines for the Diagnosis and Management of Heart Failure in Adults: a report of the American College of Cardiology Foundation/American Heart Association Task Force on Practice Guidelines: developed in collaboration with the International Society for Heart and Lung Transplantation. *Circulation*. 2009;119:e391-479.
- Imbalzano E, Zito C, Carerj S, et al. Left ventricular function in hypertension: new insight by speckle tracking echocardiography. *Echocardiography*. 2011;28:649-57.
- Kuznetsova T, Cauwenberghs T, Knez J, et al. Additive prognostic value of left ventricular systolic dysfunction in a population-based cohort. *Circ Cardiovasc Imaging* 2016; 9:e004661.
- Lee WH, Liu YW, Yang LT, Tsai WC. Prognostic value of longitudinal strain of subepicardial myocardium in patients with hypertension. *J Hypertens* 2016; 34:1195-1200.
- Oh JK, Park JH. Role of strain echocardiography in patients with hypertension. *Clin Hypertens*. 2022;28:6-11.
- Ponikowski P, Voors AA, Anker SD, et al. 2016 ESC Guidelines for the diagnosis and treatment of acute and chronic heart failure: The Task Force for the diagnosis and treatment of acute and chronic heart failure of the European Society of Cardiology (ESC) Developed with the special contribution of the Heart Failure Association (HFA) of the ESC. *Eur Heart J*. 2016;37:2129-2200
- Qingfeng Z, Yi W, Wenhua L, et al. Evaluation of left ventricular function by treadmill exercise stress echocardiography combined with layer-specific strain technique in essential hypertension patients. *J Clin Hypertens (Greenwich)*. 2022;24:312-319.
- Rapsomaniki E, Timmis A, George J, et al. Blood pressure and incidence of twelve cardiovascular diseases: lifetime risks, healthy life-years lost, and age-specific associations in 1.25 million people. *Lancet* 2014;383:1899-1911.
- Roger VL. Epidemiology of heart failure. *Circ Res* 2013;113:646-659.
- Salas-Pacheco JL, Lomelí-Sánchez O, Baltazar-González O, Soto ME. Longitudinal systolic dysfunction in hypertensive cardiomyopathy with normal ejection fraction. *Echocardiography*. 2022;39:46-53.
- Soufi Taleb Bendiab N, Meziane-Tani A, Ouabdesselam S, et al. Factors associated with global longitudinal strain decline in hypertensive patients with normal left ventricular ejection fraction. *Eur J Prev Cardiol*. 2017;24:1463-72
- Stanton T, Leano R, Marwick TH. Prediction of all-cause mortality from global longitudinal speckle strain: comparison with ejection fraction and wall motion scoring. *Circ Cardiovasc Imaging*. 2009;2:356-64.
- Tadic M, Sala C, Carugo S, Mancina G, Grassi G, Cuspidi C. Myocardial strain in hypertension: a meta-analysis of two-dimensional speckle tracking echocardiographic studies. *J Hypertens*. 2021;39:2103-2112.a
- Tadic M, Sala C, Carugo S, Mancina G, Grassi G, Cuspidi C. Myocardial strain and left ventricular geometry: a meta-analysis of echocardiographic studies in systemic hypertension. *J Hypertens*. 2021;39:2297-2306.b
- Takahashi T, Kusunose K, Zheng R, et al. Association between cardiovascular risk factors and left ventricular strain distribution in patients without previous cardiovascular disease. *J Echocardiogr*. 2022:1-8.
- Voigt JU, Pedrizzetti G, Lysyansky P, et al. Definitions for

a common standard for 2D speckle tracking echocardiography: consensus document of the EACVI/ASE/Industry Task Force to standardize deformation imaging. *Eur Heart J Cardiovasc Imaging*. 2015;16:1-11.

Williams B, Mancia G, Spiering W, et al. 2018 ESC/ESH Guidelines for the management of arterial hypertension: The Task Force for the management of arterial hypertension of the European Society of Cardiology and the European Society of Hypertension: The Task Force for the management of arterial hypertension of the European Society of Cardiology and the European Society of Hypertension. *J Hypertens* 2018;36:1953-2041.



Citation: Manlio Santilli, Bruna Sinjari, Oriana Trubiani, Gianmaria d'Addazio, Imena Rexhepi, Giuseppe Tafuri, Eugenio Manciocchi, Sergio Caputi (2022) Prevalence and localization of Maxillary Sinus Septa: a mini review. *Italian Journal of Anatomy and Embryology* 126(2): 81-85. doi: 10.36253/ijae-13781

Copyright: ©2022 Manlio Santilli, Bruna Sinjari, Oriana Trubiani, Gianmaria d'Addazio, Imena Rexhepi, Giuseppe Tafuri, Eugenio Manciocchi, Sergio Caputi. This is an open access, peer-reviewed article published by Firenze University Press (<http://www.fupress.com/ijae>) and distributed under the terms of the Creative Commons Attribution License, which permits unrestricted use, distribution, and reproduction in any medium, provided the original author and source are credited.

Data Availability Statement: All relevant data are within the paper and its Supporting Information files.

Competing Interests: The Author(s) declare(s) no conflict of interest.

Prevalence and localization of Maxillary Sinus Septa: a mini review

MANLIO SANTILLI*, BRUNA SINJARI, ORIANA TRUBIANI, GIANMARIA D'ADDAZIO, IMENA REXHEPI, GIUSEPPE TAFURI, EUGENIO MANCIOCCHI, SERGIO CAPUTI

Department of Innovative Technologies in Medicine & Dentistry, University "G. d'Annunzio" Chieti Pescara, 66100, Chieti, Italy

*Corresponding author. E-mail: santilliman@gmail.com

Abstract. The anatomy of the maxillary sinus has been widely analysed over the last few years, specifically when it comes to its vascular anatomy, relationship to the teeth, and alveolar process. In fact, surgical procedures require the most accurate knowledge of anatomical structures, facilitated by the use of some state-of-the-art imaging technologies such as the cone beam computed tomography (CBCT). Such systems are constantly evolving in terms of quality, definition, image detail, and accuracy. This review aims to analyse the international literature of the last decade that has dealt with the topic of sinus anatomy, especially looking at the presence, percentage and localization of Underwood's septa, with the aim of supporting dentists to diagnose these anatomical structures in as much detail as possible and to perform surgery in this area with greater confidence.

Keywords: CBCT, maxillary sinus septa, oral surgery.

INTRODUCTION

The presence of adequate bone volume is crucial and represents a prerequisite for predictable results in implantology and implant prosthetics. Considering the upper jaw, large bone defects are rather treated with both autologous and/or non-autologous bone grafts but they are often associated with issues having different nature, such as the need for additional surgery, the limited availability of bone graft material, the short-time resorption, the inability to have intrinsic osteogenic (heterologous biomaterials) and the volumetric contraction of the material itself. Moreover, several anatomical complications are implicated in the upper jaw during sinus floor augmentation procedures. In fact, the presence of anatomical variants, such as the presence of one or more septa (as described by Underwood in 1910), also increases the risk of sinus membrane perforation during surgeries. Sinus septa are walls of cortical bone, located inside the sinus, whose shape has been described as an inverted Gothic arch arising from the sinus' lower or lateral walls and can even divide it into two or more cavities (Whyte A. et al, 2019;

Lorkiewicz-Muszynska D., 2015). Radiographic identification of these structures is extremely important since the design of the lateral hatch is based on the presence and size of the maxillary sinus septa, during sinus floor augmentation procedures (Von Arx et al, 2019). Therefore, the rapid progress made in recent years in dental radiology, specifically in cone beam computed tomography (CBCT), allowing for high detail and resolution images has been considered, also in light of the progressively frequent use of this technology made by dental specialists. Accordingly, this review aims to analyse the main articles published in the last decade on the presence, percentage, location, and average size of Underwood septa in the maxillary sinuses.

MATERIALS AND METHODS

Study design

Firstly, a Pubmed and Hand-Search were performed with the following keywords: “*maxillary sinus septa*”, “*sinus anatomy*”, “*maxillary sinus anatomy*”, “*paranasal sinus septa*”. These keywords were then combined with the Boolean operators ‘AND’, ‘OR’, ‘NOT’. The following filters were applied: in the last 10 years, Meta-Analysis, Review, Systematic Reviews, and clinical trial. For what concerns the Hand-Search, references from the following journals were also consulted: Clinical Implant Dentistry, Journal of Periodontal and Implant Science, Clinical Oral Implants Research, Implant Dentistry. Therefore, the following inclusion criteria were considered: trials investigated using 3D radiographs that presented data on the prevalence and location of septa (primary outcome). The words “augmentation” and “elevation” were excluded, as well as all studies presenting secondary outcome data related to septa integrity, septa orientation, and septa diagnosis only by orthopantomography (OPT). Below is the flow chart (Figure 1) of the research:

RESULTS

Table 1 below summarises the results of the study. A total of 16 scientific papers were included (e.g., Books, Clinical Trials and Systematic Reviews) and analysed with respect to the number of sinuses studied, number of septa found, and respective percentages. Moreover, the most frequent location and the average size of septa were analysed as detailed in Table 1.

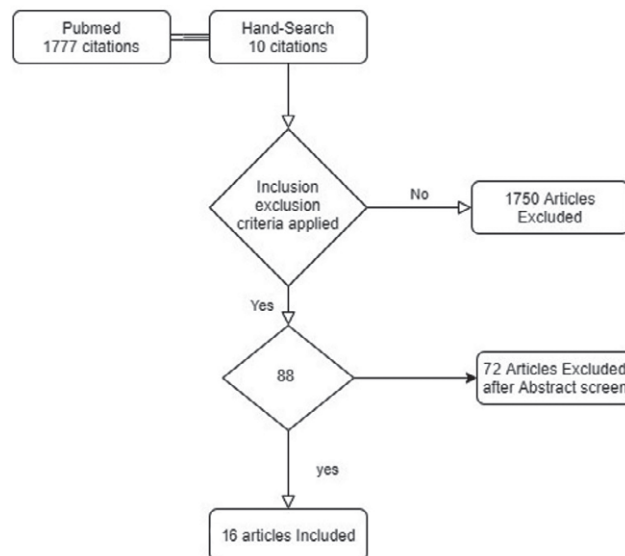


Figure 1. Flow-chart.

DISCUSSION

Sinus Floor Augmentation surgery can cause perforations of the membrane due to anatomical changes and septa.. Schneider’s membrane perforation can lead to postoperative complications, including acute or chronic sinus infections with bacterial invasion, swelling, and bleeding. Dislodgement of biomaterial within the sinus membrane causing sinusitis, chronic or acute, may also occur. Careful radiographic assessment of the size and position of the septa prevents complications both during and after sinus floor augmentation surgery. Based on the findings of the present study, the prevalence of septa in maxillary sinuses ranges between 6% and 68.4%. Specifically, the percentage ranges between 22.93% and 68.4%, while the size varies from 3.6mm to 7.36mm, except for a case study carried out in 2019 (Anbiaee N. et al,2019). This wide variation could be attributed to the fact that single studies differ based on the radiographic methods used, the criteria for septa identification, and the samples. In particular, various radiographic methods such as panoramic radiography (OPT), computed tomography (CT), and CBCT have been used to assess the presence and the anatomy of sinus septa. However, the present review has excluded those studies assessing this by only means of orthopantomography, which has represented the gold standard in literature for several years. In fact, CBCT has now become the gold standard for identifying the presence of septa, since this facilitates a detailed assessment of the maxillary sinus anatomy. Some researchers define a septum as being more than 2.5 mm

Table 1.

Author	Year	CBCT/CT	N ^o =Sinus	N ^o =Septa	%	Localization	Size
<i>Hungerbühler et al</i>	2019	CBCT	602	188	31.2%	Anterior 56 (29.8%) Middle 70(37.2%) Posterior 62(33%)	N.A.
<i>Zhang et al</i>	2019	CBCT	N.A.	355	N.A.	Anterior 108 (30.4%) Middle 180 (50.7%) Posterior 67 (18.9%)	N.A.
<i>Al-Zahrani et al</i>	2020	CBCT	1010	370	45.9%	Anterior 23 (6.2%) Middle 233(63%) Posterior 114 (30.8)	6.06±0.84 Right 5.70±0.93 Left
<i>Talo et al</i>	2017	CBCT	1000	297	29.7%	Anterior 44(8.7%) Middle 123 (24.5%) Posterior 131(26.4%)	4.62±2.50 mm
<i>Rancitelli et al</i>	2015	CBCT	228	87	38.1%	Anterior (29.4%) Middle (35.7%) Posterior (34.7%)	5.5 mm ± 1.19
<i>Kocac et al</i>	2019	CBCT	500	287	47.6%	Anterior 23.7% Middle 57.49% Posterior 18.81%	7.36mm
<i>Qian L et al</i>	2016	CBCT	1,012	390	48.2%	Anterior 136(34.8%) Middle 160 (41%) Posterior 94 (24.2%)	5.56 mm
<i>Toraman Alkurt M et al</i>	2016	CBCT	104	31	29.8%	Anterior 2(6.5%) Middle 23(74.2%) Posterior 6(19.35%)	N.A.
<i>Taleghani et al</i>	2017	CBCT	300	132	44%	Anterior (32.6%) Middle (34.8%) Posterior (32.6%)	3.6 ± 1.56 mm
<i>Anbiaee N et al</i>	2019	CT	199	23	6%	N.A.	N.A.
<i>Khalighi Sigaroudi et al</i>	2017	CBCT	444	265	68.4%	N.A.	N.A.
<i>Velasco-Torres M et al</i>	2017	CBCT	394	260	65.99%	N.A.	N.A.
<i>Chitsazi MT et al</i>	2017	CBCT	400	N.A.	26%	N.A.	N.A.
<i>Orhan K et al</i>	2013	CBCT	554	316	58%	Anterior 45 (12.2%) Middle 254 (69.1%) Posterior 70(18.6%)	5.12 mm
<i>Shen EC et al</i>	2012	CT	846	194	22.93%	Anterior 31 (15.98%) Middle 105 (54.12%) Posterior 53 (27.32%)	N.A.
<i>Jang SY et al</i>	2014	CBCT	200	63	26%	Anterior (47.6%) Middle (34.9%) Posterior (17.5%)	6.01 ± 2.21 mm

high, while for others, as in the case of Jang et al (Jang et al, 2014), a septum occurs when the bony walls are at least 4 mm. This is a key factor that should not be underestimated as this could justify the considerable discord-

ance in the data found in the literature. When describing the location of the septa, it is usually referred to location in the anterior region when the septum is in a mesial position to the root of the second premolar, in the central

region when it is in a mesial position to the distobuccal root of the second molar and the distal root of the second premolar, and in the posterior region when it is in a distal position to the distobuccal root of the second molar. Also in this case, there is a broad debate about the prevalence of one area over another (Lovasova et al, 2018). In fact, some studies have more frequently shown the presence of septa in the central region, while for others the most frequent location is indeed the anterior region, and finally, only for the study by Talo et al in 2017 (Talo et al, 2017) and Khalighi Sigaroudi et al (Khalighi Sigaroudi et al, 2017) the posterior region resulted to be the most frequent one. However, in 10 out of the 16 articles analysed in the present study, septa were most frequently found in the middle region, consistently with most of the data in the literature. This is considered to be an interesting finding that should not be overlooked and certainly deserves further investigation. One of the limitations of the present study may rely in the fact that the division between edentulous and non-edentulous patients was not taken into account, with respect to localization. So, further studies could be carried out.

FUNDING

This research received no external funding

REFERENCES:

- Anbiaee N., Khodabakhsh R., Bagherpour A. Relationship between Anatomical Variations of Sinonasal Area and Maxillary Sinus Pneumatization. (2019) *Iran J Otorhinolaryngol.* Jul;31(105):229-234. PMID: 31384589; PMCID: PMC6666940.
- Al-Zahrani M.S., Al-Ahmari M.M., Al-Zahrani A.A., Al-Mutairi K.D., Zawawi K.H. Prevalence and morphological variations of maxillary sinus septa in different age groups: a CBCT analysis. (2020) *Ann Saudi Med.* 40(3): 200-206.
- Chitsazi M.T., Shirmohammadi A., Faramarzi M., Esmaili F., Chitsazi S. Evaluation of the position of the posterior superior alveolar artery in relation to the maxillary sinus using the Cone-Beam computed tomography scans. (2017) *J Clin Exp Dent.* 9(3):e394-e399.
- Hungerbühler A., Rostetter C., Lübbers H.T., Rücker M., Staglinger B. Anatomical characteristics of maxillary sinus septa visualized by cone beam computed tomography. (2019) *Int J Oral Maxillofac Surg.* 48(3):382-387
- Jang S.Y., Chung K., Jung S., Park H.J., Oh H.K., Kook M.S. Comparative study of the sinus septa between dentulous and edentulous patients by cone beam computed tomography. (2014) *Implant Dent.* 23(4):477-81.
- Khalighi Sigaroudi A., Dalili Kajan Z., Rastgar S., Neshandar Asli H. Frequency of different maxillary sinus septal patterns found on cone-beam computed tomography and predicting the associated risk of sinus membrane perforation during sinus lifting. (2017) *Imaging Sci Dent.* 47(4):261-267.
- Kocak N., Alpoz E., Boyacıoğlu H. Morphological Assessment of Maxillary Sinus Septa Variations with Cone-Beam Computed Tomography in a Turkish Population. (2019) *Eur J Dent.* 13(1):42-46.
- Lorkiewicz-Muszynska D., Kociemba W., Rewekant A., Sroka A., Jonczyk-Potoczna K., Patelska-Banaszewska M., Przytanska A. (2015) Development of the maxillary sinus from birth to age 18. Postnatal growth patterns. *International Journal of Paediatric Otorhinolaryngology* 79 : 1393–1400
- Lovasova K., Kachlik D., Rozpravkova M., Matusevska M., Ferkova J., Kluchova D. (2018) Threedimensional CAD/CAM imaging of the maxillary sinus in ageing process. *Annals of Anatomy.* 218 69–82
- Orhan K., Kusakci Seker B., Aksoy S., Bayindir H., Berberoğlu A., Seker E. Cone beam CT evaluation of maxillary sinus septa prevalence, height, location and morphology in children and an adult population. (2013) *Med Princ Pract.* 22(1):47-53.
- Qian L., Tian X.M., Zeng L., Gong Y., Wei B. Analysis of the Morphology of Maxillary Sinus Septa on Reconstructed Cone-Beam Computed Tomography Images. (2016) *J Oral Maxillofac Surg.* 74(4):729-37.
- Rancitelli D., Borgonovo A.E., Cicciù M., Re D., Rizza F., Frigo A.C., Maiorana C. (2015) Maxillary Sinus Septa and Anatomic Correlation With the Schneiderian Membrane. *J Craniofac Surg.* 26(4):1394-8.
- Shen E.C., Fu E., Chiu T.J., Chang V., Chiang C.Y., Tu H.P. Prevalence and location of maxillary sinus septa in the Taiwanese population and relationship to the absence of molars. (2012) *Clin Oral Implants Res.* 23(6):741-745.
- Taleghani F., Tehranchi M., Shahab S., Zohri Z. Prevalence, Location, and Size of Maxillary Sinus Septa: Computed Tomography Scan Analysis. (2017) *J Contemp Dent Pract.* 18(1):11-15.
- Talo Yildirim T., Güncü G.N., Colak M., Nares S., Tözüm T.F. Evaluation of maxillary sinus septa: a retrospective clinical study with cone beam computerized tomography (CBCT). (2017) *Eur Rev Med Pharmacol Sci.* 21(23):5306-5314.

- Toraman Alkurt M., Peker I., Degerli S., Cebeci ARİ., Sadik E. Comparison of cone-beam computed tomography and panoramic radiographs in detecting maxillary sinus septa. (2016) *J Istanbul Univ Fac Dent*. 50(3):8-14.
- Velasco-Torres M., Padiál-Molina M., Avila-Ortiz G., García-Delgado R., O'Valle F., Catena A., Galindo-Moreno P. Maxillary Sinus Dimensions Decrease as Age and Tooth Loss Increase.(2017) *Implant Dent*. 26(2):288-295.
- Von Arx T., Lozanoff S., Bornstein MM.(2019) Extraoral anatomy in CBCT – a literature review. Part 1: Nasoethmoidal region. *Swiss Dent J*. 129(10):804-815.
- Whyte A., Boeddinghaus R.(2019) The maxillary sinus: physiology, development and imaging anatomy. *Dentomaxillofac Radiol*.48(8).
- Zhang Y.Q., YAN X.B.,Meng Y.,Zhao Y.N., Liu D.G. Morphologic Analysis of Maxillary Sinus Floor and its Correlation to molar roots using cone beam computed tomography.(2019) 22(1):29-36.



Citation: Maria Enrica Miscia, Pasquale Simeone, Giuseppina Bologna, Paola Lanuti, Gabriele Lisi, Laura Pierdomenico, Dacia Di Renzo, Marco Marchisio, Sebastiano Miscia, Pierluigi Lelli Chiesa (2022) Circulating endothelial cells and endothelial-derived vesicles identification in patients with infantile hemangioma: preliminary results of a prospective cohort study. *Italian Journal of Anatomy and Embryology* 126(2): 87-91. doi: 10.36253/ijae-13833

Copyright: © 2022 Maria Enrica Miscia, Pasquale Simeone, Giuseppina Bologna, Paola Lanuti, Gabriele Lisi, Laura Pierdomenico, Dacia Di Renzo, Marco Marchisio, Sebastiano Miscia, Pierluigi Lelli Chiesa. This is an open access, peer-reviewed article published by Firenze University Press (<http://www.fupress.com/ijae>) and distributed under the terms of the Creative Commons Attribution License, which permits unrestricted use, distribution, and reproduction in any medium, provided the original author and source are credited.

Data Availability Statement: All relevant data are within the paper and its Supporting Information files.

Competing Interests: The Author(s) declare(s) no conflict of interest.

Circulating endothelial cells and endothelial-derived vesicles identification in patients with infantile hemangioma: preliminary results of a prospective cohort study

MARIA ENRICA MISCIA^{1,*}, PASQUALE SIMEONE¹, GIUSEPPINA BOLOGNA¹, PAOLA LANUTI¹, GABRIELE LISI¹, LAURA PIERDOMENICO¹, DACIA DI RENZO², MARCO MARCHISIO¹, SEBASTIANO MISCIA¹, PIERLUIGI LELLI CHIESA¹

¹ Department of Medicine and Aging Science, “G.d’Annunzio” University, Chieti-Pescara, 66100 Chieti, Italy; Pediatric Surgery Department, “Spirito Santo” Hospital, Pescara, 65124 Pescara, Italy

² Pediatric Surgery Department, “Spirito Santo” Hospital, Pescara, 65124 Pescara, Italy

*Corresponding author. E-mail: mariaenrica.miscia@unich.it

Abstract. Circulating Endothelial Cells (CEC) and Circulating Extracellular Vesicles (cEVs) are biological markers of endothelial activity/dysfunction and may play a pivotal role in the evolution of IH. Our aims were to detect variations in CEC and cEVs concentration: 1. in IH versus healthy controls; 2. in IH before and after propranolol administration. Twenty-two children (15 cases; 7 controls) from our Department underwent peripheral blood sampling to study CECs, EPCs and EVs via cytofluorimetry. Statistical analyses were performed using XLSTAT ver. 2014.5.03 and GraphPad Prism ver. 8.0. Data were expressed as mean ± standard deviation, median, 5-95th percentile. The number of CEC and HSC was higher among cases than controls, even if not statistically significant. The number of CEC decreased with the evolution of the hemangioma; number of HSC decreased proportionally with the age of the patient. Number of EVs tended to increase when the CECs decrease and vice-versa in the group of cases but not among controls. Number of CEC and HSC was significantly reduced after oral propranolol administration (p: <0,0001). In conclusion CECs may represent a marker of progression of disease. Propranolol seems to affect the number of CECs and HSCs.

Keywords: circulating endothelial cells, extracellular vesicles, children, infantile hemangioma, propranolol.

INTRODUCTION

Infantile Hemangioma (IH) is the most common vascular tumor of infancy, affecting up to 10% of children, especially premature with low birth weight, with a female predominance [Mattassi R et al., Darrow DH et al. 2015, Huang J et al. 2019, Satterfield KR 2019, Bauland GC et al. 2006]. They are characterized by an abnormal proliferation of endothelial cells that

express the Glucose Transporter-1 protein (GLUT1), which is not usually expressed by normal endothelial cells, and that do not show a regular vascular architecture [Huang J et al. 2019, Bauland GC et al. 2006].

Oral propranolol, a non-selective beta-blocker, is the therapy of choice in the treatment of “complicated” IH [Huang J et al. 2019, Satterfield KR 2019, Bauland GC et al. 2006].

It is well known that the endothelial homeostasis is highly influenced by the evolution of the tumors and Circulating Endothelial Cells (CEC), Endothelial Progenitor Cells (EPC) and Circulating Extracellular Vesicles (cEV) are recognized biological markers used for monitoring the endothelial activity/dysfunction [Lanuti P et al. 2012].

Therefore, it is likely that CEC, EPC and cEV may be used as markers of progression of the disease.

The aims of our study were to detect:

1. variations in CEC and cEVs concentration and in the CEC/EPCs ratio in children with IH versus healthy controls;
2. changes in concentration of CEC and cEVs after oral propranolol administration.

MATERIALS AND METHODS

Patients

After local ethical committee approval (V 1.0, 4 February 2016), 22 children (15 cases and 7 controls) were enrolled in the study from the “Department of Pediatric Surgery”, “Santo Spirito” Hospital of Pescara, Italy.

After written informed consent was obtained from the parents or guardians, a peripheral blood sample was withdrawn from each child and repeated in cases after 1 month of oral propranolol therapy.

Data acquisition

10 × 10⁶ events/sample were acquired by flow cytometry (FACSCanto II, BD Biosciences) at “medium” flow rate mode.

CEC and cEV were identified as previously reported [Lanuti P et al. 2018, Marchisio M et al. 2016, Lanuti P et al. 2020].

Statistical analysis

Statistical analyses were performed using XLSTAT ver. 2014.5.03 (Addinsoft, Paris, France) and GraphPad

Prism ver. 8.0 (GraphPad Software Inc., La Jolla, Ca, USA).

Parametric or non-parametric tests were used as appropriate.

Data were expressed as mean ± standard deviation (SD), median, 5-95th percentile.

RESULTS

Twenty-two infants and children were included in the study, 15 cases and 7 controls.

We identified the Circulating Endothelial Cells (CEC) as CD45-/ CD34bright/ CD146+ events by flow cytometry, while Hematopoietic Stem Cells (HSC) as CD45dim/ CD34+ events. We also analyzed the extracellular vesicles (EV) whose origin was endothelial (CD31+) or staminal (CD133+).

Among the whole population, mean CEC number was 29,55 ± 39,12 (range 0-159,8), while mean HSC number was 4015 ± 4865 (range 79,39-18983). Mean number of EV CD31+ was 114,6 ± 202,6/ml (range 0-700,00) and mean number of EV CD133+ was 66,89 ± 103,9/ml (range 0-355,6).

When comparing cases versus controls, we found a higher number of CEC and HSC among cases than controls, even if not statistically significant (table 1).

We did not find any statistical significance also when comparing the number of EV CD31+ and CD133+ in cases versus controls (table 1). However, the number of EV CD 133+ was higher in cases than controls, even if not statistically significant.

We then analyzed the number of CEC and HSC in cases in relation to the phase of the evolution of the infantile hemangioma (IH). We found that the number of CEC and HSC decreased proportionally with the evo-

Table 1. Comparison between cases and controls. p significative when <0.05.

	Cases (n=15)	Controls (n=6)	p value
CEC (mean ± SD) (range)	36,5 ± 43,55 (1,96-159,8)	8,732 ± 8,783 (0-20,17)	0.1444
HSC (mean ± SD) (range)	4866 ± 5359 (647,4-18983)	1503 ± 1713 (79,39-45,46)	0.1549
EV CD31+/ml (mean ± SD) (range)	117,7 ± 211,8 (0-700,00)	121,8 ± 206,9 (0-617,4)	0.9642
EV CD133+/ml (mean ± SD) (range)	86,05 ± 115,9 (2,8-355,6)	36,93 ± 75,67 (0-222,6)	0.2907

CEC: circulating endothelial cells, HSC: hematopoietic stem cells, EV: extracellular vesicles. Mann-Whitney U test.

Table 2. Number of CEC and HSC according to the stage of the infantile hemangioma. The patient HRA was analyzed before (HRA_16) and after (HRA_18) oral propranolol administration.

ID	DOB	Gender	Phase of IH	CEC (n)	HSC (n)
HRA_16	01/01/20	F	proliferation	87,43	3906,91
CM_22	08/07/20	F	proliferation	32,6	3495,79
RR_9	16/06/19	M	proliferation	65,73	18982,97
DMA_12	20/01/19	F	proliferation	50,61	3197,01
GD_11	31/07/19	F	proliferation	13,48	4210,24
TM_23	14/05/20	F	proliferation	29,44	2637,97
AI_15	19/05/19	F	quiescence	7,20	2800,75
MD_24	25/11/19	M	quiescence	9,02	1399,82
PC_20	16/07/19	F	involution	159,83	14478,02
VE_06	06/10/12	M	involution	25,86	2218,27
HRA_18	01/01/20	F	involution	14,28	2066,56
DCS_13	13/07/17	F	involution	9,91	647,43
DBA_8	18/07/19	M	involution	3,67	7236,06

DOB: date of birth, IH: infantile hemangioma; CEC: circulating endothelial cells, HSC: hematopoietic stem cells.

lution of the hemangioma and this association was clearer when eliminating patient nr.20 (PC_20; table 2).

Of note, the number of CEC and HSC was significantly reduced in the patient HRA, before (HRA_16: CEC 87,43; HSC 3906,91) and after oral propranolol administration (HRA_18: CEC 14,28; HSC 2066,56; $p < 0,0001$) [table 2, figure 1].

Moreover, we found that the number of HSC tends to decrease when the child becomes older, and this correlation appears to be clear also when analyzing cases and controls separately.

Among the HSC population, we found a subgroup of HSC CD117+ which was highly expressed in cases but not in controls (3477 ± 4752 , range 286,4-15043 in cases; $654,7 \pm 614,9$, range 42,34-1428 in controls; $p = 0.0003$).

DISCUSSION

It is well known that the endothelial homeostasis depends on the equilibrium between CECs and EPCs [Lanuti P et al. 2015, Sabatier F et al. 2009, Najjar F et al. 2018].

Any variation in their concentration may represent a marker of endothelial activity or damage: in fact, their changes have been studied in cardiovascular diseases and tumors [Bauland GC et al. 2006, Lanuti P et al. 2016, Najjar F et al 2018, Shantsila E et al. 2008].

However, there are no studies which focused their attention on the role of the CECs in the etiopathogenesis and development of IH.

In a recent study on healthy adults, the normal values of CECs were determined which were different in females compared to males ($12,10 \pm 10,02$ versus $13,69 \pm 9,19$; $p = 0,0218$) [Lanuti P et al. 2012].

However, there are no studies that define a normal range of CECs in children. In our study, we found that the mean CEC count in the whole population was slightly higher than the one found in adults ($22,04 \pm 25,78$). Moreover, the number of CECs was higher in children affected by IH than in controls ($p = ns$).

The number of CECs in cases decreases proportionally with the evolution of the IH and this is maybe due to the reduction of the endothelial activity in the involutive and involute phases, when the vessels are replaced by fatty tissue. Therefore, the number of CECs may be identified as biomarker of evolution of the IH.

It has also been demonstrated that in peripheral blood of healthy adults the number of HSC is about $2663,3 \pm 1288,33$ [Marchisio M et al. 2020]. We found a higher number of HSC in our population (4015 ± 4865) compared to adults, which is even higher when analyzing only the IH group (4866 ± 5359), thus reflecting a higher recruitment of the staminal compartment.

Moreover, we found a subgroup of CD117+ cells which are highly expressed only in cases than controls. This subpopulation needs to be further investigated.

Propranolol seems to influence cells viability and proliferation [Erdbruegger U et al. 2010]. We found it to affect the number of CECs and HSCs; however larger studies are needed to confirm this assumption.

The number of EVs itself does not seem to be a marker of the disease, but the study of their molecular cargo will help in elucidating the mechanisms at the basis of the evolution of the IH.

FUNDING

This research received no external funding.

REFERENCES

- Mattassi R et al. Hemangiomas and Vascular Malformations. An Atlas of Diagnosis and Treatment. Second Edition. Springer.
- Darrow DH et al. Diagnosis and Management of Infantile Hemangioma: Executive Summary. PEDIATRICS Volume 136, number 4, October 2015.
- Huang J et al. Propranolol suppresses infantile hemangioma cell proliferation and promotes apoptosis by upregulating miR-125b expression. Anti-Cancer Drugs 2019, Vol 30 No 5: 501-507.

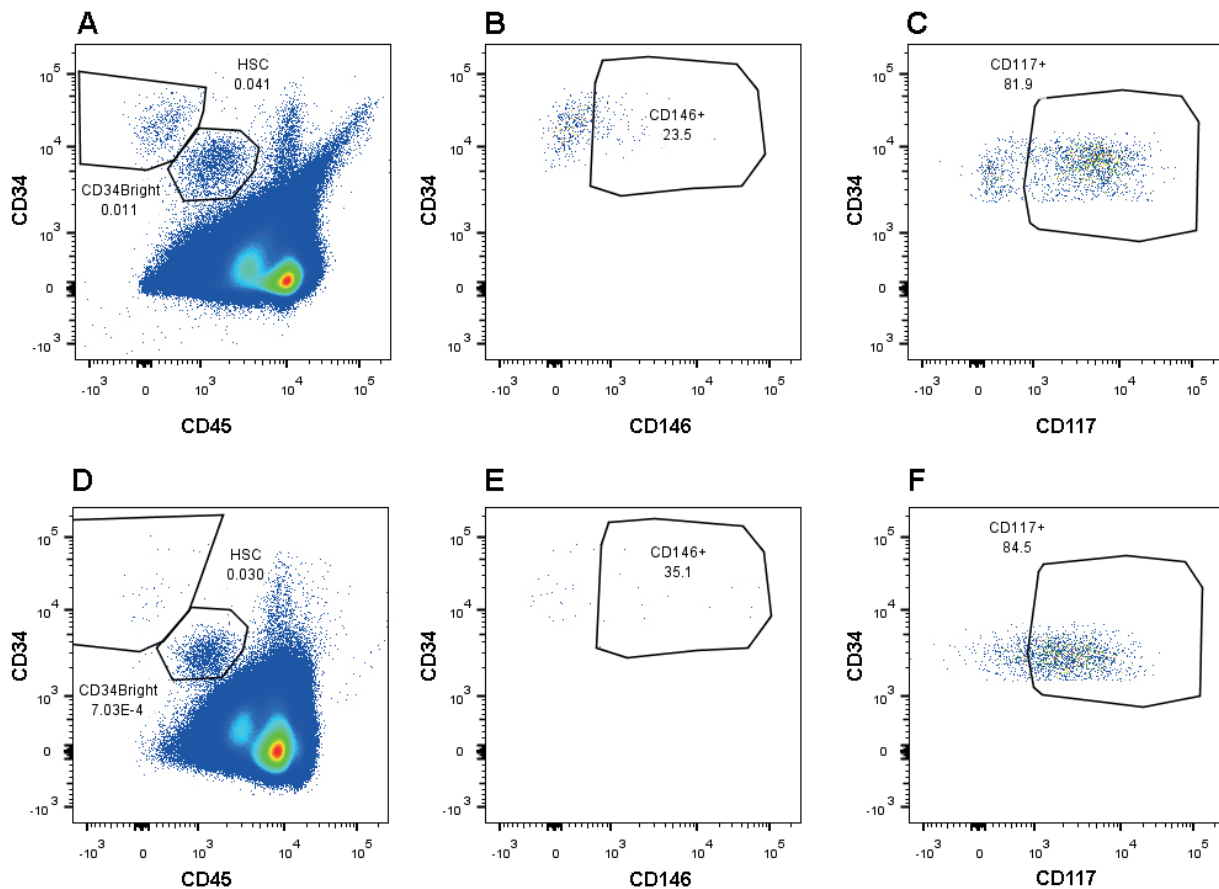


Figure 1. Flow cytometry identification of CEC and HSC in PB samples. **A, D** Cells displaying the lymph-monocyte morphology, alive and nucleated were analyzed for CD45 and CD34 expression (on a CD45/CD34 dot plot). The whole CD34pos cell compartment was identified and two subpopulations, displaying different levels of CD34 surface expression, were identified and gated separately: CD34 positive cells, which are CD45dim and represent the hematopoietic stem cell compartment (HSC), and a CD34 bright population, which resulted CD45 negative (CD34 bright). **B, E** CD34 bright/CD45neg cell populations were then analyzed for CD146 expression, on a CD146/CD34 dot plot and represent CEC compartment. **C, F** The hematopoietic stem cell compartment (HSC) was analyzed for CD117 expression, on a CD117/CD34 dot plot.

Satterfield KR, Chambers CB. Current treatment and management of infantile hemangiomas. *Survey of ophthalmology* 64 (2019) 608-618.

Bauland GC et al. The Pathogenesis of Hemangiomas: A Review. *Plast. Reconstr. Surg.* 117: 29e, 2006.

Lanuti P et al. A novel flow cytometric approach to distinguish circulating endothelial cells from endothelial microparticles: Relevance for the evaluation of endothelial dysfunction. *Journal of Immunological Methods* 380 (2012) 16-22.

Lanuti P et al. A standardized flow cytometry network study for the assessment of circulating endothelial cell physiological ranges. *Scientific Reports* (2018) 8:5823 | DOI:10.1038/s41598-018-24234-0 (ex 8)

Marchisio M et al. Flow Cytometry Analysis of Circulat-

ing Extracellular Vesicles Subtypes from Fresh Body Fluids. *Int J Mol Sci.* 2020 Dec 23;22(1):E48. doi: 10.3390/ijms22010048. (ex12)

Lanuti P et al. Endothelial Progenitor Cells, defined by the Simultaneous Surface Expression of VEGFR2 and CD133, are not Detectable in Healthy Peripheral and Cord Blood. *CytometryPartA.* 89A:259-270,2016. DOI: 10.1002/cyto.a.22730 (ex25)

Sabatier F et al. Circulating endothelial cells, microparticles and progenitors: key players towards the definition of vascular competence. *J. Cell. Mol. Med.* Vol 13, No 3 (2009) 454-471. (ex7)

Najjar F et al. Circulating endothelial cells and microparticles as diagnostic and prognostic biomarkers in small-cell lung cancer, *Lung Cancer* (2018), <https://>

doi.org/10.1016/j.lungcan.2018.06.033. (ex27)

Shantsila E et al. Circulating endothelial cells: from bench to clinical practice. *Journal of Thrombosis and Haemostasis*, 2008 6: 865-868.(ex10)

Erdbruegger U et al. Circulating Endothelial Cells: Markers and Mediators of Vascular Damage. *Current Stem Cell Research & Therapy*, 2010, 5, 294-302. (ex9)

Zhao F et al. Propranolol suppresses HUVEC viability, migration, VEGF expression, and promotes apoptosis by downregulation of miR-4295. *J Cell Biochem*. 2018;1-10. <https://doi.org/10.1002/jcb.27957> (ex19)



Citation: Federica Giuliani, Giulio Gualdi, Paolo De Sanctis, Paolo Amerio (2022) Case series of two different dose regimen Rituximab therapy for severe Pemphigus. *Italian Journal of Anatomy and Embryology* 126(2): 93-96. doi: 10.36253/ijae-13919

Copyright: © 2022 Federica Giuliani, Giulio Gualdi, Paolo De Sanctis, Paolo Amerio. This is an open access, peer-reviewed article published by Firenze University Press (<http://www.fupress.com/ijae>) and distributed under the terms of the Creative Commons Attribution License, which permits unrestricted use, distribution, and reproduction in any medium, provided the original author and source are credited.

Data Availability Statement: All relevant data are within the paper and its Supporting Information files.

Competing Interests: The Author(s) declare(s) no conflict of interest.

Case series of two different dose regimen Rituximab therapy for severe Pemphigus

FEDERICA GIULIANI*, GIULIO GUALDI, PAOLO DE SANCTIS, PAOLO AMERIO

Dermatologic Clinic, Department of Medicine and Aging Science, University “G. D’Annunzio” of Chieti-Pescara, Chieti, Italy

*Corresponding author. E-mail: federica.giuliani@asl2abruzzo.it

Abstract. Rituximab is a monoclonal antibody approved for treatment of adults with severe and refractory pemphigus vulgaris. Concerns about side effects and high costs of conventional doses have risen the hypothesis that low-dose rituximab regimen may be cost-effective with a better safety profile. Here we report our experience of seven patients with extensive/recalcitrant pemphigus, who either were steroid dependent, had contraindications or refused conventional treatment. Two patients received conventional rituximab (1000 mg 2 weeks apart) while five received ultra low-dose rituximab (200 mg 2 weeks apart). At 3 months, the two patients treated with high Rituximab regimen showed respectively a complete remission off therapy (CROT) and a complete remission on minimal therapy (CRMT), while among the five patients treated with ultra low-doses, three achieved CROT, one achieved CRMT and one a partial remission off therapy (PROT). All patients treated with ultra low-dose rituximab achieved complete depletion of cd19+ and cd19/45+ B lymphocytes after three months and all patients except one male maintained the zeroing after 6 months. No serious side effect was documented with low dose regimen except for a case of dizziness. Our data suggest that ultra low-dose rituximab can be effective even in patients with extensive/recalcitrant pemphigus, with a lower probability of side-effects respect to higher dose regimen and may act as a steroid sparing strategy.

Keywords: Rituximab, Pemphigus, low-dose therapy, ultra low-dose regimen.

INTRODUCTION

Pemphigus includes a group of rare autoimmune bullous diseases characterized by flaccid blisters and erosions of the mucous membranes and skin. This sometimes life-threatening condition, is characterized by the presence of IgG autoantibodies against the desmosomal adhesion proteins, desmoglein 3 and/or desmoglein 1, on epidermal keratinocytes, that are responsible of intraepithelial blister formation.

The severity of the disease is based on its progressive course which is accompanied by an increased body catabolism with loss of body fluids and proteins and secondary bacterial and viral infections which may lead to sepsis and heart failure.

Rituximab is a chimeric monoclonal antibody approved for treatment of adults with severe and refractory pemphigus vulgaris. Recent studies have focused on assessments of efficacy and safety of low-dose rituximab (<2 gram in each cycle)[2-8].

We reported our experiences based on a case series of seven patients treated with Rituximab at rheumatologic dose regimen (1000) and ultra-low (200) dose regimen.

MATERIALS AND METHODS

Seven patients with extensive pemphigus were selected (Table 1), who either had recalcitrant pemphigus, were steroid dependent, had relapsed after pulse therapy, had contraindications to conventional treatment or wanted to avoid conventional treatment and its side effects. Two doses of conventional rituximab (1000 mg) or ultra low-dose rituximab (200 mg) were given 2 weeks apart and patients were regularly followed up every 2 weeks for the first month and then every three months. Complete blood counts, liver function tests, renal function tests, flow cytometry assessments of B-cell subtypes, skin biopsy, direct immunofluorescence and desmoglein levels were checked before and after rituximab administration. Pre-rituximab chest X-ray, electrocardiograph, oculistic evaluation and computed bond mineral density were also obtained. Clinical response was defined by the criteria outlined in the consensus statement on definitions of endpoints and therapeutic response for pemphigus [1] Complete remission off therapy (CROT) was defined as complete epithelialization and absence of new or established lesions while the patient is off all systemic therapy for at least 2 months while complete remission on minimal therapy (CRMT) was defined as the absence of new lesions while the patient is receiving minimal doses of systemic therapy. Partial remission off therapy (PROT) was defined as the presence of transient new lesions that healed within 1 week without treatment and while off all systemic

therapy. Minimal therapy was defined as prednisone up to 10 mg/day or azathioprine up to 1.25 mg/kg/day. Relapse was defined as the appearance of at least three new lesions in 1 month that did not heal spontaneously within 1 week or the extension of established lesions in a patient who had previously achieved disease control.

RESULTS

We recruited seven patients with an average age of 63.1 years old, three were males and four females (Table 1). All of them undergoing and failed previous systemic corticosteroid therapy (Metilprednisolone 1 mg/kg/die or multiple boluses of 1 gr) and/or systemic immunosuppressant (Azathioprine or Mycophenolate). Two male patients were treated with two doses of Rituximab at rheumatologic regimen (1000 mg) two weeks away. One male patient and three female patients were treated with two ultra-low doses of Rituximab (200 mg) two weeks away. At 3 months, the two patients treated with Rituximab at rheumatologic regimen (1000 mg) showed respectively a complete remission off therapy (CROT) and a complete remission on minimal therapy (CRMT). At 3 month, the five patients treated with ultra-low doses of Rituximab (200 mg) achieved respectively: three patients a complete remission off therapy (CROT), one patient a complete remission on minimal therapy (CRMT) and one patient a partial remission off therapy (PROT) (Table 2; Graphic 1).

Two patients showed adverse events, in detail, one patient treated with Rituximab 1000 mg showed defect of vision like visual blurring and one patient treated with Rituximab 200 mg developed dizziness (Table 2).

Flow cytometry assessments of B-cell subtypes displayed a lasting maintenance of the zeroing of linf B cd19 + and cd19 / 45 + at three months and at 6 months in all patient except one male patient treated with 200 mg (Table 2; Graphic 2).

Table 1. Population dermatographic characteristics

Patients	Age	Sex	Desease	Previous therapy	Dose T0	Dose T1 (2w)
1	82	M	Pemfigo	CS	1000	1000
2	32	M	Pemfigo	CS, AZT	1000	1000
3	74	M	Pemfigo	CS	200	200
4	66	F	Pemfigo	CS	200	200
5	55	F	Pemfigo	CS, MMF, AZT	200	200
6	64	F	Pemfigo	CS, Dapsone, MMF, evIG	200	200
7	69	F	Pemfigo	CS, RTX	200	200

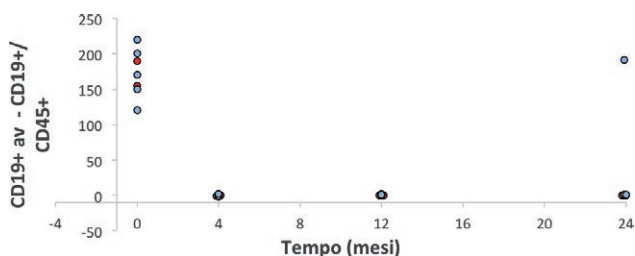
Table 2. Results of efficacy and safety in patients undergoing Rituximab at conventional and ultra low-dose regimen.

Patients	Age	Sex	Dose T0	Results (12w)	Cd19+ Cd19+/ Cd45+% (4 W)	Cd19+ / Cd19+/ Cd45+% T2 (12w)	Cd19+ / Cd19+/ Cd45+% T3 (24w)	Aes
1	82	M	1000	CROT	0/0	0/0	0/0	-
2	32	M	1000	CRMT	0/0	0/0	0/0	EP
3	74	M	200	CROT	2/0	2/0	1/0	headache
4	66	F	200	PROT	0/0	0/0	191/10	dizziness
5	55	F	200	CROT	0/0	0/0	0/0	-
6	64	F	200	CROT	0/0	1/0	1/0	-
7	69	F	200	CRMT	0/0	1/0	1/0	-

Results



Graphic 1. Results at week 12, in patients undergoing two doses of low-dose Rituximab (200 mg). CROT complete remission off therapy; CRMT: complete remission on minimal therapy; PROT: partial remission off therapy.



Graphic 2. Maintenance of zeroing cd19+ and cd19+/45+ B lymphocytes since first week, maintained after 3 and 6 months from the first infusion.

DISCUSSION

Rituximab has been approved as a treatment for moderate-to-severe Pemphigus Vulgaris (PV). By depleting B cells, rituximab decreases circulating anti-desmoglein autoantibodies. However, the optimal dosage has not been standardized. Since the B-cell burden in autoimmune blistering skin diseases is much lower than that in lymphoproliferative disorders, lower dosage regimens, as low as a single infusion of 200 mg has been reported to be effective for

PV (Ailabac et al [4]). Schoergenhofer et al. [5] showed that CD20+ cells were depleted by 68%, 74%, and 97% at 1 h after the infusion of rituximab at the doses of 0.1, 0.3, and 1 mg/m², respectively, and the CD20+ cell counts gradually returned to baseline in 1–9 months. Therefore, the authors extrapolated that 100 mg Rituximab may be sufficient to fully suppress CD20+ cells for 3 months.

In our series low-dose Rituximab regimen was associated with a good and prolonged clinical response with zeroing of cd19+ and cd19+/45+ B lymphocytes since first week, maintained after 3 and 6 months from the first infusion (Graphic 2). No serious side adverse events was reported, and only one male developed dizziness.

Our data show that this strategy can be effective even in patients with extensive and recalcitrant pemphigus, with a lower probability of side-effects, thus potentially reducing the negative consequences deriving from long-term use of corticosteroids and other immunosuppressive drugs.

Instead higher Rituximab doses “at rheumatologic regimen”, may be necessary in very severe cases with high levels of anti-desmoglein 3 antibodies, which are considered predictive of therapy failure.

Such preliminary hypothesis need to be confirmed on larger and possibly randomized prospective clinical trials.

CONCLUSIONS

Our results suggest that ultra low-dose rituximab can be a well-tolerated and effective adjuvant therapy in recalcitrant and/or severe pemphigus which may also act as a steroid-sparing strategy, avoiding long-term side effects of chronic corticosteroids intake.

FUNDING

This research received no external funding.

REFERENCES

1. Murrell DF, Dick S, Ahmed AR, Amagai M, Barnadas MA, Borradori L, et al. Consensus statement on definitions of disease, end points, and therapeutic response for pemphigus. *J Am Acad Dermatol* 2008;58:1043–6.].
2. Lemieux A, Maho-Vaillant M, Golinski ML, et al. Evaluation of Clinical Relevance and Biological Effects of Antirituximab Antibodies in Patients With Pemphigus. *JAMA Dermatol*. 2022 Jun 22. doi: 10.1001/jamadermatol.2022.2149. Epub ahead of print. PMID: 35731529.
3. Singh N, Handa S, Mahajan R, et al. Comparison of the efficacy and cost-effectiveness of an immunologically targeted low-dose rituximab protocol with the conventional rheumatoid arthritis protocol in severe pemphigus. *Clin Exp Dermatol*. 2022 Apr 5. doi: 10.1111/ced.15213. Epub ahead of print. PMID: 35384021.
4. Russo I, Miotto S, Saponeri A, Alaibac M. Ultra-low dose rituximab for refractory pemphigus vulgaris: a pilot study. *Expert Opin Biol Ther*. 2020;20:673–8.
5. Schoergenhofer C, Schwameis M, Firbas C, Bartko J, Derhaschnig U, Mader RM, et al. Single, very low rituximab doses in healthy volunteers—a pilot and a randomized trial: implications for dosing and bio-similarity testing. *Sci Rep*. 2018;8:124
6. Tavakolpour A systematic review on efficacy, safety, and treatment-durability of low-dose rituximab for the treatment of Pemphigus: special focus on COVID-19 pandemic concerns
7. Keeley JM, Bevans SL, Jaleel T, Sami N. Rituximab and low dose oral immune modulating treatment to maintain a sustained response in severe pemphigus patients. *J Dermatolog Treat*. 2019 Jun;30(4):340-345. doi: 10.1080/09546634.2018.1510173. Epub 2018 Sep 7. PMID: 30086663.
8. Gupta J, Raval RC, Shah AN, et al. Low-dose rituximab as an adjuvant therapy in pemphigus. *Indian J Dermatol Venereol Leprol*. 2017 May-Jun;83(3):317-325. doi: 10.4103/ijdv.IJDVL_1078_14. PMID: 28366912.

Finito di stampare da
Logo s.r.l. – Borgoricco (PD) – Italia

<p>The vascular structure of the urethra: a historical overview Gianfranco Natale, Emanuele Armocida</p> <p>Bioarcheological and paleopathological study of a multiple deposition burial from S. Antine- Genoni (SU) – Sardegna - Italy Rita M. Serra, Paolo Melis, Andrea Montella, Pasquale Bandiera</p> <p>Off-line or on-line? – near-peer assisted anatomy education in the time of Covid-19 pandemic – a single center randomized controlled study Jurand Domański, Marta Wanat, Jacek Ciach, Angelika Osuch, Bożena Kurc-Darak, Sławomir Woźniak, Zygmunt Domagała</p> <p>Utility of the Movat pentachrome stain technique in the microanatomical analysis of the human placenta Zygmunt Domagała, Agnieszka Pinkowska, Aleksandra Piotrowska, Jurand Domański, Victoria Tarkowski, Aleksandra Zimmer-Stelmach, Jakub Śliwa</p> <p>Special issue on Innovative Technologies in Clinical Medicine & Dentistry (InTEchMed) Oriana Trubiani</p> <p>Role of extracellular vesicles derived by human gingival mesenchymal stem cells in cardiomyocytes acute hypoxia Ylenia Della Rocca, Jacopo Pizzicannella, Guya Diletta Marconi, Luigia Fonticoli, Oriana Trubiani, Francesca Diomedede</p> <p>The role of the applied load in bone homeostasis and its implications in implant dentistry: a mini-review Francesco Valente, Oriana Trubiani, Tonino Traini</p> <p>Presepsin: a biomarker of early-onset neonatal sepsis Valentina Botondi, Ebe D'Adamo, Oriana Trubiani, Diego Gazzolo</p> <p>Autophagy inhibitors in the treatment of colorectal cancer: a brief review Martina Ceci, Manuela Iezzi, Marco Trerotola</p> <p>A prospective, blinded, randomized-controlled study on regressive bone modeling around dental implants with different machined coronal portion Stefano Oliva, Antonio Scarano, Oriana Trubiani, Bruna Sinjari, Maurizio Piattelli</p>	<p>3</p> <p>9</p> <p>17</p> <p>25</p> <p>33</p> <p>35</p> <p>39</p> <p>43</p> <p>47</p> <p>51</p>	<p>Presepsin assessment in maxillo-facial infections: a new early biomarker of sepsis? Luigi Falconio, Oriana Trubiani, Diego Gazzolo, Francesco Valente, Tonino Traini</p> <p>Effects of <i>Fusobacterium nucleatum</i> on migration and cytokines production of ags gastric adenocarcinoma cell line Mariangela Mazzone, Maria Carmela Di Marcantonio, Valentina Puca, Beatrice Marinacci, Giulia Nannini, Simone Guarnieri, Amedeo Amedei, Gabriella Mincione, Raffaella Muraro¹</p> <p>Inflammatory Bowel Disease (IBD): a novel biological role of saffron petal extracts as a modulator of phlogistic pathway <i>via</i> FBW7/NF-κB in Caco-2 cell line LPS-stimulated Federica De Cecco, Sara Franceschelli, Lorenza Speranza</p> <p>Genotype-phenotype correlation and adaptive proteome reorganization in Marinesco-Sjögren syndrome Anna Giulia Ruggieri, Michele Sallese</p> <p>Left ventricular global longitudinal strain by speckle tracking echocardiography in hypertension: a mini-review Francesca Coccina, Rosa Scurti, Oriana Trubiani, Sante D. Pierdomenico</p> <p>Prevalence and localization of Maxillary Sinus Septa: a mini review Manlio Santilli, Bruna Sinjari, Oriana Trubiani, Gianmaria d'Addazio, Imena Rexhepi, Giuseppe Tafuri, Eugenio Manciocchi, Sergio Caputi</p> <p>Circulating endothelial cells and endothelial-derived vesicles identification in patients with infantile hemangioma: preliminary results of a prospective cohort study Maria Enrica Miscia, Pasquale Simeone, Giuseppina Bologna, Paola Lanuti, Gabriele Lisi, Laura Pierdomenico, Dacia Di Renzo, Marco Marchisio, Sebastiano Miscia, Pierluigi Lelli Chiesa</p> <p>Case series of two different dose regimen Rituximab therapy for severe Pemphigus Federica Giuliani, Giulio Gualdi, Paolo De Sanctis, Paolo Amerio</p>	<p>55</p> <p>59</p> <p>65</p> <p>71</p> <p>77</p> <p>81</p> <p>87</p> <p>93</p>
--	---	---	---